ACTA PROTOZOOLOGICA

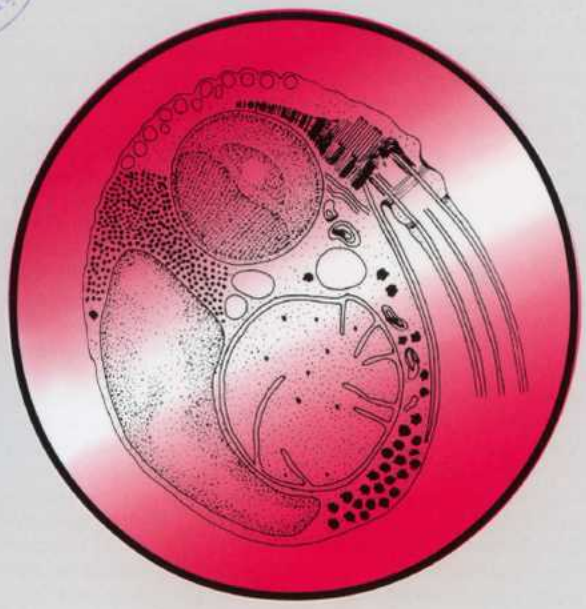

NENCKI INSTITUTE OF EXPERIMENTAL BIOLOGY
WARSAW, POLAND

2004

VOLUME 43 NUMBER 4
ISSN 0065-1583

Polish Academy of Sciences
Nencki Institute of Experimental Biology
and
Polish Society of Cell Biology

ACTA PROTOZOOLOGICA
International Journal on Protistology

ACTA PROTOZOOLOGICA appears quarterly.

The price (including Air Mail postage) of subscription to *Acta Protozoologica* at 2005 is: 200.- € by institutions and 120.- € by individual subscribers. Limited numbers of back volumes at reduced rate are available. Terms of payment: check, money order or payment to be made to the Nencki Institute of Experimental Biology account: 91 1060 0076 0000 4010 5000 1074 at BPH PBK S.A. Warszawa, Poland. For the matters regarding *Acta Protozoologica*, contact Editor, Nencki Institute of Experimental Biology, ul. Pasteura 3, 02-093 Warszawa, Poland; Fax: (4822) 822 53 42; E-mail: j.sikora@nencki.gov.pl For more information see Web page **http://www.nencki.gov.pl/ap.htm**

Front cover: Pekkarinen M., Lom J., Murphy C. A., Ragan M. A. and Dyková I. (2003) Phylogenetic position and ultrastructure of two *Dermocystidium* species (Ichthylosporea) from the common perch (*Perca fluviatilis*). *Acta Protozool.* **42:** 287-307

This publication is supported by the State Committee for Scientific Research

Desktop processing: Justyna Osmulska, Information Technology Unit of the Nencki Institute
Printed at the MARBIS, ul. Poniatowskiego 1
05-070 Sulejówek, Poland

Acta Protozool. (2004) 43: 291 - 301

ACTA
PROTOZOOLOGICA

Syndrome of the Failure to Turn off Mitotic Activity in *Tetrahymena thermophila*: in *cdaA1* Phenotypes

Ewa JOACHIMIAK, Janina KACZANOWSKA, Mauryla KIERSNOWSKA and Andrzej KACZANOWSKI

Department of Cytophysiology, Institute of Zoology, Warsaw University, Warsaw, Poland

Summary. During early micronuclear mitosis of a wild type *Tetrahymena thermophila,* basal body proliferation and cortical growth are localized in the equatorial region of the pre-dividing cell. These processes are arrested prior to cytokinesis when the fission line gaps appear in ciliary rows. Then a putative marker of cellular polarity, the fenestrin antigen, appears in the apical zone of the dividing cell and around the old oral apparatus (OA1) and in the cortex localized posterior to the fission line gaps and around the new oral apparatus (OA2) i.e. in the apical cortex of the prospective posterior daughter cell. Prior to cytokinesis, the membranelles within OA1 and OA2 oral apparatuses are strongly labeled with the MPM2 antibody against mitotic phosphoproteins. The transition to cytokinesis is correlated with disappearance of both the polar fenestrin staining and of the phosphoprotein antigens in OA1 and OA2. *cdaA1* (cell division arrest) mutant cells grown at the restrictive temperature do not produce a fission line and they do not undergo cytokinesis thereby generating irregular chains. The *cdaA1* phenotypes continue elongation of their ciliary rows in equatorial regions, mostly without formation of the fission line gaps, accompanied with repetitive micronuclear mitoses and repetitive formation of the defective oral structures. In *cdaA1* cells at restrictive temperature, the fenestrin antigen was recruited and then permanently found in the apical regions and around all oral apparatuses, and was always absent in equatorial regions, in spite of variability of immunostaining patterns, sizes and advancement of organization of OAs in different specimens of the same sample. The MPM2- tagged phosphoproteins were retained in all oral apparatuses in different *cdaA 1* phenotypes. We suggest that the *cdaA1* phenotypes produced at restrictive temperature behave as cells trapped in a metastable phase with a syndrome of an arrest of the mechanism required to regain the morphostatic stage of a non-dividing cell.

Key words: *cdaA1* mutation, cell cycle, fenestrin, MPM2 phosphoproteins, *Tetrahymena thermophila.*

INTRODUCTION

In yeasts many regulators define the spatial pattern of cell growth, positioning of the fission line, cytokinesis (Ayscough *et al*. 1997, Finger *et al*. 1998) and pattern the of acquisition of cell polarity during the cell cycle (Casamayor and Snyder 2002, Niccoli and Nurse 2002). The cell cycle is ended with an activation of the mitotic exit network (MEN) of events stimulated by an activation of the specific phosphatase (Cdc 14) and then turned off by an activation of the specific inhibitor of G protein signaling involved in acquisition of cell polarity to reset the whole cell cycle (Visintin *et al*. 1998, Wang *et al*. 2003).

The regulators corresponding to yeast's regulators of the patterned growth, mitotic exit and resetting of the cell cycle remain unknown in the ciliate cells. Biometrical

Address for correspondence: Janina Kaczanowska, Department of Cytophysiology, Institute of Zoology, Warsaw University, Miecznikowa str. 1, 02-096 Warszawa, Poland; Fax: (0-48) 22 554 1203; E-mail: kaczan@biol.uw.edu.pl

analysis showed that localization of the oral primordium for the prospective posterior cell division product in *T. thermophila* (OA2), is specified by two gradients of ciliary basal body proliferation within ciliary rows: an antero-posterior gradient and a dorso-ventral gradient (Kaczanowski 1978). In the later stages of divisional morphogenesis, the proliferation of the basal bodies is arrested, resulting in fission zone gaps within ciliary meridians that localizes the equatorial position of a fission line (Kaczanowska *et al*. 1992, 1993). The fission line separates nascent posterior and anterior poles of prospective daughter cells (Frankel *et al*. 1981, Kaczanowska *et al*. 1999). The metamery of divisional morphogenesis and the asymmetry of the fission zone correlates with a transient appearance of the fenestrin antigen in the apical region of the parental dividing cell and in a belt localized posterior to its fission line (Nelsen *et al*. 1994). Thus the fenestrin antigen is a transient cortical marker of an anterior pole character (Kaczanowska *et al*. 2003), and this patterned cortical growth during divisional morphogenesis is also associated with stage-dependent patterns of phosphorylation of proteins in oral membranelles (Kaczanowska *et al*. 1999). Subdivision of the anterior-posterior axis of the mother cell into two axes of prospective daughter cells is correlated with a transient appearance of the anterior marker of the submembrane protein - fenestrin (Nelsen *et al*. 1994) and with a transient decrease of the B antigen against the submembrane cytoskeletal epiplasm (Williams *et al*.1987,1995; Kaczanowska *et al*. 1993, 1999; Honts and Williams 2003). The apical staining with the anti-fenestrin antibody (Nelsen *et al*. 1994) appears at specific stages of oral development both in dividing and in reorganizing cells (Kaczanowska *et al*. 2003).

The MPM2 antibody. directed against some mitotic phosphoproteins (Davies *et al*. 1983, Westendorf *et al*. 1994, Ding *et al*. 1997) permanently labeled basal bodies of ciliary rows and other cortical organelles (like the contractile vacuole pores and cytoproct), but during morphogenesis this label only transiently appears in the oral membranelles of the developing or reorganizing oral apparatus and increases in surrounding cortical regions, then disappears during the transition to a morphostatic state (Kiersnowska and Golinska1996, Kaczanowska *et al*. 1999). Thus both the fenestrin and MPM2 antibodies may be used as markers of the exit of a cell from a metastable phase to the morphostatic condition of the quiescent cell.

To address this problem, we used the *cdaA1* mutant. At the restrictive temperature, the *cdaA1* mutant of *T. thermophila* (Frankel *et al*. 1976, 1977) shows complete arrest in cytokinesis, general increase of cell size, consecutive rounds of incomplete oral morphogenesis, repetitive micronuclear divisions, repetitive macronuclear DNA synthesis leading to a 2-4 fold increase of DNA content in the macronucleus (Frankel *et al*. 1976, 1980; Cleffmann and Frankel 1978). This resulted in formation of an array of *cdaA1* phenotypes with: disturbed cortical polarity of ciliary rows (Ng and Frankel 1977), which are folded in irregular cortical protrusions within the cortex of the prospective fission zone (Buzanska *et al*. 1989), and with repetitive but curtailed and defective stomatogenesis (Frankel *et al*. 1977, 1980; Kaczanowska 1990).

The aim of this report is to characterize the *cdaA1* phenotypes (Frankel *et al*. 1976) by an analysis of the patterns of immunofluorescence with the anti-fenestrin marker (Nelsen *et al*. 1994) and with the MPM-2 antibody against the phosphorylated epitopes of cytoskeletal mitotic phosphoproteins (Davies *et al*. 1983) in the *cdaA1* cells. Therefore the following questions were asked in this study: (1) whether in cytokinesis - arrested *cdaA1,* the fenestrin antigen will appear in the putative fission line zones and in the anterior apical region, (2) whether the variability of phenotypes correlates with the defined anti-fenestrin immunostained internal oral patterns, or with the advancement of development achieved by particular oral structures in the specimen, and (3) whether parallel correlations affect MPM2 immunostaining of oral patterns in particular specimens in the array of phenotypes.

MATERIALS AND METHODS

Material. *Tetrahymena thermophila cdaA1* (previously *mol^a/mol^a*, Frankel *et al.* 1976) strain IA104 was kindly provided by Dr J. Frankel, Iowa University, U.S.A. For inducing expression of the *cdaA1* mutation 300 ml Erhlenmeyer flasks containing 50 ml of the growth medium (1% PPY supplemented with iron and antibiotics, Nelsen *et al*. 1981) were inoculated with the mutant strain and incubated overnight at the 28°C to yield densities about 1000 cells/ml. Then some flasks were shifted to the 36°C restrictive temperature and other (controls) were left at the 28°C. The cell samples were immunostained at different times after shifting the cells to the restrictive temp (2, 2.5, 4 and 7 h). In one control experiment, the wild type conjugants of two complementary strains of *T. thermophila* CU427 (mt VI) and CU428 (mt VII) mixed for 4.5 h at 28°C were used. These strains were derived from Cornell University Athens, U.S.A and obtained from Dr J. Gaertig.

Antibodies. The monoclonal antibodies: FXIX-9A7 (against 64 kDa polypeptide - fenestrin) and MPM-2 (against phosphopro-

teins) were generously supplied by Drs: N. Williams, J. Frankel, and M. Nelsen, and by Dr P. Rao, Houston, U.S.A respectively. The secondary antibody was FITC - conjugated goat anti-mouse IgG (SIGMA).

Indirect immunofluorescence. The fenestrin epitopes were labeled according to Williams *et al*. (1990). The cells were collected by the low speed centrifugation , washed with 10 mM Tris - HCl (pH 7.4), permeabilized and fixed for 5-10 min on ice, with a solution of 0.2% Triton X-100 in 50% ethanol. The extracted cells were washed 2 × 10 min with blocking solution: of 0.2% BSA/TBS (bovine serum albumin - 20 mM Tris-HCl, 150 mM NaCl, pH 8.2). After 2 h of incubation with the primary antibody diluted 1:50 with 0.2% BSA/TBS at 30°C the pellet of cells was washed 3 × 10 min with the blocking buffer, and secondary antibody (diluted 1:200 with 0.2% BSA/TBS) was added for 2 h. Then the cells were washed 3-4 times and suspended on a slide in DAKO fluorescent mounting medium (anti quenching of the fluorescent label agent) and observed in a NIKON ECLYPSE E - 600 microscope.

The cells were labeled with the MPM2 antibody according to Kiersnowska and Golinska (1996). The growing cells were collected by low speed centrifugation and after washing with the 10 mM TRIS - HCl (pH 7.4) they were extracted for 3-5 min with 0.5% Triton X-100 in PHEM buffer, pH 6.9 (Schliwa and Van Blerkom 1981), fixed for 30 min with 2% paraformaldehyde, washed 4 × 10 min with 0.1% BSA / PBS (bovine serum albumin /phosphate buffer) and incubated overnight in 4°C with primary antibody at dilution 1: 200 in1% BSA/PBS. Then the cell samples were incubated with the secondary antibody and prepared for microscopic examination in the same way as those cells labeled with the anti-fenestrin antibody, except that PBS buffer solution was applied for washing.

Western blotting. Microtubule-free cortical residues were isolated from *cdaA1 Tetrahymena thermophila* grown at permissive temperature 28°C (as described above), and from cell samples shifted to the restrictive temperature 36°C for 2.5, 4 and 7 h. The samples were washed with 10 mM Tris-HCl, pH 7.4 and extracted with a cold solution containing of Triton X-100 in a high salt solution, with a cocktail of proteolysis inhibitors as described by Williams *et al*. (1990). SDS-PAGE electrophoresis and immunoblotting were carried out with the anti-fenestrin antibody diluted 1:200 incubated overnight at 4°C, and then the second anti-body the anti-mouse IgG- AP conjugated was developed with BCIP/NBT (Sigma) protocol according to producer's instruction. Three independent experiments were performed and one was supplemented with the sample of the wild type conjugating cells kept at 28°C for 4.5 h as the case of *wt* starved cells but nevertheless involved in morphogenetic activity.

RESULTS

Cortical patterns of anti- fenestrin immunofluorescence in *cdaA1* phenotypes

Cells incubated at permissive temperature (28°C). The morphostatic *cdaA1* cells showed slight fluorescence of the collar of the oral apparatus (OA) and a weak fluorescence around basal body domains in the middle segments of ciliary rows (Fig. 1). In dividing cells, a weak apical fluorescence intensified (Fig. 2, arrowhead) and the newly developing oral primordium (OA2) gradually differentiates a "negative pattern of oral membranelles" in which the three membranelles are not immunostained, while the oral matrix around them is stained (Fig. 2, OA2). Thereafter, with some delay, this "negative pattern of membranelles" also appears in the parental OA1 (not shown). In the next stage, the fluorescence of the apical cortex and of the belt localized posterior to the fission line appears (Fig. 3, arrowheads), while the negative labeling of the membranelles gradually disappears in both oral apparatuses (Fig. 3, OA1 and OA2), whereas, the residual labeling outlines the OAs. During cytokinesis, the polar immunostaining of both offspring gradually diminishes while residual labeling outlining the OAs persists (not shown). Thus at the permissive temperature, the patterns of cortical labeling of morphostatic and dividing *cdaA1* cells with the anti-fenestrin antibody were the same as those in the w*t* cells (Kaczanowska *et al*. 2003).

Cells incubated 2h or more at restrictive temperature. Growing c*daA1* cells expressed cell division arrest (their mutant phenotypes) as soon as 2 h after shifting to the restrictive temperature, what was monitored under the microscopy, and became majority in a sample incubated for 2.5 h. Practically all specimens expressed *cdaA1* phenotypes after 4 h of incubation, whereas after 7 h of incubation some cells became immobile (possibly dying cells). *cdaA1* phenotypes taken from the after 2 h of incubation at 36°C sample are very variable. Some of them (for instance Fig. 4) keep a normal size and shape, whereas others exhibit very different sizes and shapes. All *cda A1* cells kept at the restrictive temperature show an apical labeling of the fenestrin marker (Figs 4-9) and absence of this marker in the equatorial regions (Figs 5-9). The first sign of an abnormality in cells shifted to restrictive temperature was found in the cell of Fig. 4, with an incomplete fluorescent belt localized posterior to the fission line (arrowhead) and with two oral apparatuses with greatly reduced internal fluorescence (as on Fig. 3). A cell (Fig. 5) from the same sample with three oral apparatuses OA1, OA2 and OA3 shows a "negative pattern of membranelles" (like in Fig. 2) only in the OA2. All these cells manifested less or more extended apical fluorescence as focused in Figs 5 and 6 (arrowheads) together with a total absence of this fluorescence in vicinity of the fission zone, in spite of gaps of some ciliary rows (Fig. 6). In contrast to Fig. 5, in Fig. 6, all three oral

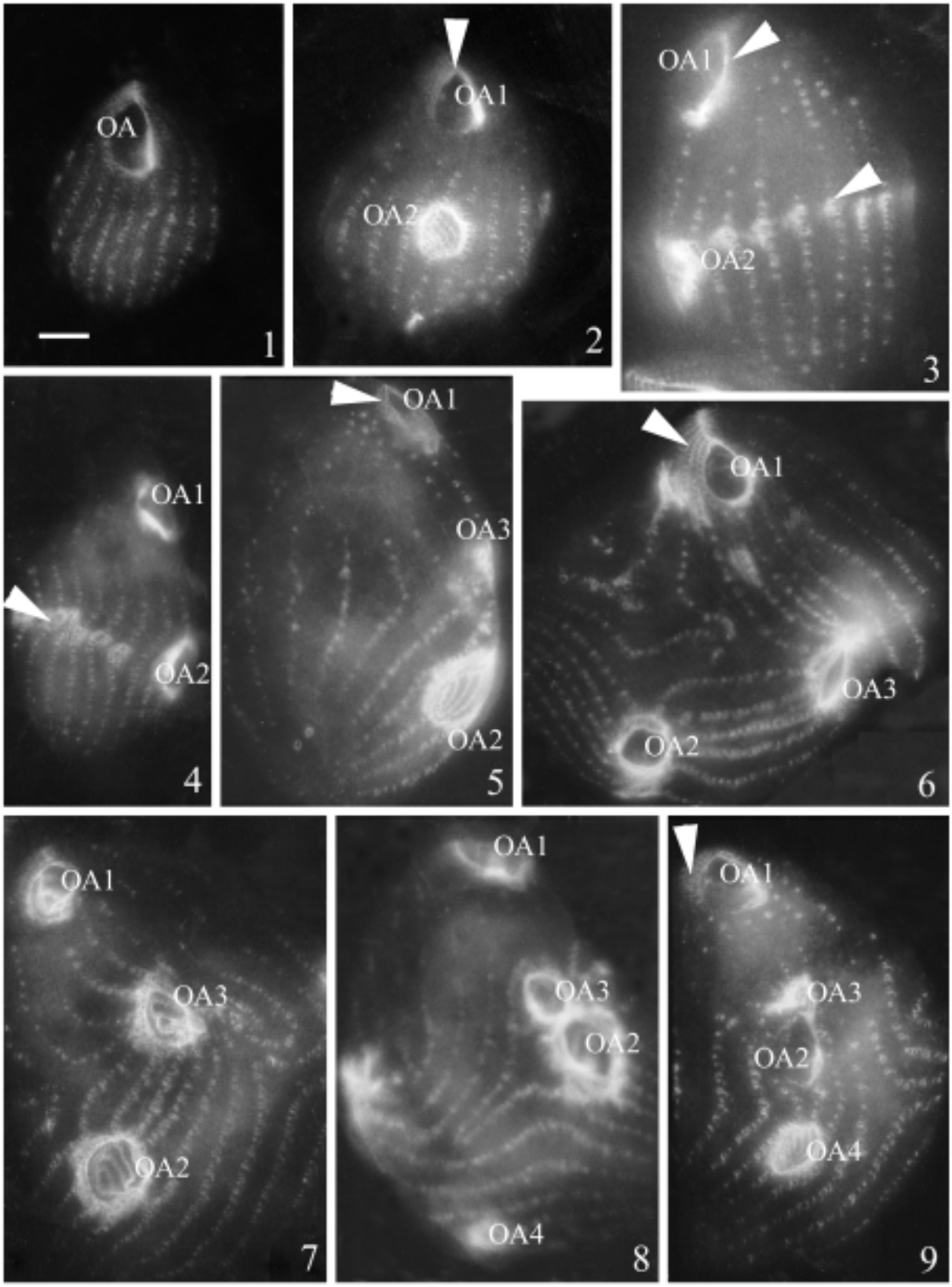
OA
1
OA1
OA2
2
OA1
OA2
3
OA1
OA2
4
OA1
OA3
OA2
5
OA1
OA3
OA2
6
OA1
OA3
OA2
7
OA1
OA3
OA2
8
OA1
OA3
OA2
OA4
9
OA1
OA3
OA2
OA4

apparatuses, OA1, OA2 and OA3 lack internal fluorescence. In the Fig. 7 another cell from the same sample shows fenestrin labeling around oral structures, which represents the same stage of a "negative pattern of membranelles" in all three oral apparatuses (OA1, OA2, and OA3). In Fig. 8, collars surround the four oral apparatuses that lack fluorescence within oral pouches of variable sizes. Finally, a cell with two apparent generations of oral apparatuses is presented in Fig. 9; OA1 and OA2 are at the stage of nearly total disappearance of fluorescence within the oral pouches, whereas the OA3 and OA4 are in stage of a "negative pattern of membranelles" (Fig. 9, OA3 and OA4). In this cell, the apical staining with fenestrin is preserved (Fig. 9, arrowhead) as in other specimens. Hence, in *cdaA1* mutants, perturbations in the pattern of ciliary rows are associated with an absence of the fenestrin marker of polarity in the prospective posterior daughter cell, whereas this marker is preserved in the apical region of phenotypes and in collars outlining all oral apparatuses. Nevertheless, the size and number of oral apparatuses, presence or absence of labeling by anti-fenestrin antibody of the "negative pattern of membranelles" are variable. The same variability is observed in samples incubated at restrictive temperature for more than 2 h (in samples incubated 4 and 7 h).

Cortical patterns of MPM2 immunofluorescence in cdaA1 phenotypes

Cells kept at permissive temperature. In non-dividing wild type *T. thermophila* as well as in *cdaA1* cells kept at a permissive condition, the MPM2- tagged phosphoproteins are detected in the inner pouch of the oral apparatus (OA), with a very strong fluorescence of the deep fiber at its bottom (Fig. 10, DF), with an absence of fluorescence of the oral membranelles, and a weak fluorescence of the oral collar and the basal bodies of ciliary rows (Fig. 10). In early dividing cells very strong fluorescence appears of the newly produced primordium of the second oral apparatus (Fig. 11, OA2), whereas the pattern of immunostaining of OA1 roughly corresponds to that of OA of a non-dividing cell (Fig. 11, DF). In this cell some apical fluorescence, and intense staining of basal bodies in middle segments of ciliary rows are observed (Fig. 11). In more advanced stage of cell division, a disappearance of the fluorescence in the bottom of the OA1 (corresponding to a site of the deep fiber in Figs 10, 11) and a start of transient immunostaining of its membranelles (Fig. 12, OA1) sharply contrasts with a very strong fluorescence of the oral region of OA2 (Fig. 12, OA2). At more advanced stage, the membranelles in both oral apparatuses (Fig. 13, OA1 and OA2) are heavily immunostained in equivalent intensities. Prior to cytokinesis, a gradual disappearance of fluorescence of membranelles in OA1 and OA2 (Fig. 14 *vs.* Fig. 13) is observed. It results in a weak "negative pattern of membranelles" in both oral apparatuses with a nearly total disappearance of fluorescence within oral apparatuses (OA1 and OA2) (not shown). After division, in quiescent daughter cells some apical fluorescence gradually diminishes, whereas the deep fiber gradually re-appears in the bottom of OA which strongly binds MPM2 antibody (Fig. 15, DF). This cell also shows a transiently appearing fluorescence of the macronucleus (Fig. 15, MA). Thus at the permissive temperature, the patterns of cortical labeling of morphostatic and dividing *cdaA1* cells with the MPM2 antibody are the same as those in the w*t* cells (Kiersnowska and Golinska 1996, Kaczanowska *et al*.1999).

Cells kept 2 h, 4 h and 7 h at restrictive temperature. A major fraction in a sample incubated at 2 h are the *cdaA1* cells arrested in cell division of a size of cells

Figs 1-9. Cortical patterns of anti-fenestrin immunostaining in *cdaA1 Tetrahymena thermophila*. **1-3** - cells grown at permissive temperature; **4-9** - cells incubated 2 h at the restrictive temperature. **1** - a nondividing cells with fluorescence of the collar around the oral apparatus (OA), and some fluorescence in the inner part of the oral pouch and of basal body domains of ciliary rows; **2** - the early dividing cell with the morphostatic pattern of the parental oral apparatus (OA1) and some apical fluorescence (arrowhead) and with a "negative pattern of tetrahymenium" of the developing OA2; **3** - an advanced dividing cell prior to cytokinesis with decreasing fluorescence. The fluorescence diminishes inside the oral apparatuses (OA1 and OA2) and outlines the collars. The apical fluorescence (out of focus) and strong belt of fluorescence posterior to the fission line are marked by arrowheads; **4** - an unusual pattern of a nearly normal-looking cell with the outlines of two apparatuses OA1 and OA2 and with incomplete belt of fluorescence (arrowhead) localized posterior to the fission line (more explanation in text); **5** - a *cdaA1* phenotype with a parental oral apparatus (OA1) and two developing oral apparatuses (OA2 and OA3) at different stages of development. The enlarged OA2 is at stage of a "negative pattern of tetrahymenium" and with apical fluorescence (out of focus, arrowhead); **6** - another cell with three oral apparatuses (OA1, OA2 and OA3) without oral internal fluorescence. The cell is focused on the apical fluorescence (arrowhead). Some ciliary rows show a fission zone discontinuities; **7** - a cell from the same sample showing three oral apparatuses (OA1, OA2 and OA3) at the same stage of a "negative pattern of tetrahymenium"; **8** - a cell with four outlined oral apparatuses (OA1, OA2, OA3 and OA4) of different sizes with some looped ciliary rows. **9** - a specimen with the four oral apparatuses of two generations; the OA1 and OA2 at a very advanced morphogenesis with diminishing internal fluorescence, OA4 at a stage of a "negative pattern of tetrahymenium" and OA3 at early primordial stage. All cells at the same magnification as indicated by the bar 10 μm in Fig.1.

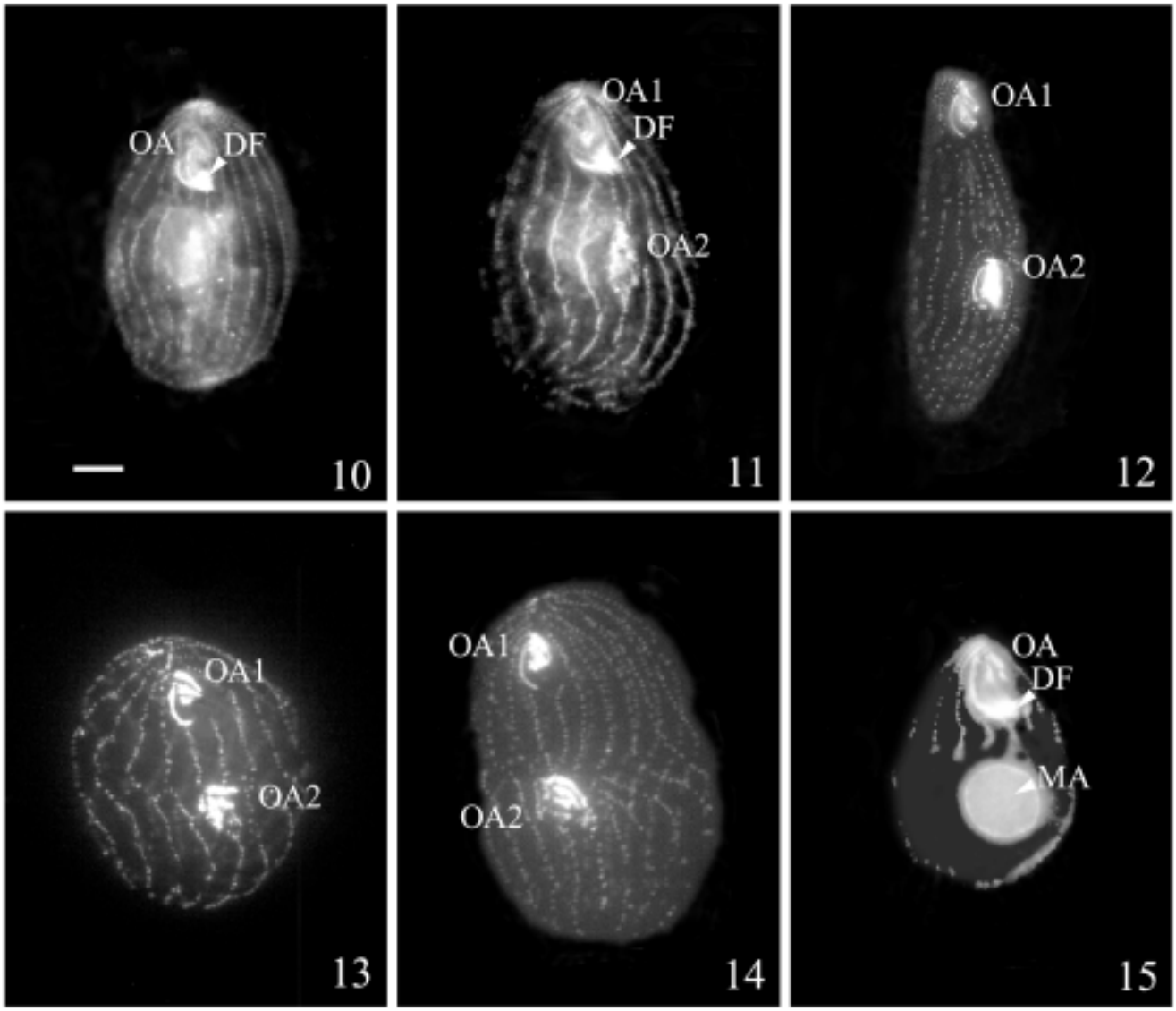

Figs 10-15. Cortical patterns of phosphoproteins immunostained with the MPM2 antibody in *cdaA1 Tetrahymena thermophila.* Cells kept at permissive temperature. **10 -** a morphostatic pattern of a *cdaA1* cell with a weak fluorescence of the oral apparatus (OA) except an intense fluorescence within the bottom of the oral pouch co-localized with a deep fiber (DF), and in the basal body domain in meridional ciliary rows; **11** - an early dividing cell with a weak fluorescence of parental oral apparatus (OA1) showing phosphorylated deep fiber (DF) with a strong fluorescence of the developing oral primordiun (OA2) and of middle segments of meridional ciliary rows; **12 -** a cell in more advanced cell division than Fig. 11. The parental oral apparatus (OA1) gains fluorescence of membranelles whereas a deep fiber is absent, the new oral apparatus (OA2) shows maximal strong fluorescence of a whole oral region; **13 -** a cell in advanced cell division showing strong fluorescence of patterns of oral membranelles of both oral apparatuses (OA1 and OA2), however lacking fluorescence of a matrix of oral regions; **14 -** a cell at beginning of cytokinesis with diminishing fluorescence of membranelles of both oral apparatuses (OA1 and OA2); **15 -** an early post-dividing cell with remnant of apical fluorescence and weak fluorescence of oral apparatus (OA1) except the re-appearing deep fiber (DF). Some fluorescence of a macronucleus (MA) is observed in early post-dividing cells. Figs 1-9 are printed at the same magnification as in and indicated by the bar 10 μm on Fig.10.

dividing in permissive temperature (Fig. 16 *vs*. Fig. 14), with two strongly fluorescent oral apparatuses (Fig. 16, OA1 and OA2) and with a more or less meridional disposition of ciliary rows of strongly fluorescent basal bodies. Nevertheless, some cells show an increase of a total dimensions, irregularities in pattern of ciliary meridians and the abnormally intensive immunostaining of both oral regions (Figs 17-20, OA1 and OA2). In the same sample, some specimens with the very bright both oral regions (Figs 18, 19; OA1 and OA2) are supplemented

with the new oral primordium. Two localizations of these primordia are discerned, either the OA3 primordium appears localized between OA1 and OA2 (Fig. 18, OA3), or in rare cases, the OA4 primordium appears at the rear end of the cell (Fig. 19, OA4). Some specimens yield three oral apparatuses of the same dimensions and brightness that seems to be equivalent (Fig. 20, OA1, OA2 and OA3). Finally, some specimens shows four oral apparatuses of different sizes and locations (Fig. 21) apparently representing two rounds of stomatogenesis; the enlarged OA1 and OA2 are accompanied with the minor ones OA3 and OA4 (Fig. 21, OA1, OA2, OA3 and OA4). In all these phenotypes all oral apparatuses kept intense fluorescence. Very few cells (except of 2% of morphostatic cells) with two or more oral apparatuses showed submaximal fluorescence of the oral regions.

In the sample taken from cells incubated 4 h, the fraction of unmodified cells with the pattern presented in Fig. 10 concerns about 2-4% and most of the specimens correspond to cortical patterns of fluorescence presented in Figs 17-21. In these phenotypes all oral apparatuses kept intense fluorescence. Apparently, the depletion of the MPM2-tagged phosphoproteins in the oral membranelles that usually occurs prior to cytokinesis is inhibited in practically all *cdaA1* cells.

The amounts of the fenestrin in cytoskeletal fraction of *cdaA1* cells kept at permissive temperature and at restrictive temperature during sequent hours of incubation

The Western blots for the presence of fenestrin antigen in the cytoskeletal fraction of the *cdaA1* cells were performed in three independent experiments according to Material and Methods. In these experiments, the growing cell cultures were shifted to a restrictive temperature and cell samples were collected after 2.5, 4, and 7 h of incubation and from a control culture that was not shifted to 36°C as well as a sample of wild type conjugating cells (see Materials and Methods). The results are presented in Fig. 22. Nearly the same amounts of the fenestrin protein are found in cells either from the culture kept at permissive temperature (first lane, 0 h of incubation), or after 2.5, 4 and 7 h of incubation. Apparently, the major fraction of non-dividing well fed control cells (first lane) and these that entered into defective divisional morphogenesis (second lane) demonstrated an amount of fenestrin protein slightly lower than the amounts found in other lanes. This means that from 2.5 h of incubation roughly the same amounts of the fenestrin are detected in all samples and they roughly correspond to amount of the fenestrin found in starved wild type conjugating for 4.5 h. It follows from the above that absence of the fenestrin within the putative fission zones of *cdaA1* phenotypes is not due to a decreased amounts of this protein in the cytoskeletal fraction.

DISCUSSION

In *cdaA1* cells kept at permissive temperature, as in *wild type* cells, the co-ordinated spatial cortical patterns of cell growth and stages of divisional morphogenesis were correlated with changes in patterns of immunofluorescence with both antibodies (Kaczanowska *et al*. 1999, 2003). In early dividing cells, the MPM-2 and fenestrin antigens appeared in the OA2 primordium and next in developing membranelles of the newly formed OA2. Prior to cytokinesis, this staining of membranelles disappeared, replaced by formation of a ”negative patterns of membranelles” of both parental OA1 and in newly formed OA2 followed by a nearly total disappearance (except of weak oral outlines and of the developing inner pouch) of fluorescence in OAs of daughter cells. Additionally, prior to cell division the fenestrin antigen appeared around the proliferating basal body domains of meridional ciliary rows, and as fluorescence of the anterior cortex pole and of the newly produced anterior pole of the posterior daughter cell. Dual metameric cortical patterns for prospective daughter cells are transiently marked by the fenestrin immunostaining of the apical cortex and of the belt of cortex localized posterior to the fission line. This labeling disappears during cytokinesis. The MPM2 phosphoproteins associated with *Tetrahymena* oral apparatuses during morphogenesis disappear prior to cytokinesis, and this labeling only partly re-appears in daughter cells reduced to a site co-localized to a developing deep fiber.

At a restrictive temperature, the *cdaA1* cells were arrested in fission line formation. Failure of the arrest of cortical growth in this equatorial region results in irregular lengthening and looping of meridional ciliary rows, and in consecutive attempts to develop a new oral apparatuses. In these *cdaA1* phenotypes, the fenestrin marker is found on the anterior pole of cells indicating that they have reached an advanced stage of divisional morphogenesis, with residual or no labeling in the fission zone. The results of Western blotting show that the amount of fenestrin in cortical residues do not decrease

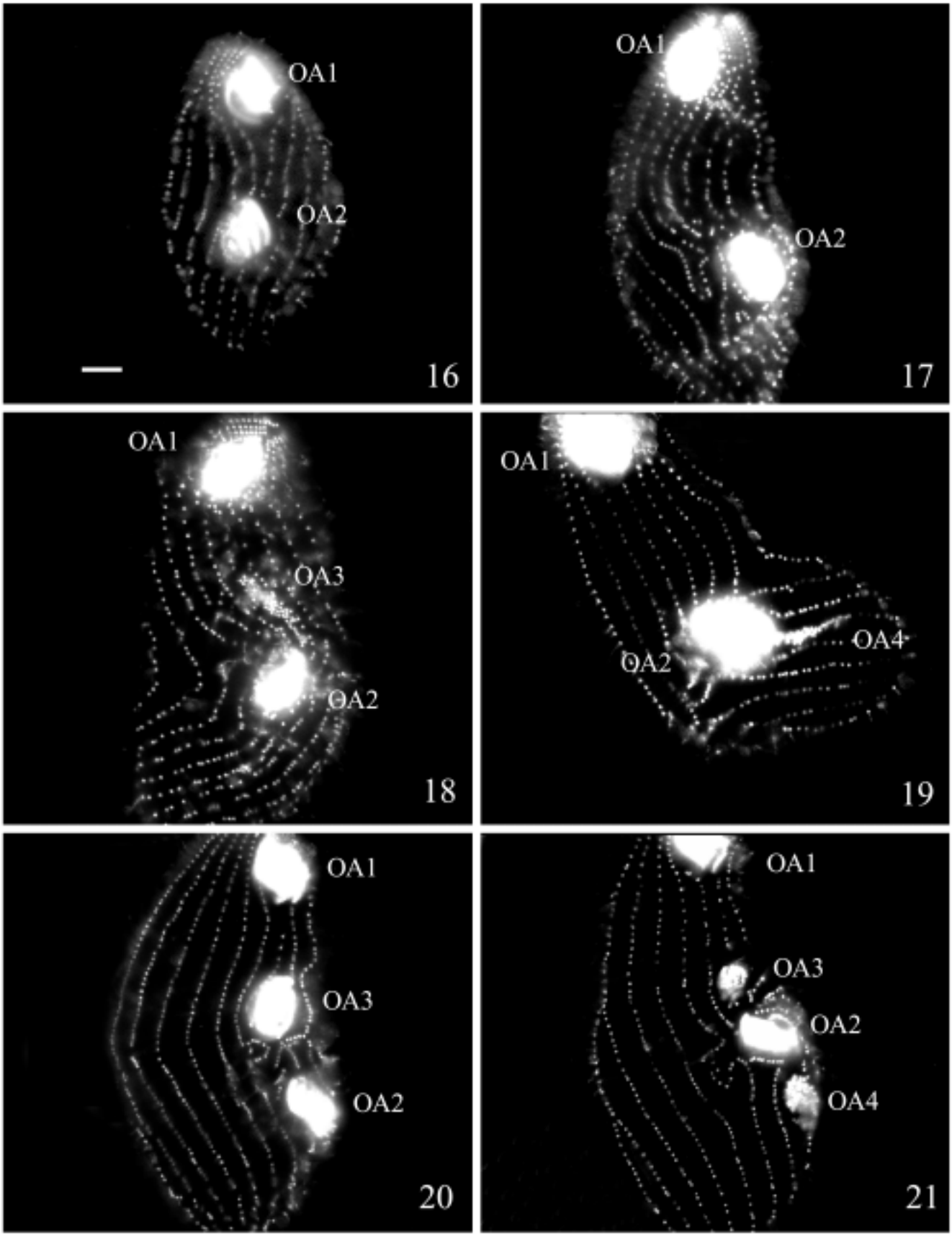
OA1
OA2
16
OA1
OA2
17
OA1
OA3
OA2
18
OA1
OA4
OA2
19
OA1
OA3
OA2
20
OA1
OA3
OA2
OA4
21

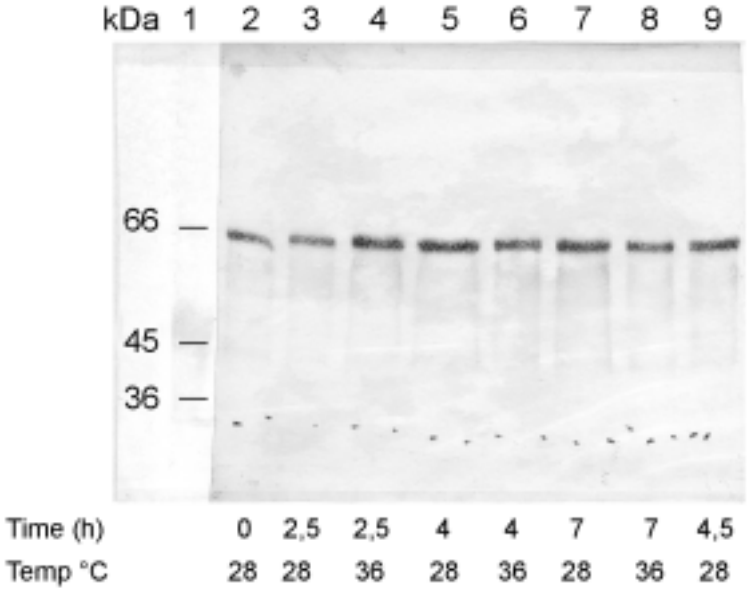

Fig. 22. A Western blot of electrophoresed proteins of cytoskeletal cortices of *cdaA1* cells marked with the anti-fenestrin antibody. The 1st lane shows the distribution of the commercial cortical markers (Sigma) of proteins of 36, 45 and 66 kDa. The 2nd lane detects the fenestrin from cells grown at permissive temperature,3rd and 4th lanes- from the cells incubated 2.5 h, 5th and 6th lanes-from the cells incubated 4 h, and 7th and 8th lanes from the cells incubated 7 h at permissive and restrictive temperatures, respectively. The 9th lane - conjugants (CU427 × CU428) after 4.5 h from mixing of mates.

in these cells. Thus the failure of cytokinesis and of immunostaining of the putative fission zone are not correlated with a decrease of the amount of cortical fenestrin. On the other hand, the fenestrin antigen appears at the anterior pole in cells in different stages of oral morphogenesis and with a variable number of oral apparatuses suggesting that *cdaA1* cells do not turn off their morphogenetic activity while they undergo successive rounds of cortical development (Kaczanowska 1990). This is consistent with data about other activities, such as repetitive micronuclear mitoses and DNA replication in macronucleus (Frankel *et al*. 1976, Cleffmann and Frankel 1978) and progressing morphological anomalies (Frankel *et al*. 1977) which may reflect the sustaining of a metastable phase in *cdaA1* cells. In support of this interpretation, the programmed depletion of the MPM2-tagged phosphoproteins found in oral apparatuses of wild type cells during cytokinesis was arrested in practically all *cdaA1* cells irrespective to the advancement of oral morphogenesis and of the internal oral patterns of the anti-fenestrin immunostaining, or of the duration of incubation at restrictive temperature. The defined and short-lasting temperature-sensitive period in the cell cycle of *cdaA1* cells for expression of abnormal phenotypes (Frankel *et al*. 1980) is taken as evidence that *cdaA1* mutation concerns fundamental failure of some transition(s) in progress of the cell cycle of *Tetrahymena*. Thus an absence of dephosphorylation of phosphoproteins within the oral apparatuses and the retention of apical fenestrin immunostaining in *cdaA1* phenotypes

Figs 16-21. *cdaA1* cells incubated 2 h at restrictive temperature. **16** - a normally looking cell with heavily stained membranelles of both oral apparatuses (OA1 and OA2); **17** - a specimen with a slight disorder in polarity of ciliary rows, and with some apical fluorescence, showing maximal, heavy fluorescence of whole oral regions of both oral apparatuses (OA1 and OA2); **18** - a specimen with the same pattern of fluorescence as shown in oral regions (OA1 and OA2) in Fig. 17 but with an additional bright primordium of next oral apparatus (OA3); **19** - a specimen with the same pattern of fluorescence as shown in oral regions (OA1 and OA2) in Figs 17 and 18 with an additional primordium of posterior oral apparatus (OA4); **20** - a cell with the three heavily labeled oral apparatuses (OA1, OA2 and OA3) with one interrupted ciliary row and with some folding of ciliary rows in area between OA3 and OA2; **21** - an enlarged undivided cell with four strongly labeled oral apparatuses of two generations (OA1 and OA2 of the first generation and OA3 and OA4 of the second generation) With some ciliary rows looped towards the oral apparatus (OA2). Figs 1-15 are printed at the same magnification as in with the bar 10 μm shown on Fig. 16.

are correlated with a failure in cytokinesis and an arrest in the transition from morphogenetic activities of dividing cell to morphostasis of divided daughter cells. Apparently, the mitotic exit network in *Tetrahymena thermophila* wild type and *cdaA1* concerns both dephosphorylating and phosphorylating events (Buzanska and Wheatley 1994).

In budding yeast, the mechanisms of transition from the metastable state of a budding cell into the quiescent state of the daughter cells by the Amn1 inhibitor was recently identified (Wang *et al*. 2003). An important step in this pathway is the release and activation of Cdc 14 serine phosphatase which inhibits Cdk1 activity (Visintin *et al*. 1998). These findings raise the question whether a mechanism corresponding to the mechanism of the mitotic exit network (MEN) of yeast, with activation of some dephosphorylation and of Amn 1 inhibitor, is present in *T. thermophila* and is affected by the *cdaA1* mutation, and whether in particular this exit depends upon the localization of protein p85 in the fission line of the *wt* cells that does not appear in equatorial regions of the *cdaA1* cells (Gonda *et al*. 1999a). The p85 is a protein partly homologous to a cdc2 kinase (Gonda *et al*. 1999b) which is sensitive to Ca^{++}/CaM signaling pathway and has the same aminoacid sequence in *wt* and *cdaA1* phenotypes (Gonda *et al*. 1999a, b; Numata and Gonda 2001). Gonda *et al*. (1999a) found a slight difference of molecular weights between p85 in the *wt* and *cdaA1* phenotypes, which is due to some unknown posttranslational modification pertinent to its proper activity at the end of the cell cycle. Recently, as many as three cyclin-dependent kinases were found in *T. thermophila,* but the regulation of their activities in the cell cycle remains unknown (Zhang *et al*. 2002).

Acknowledgements. The authors thank Dr Joseph Frankel (Iowa Univ., U.S.A.) for supplying *cdaA1 Tetrahymena thermophila.* We are very thankful to Drs J. Frankel, N.E. Williams, M Nelsen and P. Rao for generous gifts of antibodies used in this study. Assistance and technical aid in preparation of western blot by Dr Dorota Wloga is also acknowledged. We are very grateful for technical assistance of MSc Marzena Kwiatkowska-Dąbrowska. This work was supported by the grant from Polish Science Committee No 6PO4C 012 19 to Dr Andrzej Kaczanowski.

REFERENCES

Ayscough K. R., Stryker J., Pokala N., Sanders M., Crews P., Drubin D. G. (1997) High rates of actin filament turnover in budding yeast and roles for actin in establishment and maintenance of cell polarity revealed using the actin inhibitor latrunculin-A. *J. Cell Biol*. **137:** 399-416

Buzanska L., Wheatley D. N. (1994) Okadaic acid promotes cell division in synchronized *Tetrahymena pyriformis* and in the cell division-arrested (*cdaA1*) temperature sensitive mutant of *T. thermophila*. *Eur. J. Cell Biol*. **63:** 149-158

Buzanska L., Gregory D. W., Wheatley D. N. (1989) Protrusion formation in the cell division-arrested mutant *Tetrahymena thermophila cdaA1*, and the elucidation of some rules governing cytoskeletal growth. *J. exp. Zool*. **251:** 27-36

Casamayor A., Snyder M. (2002) Bud-site selection and cell polarity in budding yeast. *Curr. Opin. Microbiol.* **5:** 179-186

Cleffmann G., Frankel J. (1978) The DNA replication schedule is not affected in a division blocked mutant of *Tetrahymena thermophila. Exp. Cell Res.* **117:** 191-194

Davies F. M., Tsao T. Y., Fowler S. K., Rao P. N. (1983) Monoclonal antibodies to mitotic cells. *Proc. Natl. Acad. Sci. USA* **80:** 2926-2930

Ding M., Feng Y., Vandre D. D. (1997) Partial characterization of the MPM-2 phosphoepitope. *Exp. Cell Res*. **231:** 3-13

Finger E. P., Hughes T. E., Novick P. (1998) Sec3p is a spatial landmark for polarized secretion in budding yeast. *Cell* **92:** 559-571

Frankel J., Jenkins L. M., DeBault L. E. (1976) Causal relations among cell cycle processes in *Tetrahymena pyriformis*. An analysis employing temperature-sensitive mutants. *J. Cell Biol*. **71:** 242-260

Frankel J., Nelsen E. M., Jenkins I. M.. (1977) Mutations affecting cell division in *Tetrahymena pyriformis Syngen I*. II. Phenotypes of single and double homozygotes. *Devel. Biol*. **58:** 255-275

Frankel J., Mohler J., Frankel A. W. K. (1980) Temperature - sensitive periods of mutations affecting cell division in *Tetrahymena thermophila*. *J. Cell Sci*. **43:** 75-91

Frankel J., Nelsen E. M., Martel E. (1981) Development of a ciliature of *Tetrahymena thermophila* II. Spatial subdivision prior to cytokinesis. *Devel. Biol*. **88:** 349-354

Gonda K., Nishibori K., Ohba H., Watanabe A., Numata O. (1999a) Molecular cloning of the gene for 85 that regulates the initiation of cytokinesis in *Tetrahymena. Biophys. Biochem. Res. Com.* **264:** 1112-118

Gonda K., Katoh M., Hanyu K., Watanabe A., Numata O. (1999b) Ca^{++}/calmodulin and p85 cooperatively regulate the initiation of cytokinesis in *Tetrahymena*. *J. Cell Sci*. **112:** 3619-3626

Honts J., Williams N. E. (2003) Novel cytoskeletal proteins in the cortex of *Tetrahymena*. *J. Eukaryot. Microbiol.* **50:** 9-14

Kaczanowska J. (1990) Integration of oral structures in *cdaA1* mutant of *Tetrahymena thermophila*. *Acta Protozool*. **29:** 275-290

Kaczanowska J., Buzanska L., Frontczak M. (1992) The influence of fission line expression on the number and positioning of oral primordia in the *cdaA1* mutant of *Tetrahymena thermophila*. *Devel. Genetics* **13:** 216-222

Kaczanowska J., Buzanska L., Ostrowski M. (1993) Relationship between spatial patterning of basal bodies and membrane cytoskeleton (epiplasm) during the cell cycle of: *cdaA* mutant and anti-membrane immunostaining. *J. Eukaryot. Microbiol*. **40:** 747-754

Kaczanowska J., Joachimiak E., Buzanska L., Krawczynska W., Wheatley D. N, Kaczanowski A. (1999) Molecular subdivision of the cortex of dividing *Tetrahymena* is coupled with the formation of the fission zone. *Devel. Biol*. **212:** 150-164

Kaczanowska J., Joachimiak E., Kiersnowska M., Krzywicka A., Golinska K., Kaczanowski A. (2003) The fenestrin antigen in submembrane skeleton of the ciliate *Tetrahymena thermophila* is proposed as a marker of cell polarity during cell division and in oral replacement. *Protist* **154:** 251-264

Kaczanowski A. (1978) Gradients of proliferation of ciliary basal bodies and the determination of the oral primordium in *Tetrahymena*. *J. exp. Zool*. **204:** 417-430

Kiersnowska M., Golinska K. (1996) Pattern of phosphorylated structures in the morphostatic ciliate *Tetrahymena thermophila*: MPM-2 immunogold labeling. *Acta Protozool*. **35:** 297-308

Nelsen F. M., Frankel J., Martel E. (1981) Development of the ciliature of *Tetrahymena thermophila*.I. Temporal co-ordination with oral development. *Devel. Biol*. **88:** 27-38

Nelsen E. M., Williams N. E., Hong Y., Knaak J., Frankel J. (1994) „Fenestrin" and conjugation in *Tetrahymena thermophila*. *J. Eukaryot. Microbiol*. **41:** 483-495

Ng S. F., Frankel J. (1977) 180° rotation of ciliary rows and its morphogenetic implications in *Tetrahymena pyriformis*. *Proc. Natl. Acad. Sci. USA* **74:** 1115-1119

Niccoli T., Nurse P. (2002) Different mechanisms of cell polarization in vegetative and shmooing growth in fission yeast. *J. Cell Sci*. **115:** 1651-1662

Numata O., Gonda K. (2001) Determination of division plane and organization of contactile ring in *Tetrahymena. Cell Struct. Func.* **26:** 591-601

Schliwa M., Van Blerkom J. (1981) Structural interaction of cytoskeletal components. *J. Cell Biol.* **90:** 222-235

Visintin R., Craig K., Hwang E.S., Prinz S., Tyers M., Amon A. (1998) The phosphatase Cdc 14 trigers mitotic exit by reversal of Cdk-dependent phosphorylation. *Mol. Cell* **2:** 709-718

Wang Y., Shirogane T., Liu D., Harper J.W., Elledge S. J. (2003) Exit from exit: resetting the cell cycle through AMN1 inhibition of G protein signaling. *Cell* **112:** 697-709

Westendorf J. M., Rao P. N., Gerace L. (1994) Clonning of cDNA for M-phase phosphoproteins recognized by the MPM2 monoclonal antibody and determination of the phosphorylated epitope. *Proc. Natl. Acad. Sci. USA* **91:** 714-718

Williams N. E., Honts J. E., Jaeckel-Williams R. F. (1987) Regional differentiation of the membrane in *Tetrahymena. J. Cell Sci*. **87:** 457-463

Williams N. E., Honts J. E, Kaczanowska J. (1990) The formation of basal body domains in the membrane skeleton of *Tetrahymena*. *Development* **109:** 935-942

Williams N. E., Honts J. E., Dress V. M, Nelsen E. M., Frankel J. (1995) Monoclonal antibodies reveal complex structure in the membrane skeleton of *Tetrahymena. J. Eukaryot. Microbiol*. **42:** 422-427

Zhang H., Huang X., Tang L., Zhang Q-J, Frankel J., Berger J. D. (2002). A cyclin dependent protein kinase homologue asssociated with the basal body domains in the ciliate. *Biochim. Biophys. Acta* **1591:** 119-128

Received on 21st January, 2004; revised version on 28th May, 2004; accepted on 3rd June, 2004

Acta Protozool. (2004) 43: 303 - 311

ACTA
PROTOZOOLOGICA

Multigene Evidence for Close Evolutionary Relations between *Gromia* and Foraminifera

David LONGET, Fabien BURKI, Jérôme FLAKOWSKI, Cédric BERNEY, Stéphane POLET, José FAHRNI and Jan PAWLOWSKI

Department of Zoology and Animal Biology, University of Geneva, Genève, Switzerland

Summary. *Gromia oviformis* is a common marine rhizopod, possessing a large ovoid membraneous theca that resembles the tests of certain monothalamous (single-chambered) foraminifers. In fact, the genus *Gromia* was initially classified among the Foraminifera, but because of its non-granular, filose pseudopodia it was later included among filopodia-bearing protists (the Filosea). Recent molecular phylogenies suggested that *Gromia* branches among Cercozoa, a heterogeneous assemblage of mainly amoeboid protists, which show some affinities to Foraminifera. To test how closely related are *Gromia* and Foraminifera, we have analysed the sequences of actin, large subunit of the RNA polymerase II (RPB1) and small subunit (SSU) rRNA genes. We also analysed the structure of the polyubiquitin gene of *G. oviformis*. Our analyses show that *Gromia*'s actin is specifically related to one of the two actin genes families known in Foraminifera. In RPB1-based phylogenies, *Gromia* appears as the closest relative of Foraminifera, while in the SSU rRNA trees it branches as sister to Foraminifera and Haplosporidia. We identified also a single serine insertion in the polyubiquitin of *Gromia*, similar to that found in Foraminifera, Plasmodiophorida and some Cercozoa. Altogether, these findings support the hypothesis that the morphological resemblance between *Gromia* and Foraminifera may be due to a shared common ancestor. If further analyses of protein-coding genes including a more representative sampling of Cercozoa confirm this relationship, then the molecular study of *G. oviformis* will be of key importance for understanding the origin of Foraminifera.

Key words: actin, Cercozoa, Filosea, foraminifera, phylogeny, polyubiquitin, RNA polymerase II largest subunit, SSU rRNA.

Abbreviations: BV - bootstrap value, LBA - long branch attraction, ML - maximum likelihood, MP - maximum parsimony, NJ - neighbor-joining, PP - posterior probability, RPB1 - RNA polymerase II largest subunit, RT-PCR - reverse-transcriptase PCR, SSU - small subunit.

INTRODUCTION

Gromia oviformis is a common marine rhizopod characterized by a large ovoid membraneous test and filose pseudopodia. Morphologically, the species is very similar to some monothalamous allogromiid foraminifers, among which it was initially classified (see review in Cifelli 1990). Detailed light microscopic studies of *Gromia* revealed, however, the non-granular, filose character of its pseudopodia and prompted de Saedeleer (1934) to transfer this genus to the order Filosea. Further electron microscopic observations revealed other distinctive features that distinguished *Gromia* from allogromiid Foraminifera, such as the presence of honeycomb-like membranes on the inner aspect of the wall (Hedley and

Address for correspondence: Jan Pawlowski, Department of Zoology and Animal Biology, University of Geneva, Sciences III, 30, Quai Ernest-Ansermet, CH-1211 Genève 4, Switzerland; Fax: + 41 22 379 67 95; E-mail: Jan.Pawlowski@zoo.unige.ch

Bertaud 1962). Nevertheless, the gross morphological similarities between gromiid and allogromiid tests led to taxonomic confusion (Hedley 1958) and left uncertain the taxonomic status of some *Gromia*-like foraminifers, such as *Allogromia marina* (Nyholm and Gertz 1973). In some recent protozoan classifications, the genus *Gromia* was included among amoebae of uncertain affinity (Patterson *et al.* 2000).

The first molecular phylogenetic study of *G. oviformis*, based on SSU rRNA gene sequences, suggested that the species belongs to the supergroup Cercozoa (Burki *et al.* 2002). The Cercozoa comprises a heterogeneous assemblage of filose testate amoebae (Testaceafilosia), cercomonads, amoeboflagellates, chlorarachniophyte algae, as well as certain protistan parasites of plants (plasmodiophorids) and invertebrates (Haplosporidia) (Bhattacharya *et al.* 1995; Cavalier-Smith and Chao 1996/7, 2003a; Bulman *et al.* 2001; Wylezich *et al.* 2002). In a recent classification of Cercozoa based on SSU rRNA analysis, the genus *Gromia* was included in the class Gromiidea within the subphylum Endomyxea (Cavalier-Smith and Chao 2003b). These authors further showed that the Filosea *sensu* de Saedeleer (1934) are polyphyletic and evolved three times separately within the Cercozoa.

Phylogenetic analyses of actin-coding genes suggested that Foraminifera are also related to Cercozoa (Keeling 2001). This affinity was subsequently confirmed by the discovery of shared one or two amino-acid inserts at the monomer-monomer junction of polyubiquitin proteins (Archibald *et al.* 2003), and by phylogenetic analysis of sequences of the largest subunit of the RNA polymerase II (RPB1) (Longet *et al.* 2003). Revised analysis of the SSU rRNA revealed that Foraminifera branch together with *G. oviformis* as a sister group of Cercozoa (Berney and Pawlowski 2003). Recently, Archibald and Keeling (2004) showed that the Plasmodiophorida, a group of intracellular parasites of plants, weakly branch as sister to Foraminifera in actin phylogenies, suggesting a possible close evolutionary relation between both groups.

To further test the phylogenetic relationship between *Gromia* and Foraminifera, we obtained the sequences of actin and polyubiquitin genes from *Gromia* sp. and *G. oviformis*, and compared them to corresponding sequences of Foraminifera and other eukaryotes. We also re-analysed the RPB1 and the SSU rRNA gene sequences of *Gromia*. Independent analyses of these four molecular markers suggest that *Gromia* is closely related to Foraminifera, although the solid establishment of its phylogenetic position will require analysis of protein-coding genes from a broader sampling of Cercozoa.

MATERIALS AND METHODS

Specimen collection and nucleic acids extractions. Several specimens of *Gromia oviformis* living on *Corallina mediterrannea* were collected in September 2003 near Marseilles (France). After transfer to the laboratory, healthy specimens were isolated, cleaned and individually conserved in small volumes of sterile seawater. Daily observations showed that certain specimens presented characteristic cytological modifications of individuals undergoing gametogenesis as described by Arnold (1966). DNA was extracted from these gametogenetic individuals prior to gametes release with the DNeasy Plant Mini Kit (Quiagen) using a single cell per extraction.

Additionally, total RNA was extracted from one hundred *Gromia* sp. specimens collected at Svalbard during the cruise of RV Jan Mayen, in July 2001. The specimens were individually cleaned with a paintbrush and rinsed in several bath of sterile seawater prior to RNA extraction using Tri-Reagent (Molecular Research Inc.) (Chomczynski and Sacchi 1987).

Isolation of actin and polyubiquitin genes. All PCR amplifications were carried out under standard amplification protocol, and purified, cloned and sequenced in both directions as described previously (Pawlowski *et al.* 1999). The actin gene of *Gromia oviformis* was amplified from genomic DNA using the forward 5'-GGT GAY GAY GCN CCA MGA GC-3' and reverse 5'-GGW CCD GAT TCA TCR TAY TC-3' primers pair. Multiple (5) independent clones were sequenced and no variability was observed. Under the canonical GT-AG splicing sites assumption, three introns of 346, 304 and 447 base pairs were identified and removed to obtain a 1032 base pairs actin open reading frame.

The actin gene of *Gromia* sp. was also obtained from a total RNA extract by RT-PCR. This procedure allows discriminating deviant actin paralogs or pseudogenes from more slowly evolving actins and relies on the assumption that transcribed gene copies are less likely to represent deviant paralogs that gene sequences amplified directly from genomic DNA. RT-PCR was carried out with the forward 5'-AAC TGG GAY GAY ATG GA-3' and reverse 5'- RTA YTT ICK YTC IGG IGG IGC-3' primers pair and the 3' end of the molecule was obtained by 3' RACE using the 5'/3' RACE kit (Roche). The length of the obtained *Gromia* sp. actin gene sequence is of 894 base pairs.

A fragment of polyubiquitin gene of *G. oviformis* encompassing one and a half ubiquitin monomers was amplified from genomic DNA following Archibald *et al.* (2003), and cloned and sequenced as described above. An intron of 318 base pairs was identified in the ubiquitin monomer of *G. oviformis*. Removal of this intron, assuming canonical GT-AG splicing sites, yielded an ubiquitin monomer consisting of a 231 base pairs uninterrupted open reading frame. The sequences of *Gromia*'s RPB1 and SSU rRNA genes were obtained as described elsewhere (Burki *et al.* 2002, Longet *et al.* 2003).

The nucleotide sequences have been submited to the GenBank under accession numbers: AY571669-AY571670.

Protein phylogenies. Actin sequences of *Gromia oviformis* and *Gromia* sp. and their homologs representing major eukaryotic groups were aligned using Clustal X (Thompson *et al.* 1994) and further adjusted by eye. The actin alignment used consists of 59 sequences and 227 unambiguously aligned amino acid positions, and includes the recently reported actin sequences of the cercozoan-related Polycystinea (Nikolaev *et al.* 2004). The RPB1 alignment was composed of 36 taxa, representing all eukaryotic RPB1 sequences available in GenBank, and 283 unambiguously aligned amino acid positions. Both proteins were analysed identically using distance and maximum likelihood methods. To accommodate rate variations among sites, maximum likelihood distances were computed under the JTT substitution model, assuming a gamma distribution with eight rate categories plus invariable sites, using TREE-PUZZLE 5 (Strimmer and von Haeseler 1996). Fitch-Margoliash distance trees were constructed from these gamma-corrected distances with FITCH 3.6a3 (Felsenstein 1993) using the global rearrangements option. Bootstrap analyses (100 replicates) was carried out for this method with SEQBOOT 3.6a3 (Felsenstein 1993) followed by PUZZLEBOOT (www.tree-puzzle.de) under the JTT substitution matrix with the alpha parameter and proportion of invariable sites calculated by TREE-PUZZLE 5 as explained above. Maximum likelihood trees were inferred with ProML 3.6a3 (Felsenstein 1993) using the JTT substitution matrix and the global rearrangements option. Rate variations among sites were modelled with the -R option and nine categories corresponding to eight rate categories plus invariable sites with rates and their frequencies estimated with TREE-PUZZLE 5 as above. Bootstrap analyses were not performed for the maximum likelihood method due to computational limitations. In the case of actin, we further performed a Bayesian analysis using Mr Bayes 3.0B4, using a gamma distribution and 1500000 generations, with all necessary parameters estimated by the program.

SSU rRNA phylogeny. The SSU rRNA sequences were manually aligned using the Genetic Data Environment software (Larsen *et al.* 1993), following secondary structure models (Neefs *et al.* 1993, Wuyts *et al.* 2000). The sequences were selected so that major taxonomic groups of eukaryotes were represented, using an extensive sampling for Cercozoa. A total of 1115 unambiguously aligned positions were used. Evolutionary trees were inferred using the maximum likelihood (ML) method (Felsenstein 1981), the neighbour-joining (NJ) method (Saitou and Nei 1987), and the maximum parsimony (MP) method, using PAUP* (Swofford 1998). The reliability of internal branches was assessed using the bootstrap method (Felsenstein 1985), with 100, 500, and 1000 bootstrap replicates for ML, MP, and NJ analyses, respectively. ML analyses were performed with the GTR model of substitution (Lanave *et al.* 1984, Rodriguez *et al.* 1990), taking into account a proportion of invariable sites (15.92%), and a gamma-shaped distribution of the rates of substitution among variable sites, with 8 rate categories (alpha = 0.4115). All necessary parameters were estimated from the data using MODELTEST (Posada and Crandall 1998). Starting trees of ML searches were obtained via NJ and swapped with the tree-bisection-reconnection algorithm. NJ analyses were performed with ML-corrected distances using the same parameters. The most parsimonious trees for each MP bootstrap replicate were determined using a heuristic search procedure with 10 random-addition-sequence replicates and tree-bisection-reconnection branch-swapping. The transversion cost was set to twice the transition cost.

RESULTS

The actin phylogeny shows that the two *Gromia* sequences branch with one of the two foraminiferan actin paralog (type 1), while the second foraminiferan actin paralog (type 2) branches with Polycystinea (Fig. 1). This topology is congruently inferred in ML and Bayesian analyses. The distance methods support a relationship between *Gromia* and Plasmodiophorida (56% BV) and weakly recover the monophyly of two foraminiferan paralog (data not shown). A clade comprising *Gromia*, Foraminifera, Plasmodiophorida, and Polycystinea is observed in all analyses (24% BV, 0.99 PP), which support also its relation to Core Cercozoa (29% BV, 0.97 PP). Within this clade, Chlorarachniophyta and cercomonads form two basal lineages in ML and Bayesian trees but are sister groups in distance analysis. Most of the other well-recognised eukaryotic groups were recovered by actin phylogeny.

The RPB1 phylogeny placed *Gromia* sp. as a sister group of Foraminifera (Fig. 2). *Gromia* sp. and Foraminifera formed a clade supported by 75% BV, while their grouping with other Cercozoa was supported by 84% BV. The monophyly of cercomonads and chlorarachniophytes observed in ML trees (Fig. 2) was not confirmed by distance analysis where the clade represented by *Gromia* sp. and Foraminifera branched within the Cercozoa (data not shown). Compared to the consensus eukaryote phylogeny, the RPB1 sequence analysis supported most of the well established eukaryotic groups, but failed to recover the monophyly of Opisthokonts (animals, fungi and choanoflagellates) and placed a heterokont *Ochromonas* among the Alveolata.

The SSU rRNA analyses confirmed the close relation between the two *Gromia* sequences and Foraminifera, but included a group of parasitic Haplosporidia into this clade (Fig. 3). In our ML and MP analyses, the Haplosporidia branched as a sister group of Foraminifera, although with a relatively low BV (56%, 64% in ML and MP, respectively). The NJ analysis showed the monophyly of *Gromia* and Foraminifera to the exclusion of Haplosporidia but this topology was supported by a BV lower than 50%. These three groups formed a relatively well supported clade (58%, 75%, 71% BV in ML, NJ, MP trees, respectively). The Plasmodiophorida appeared next to this clade as a sister group of Core Cercozoa. All remaining cercozoan sequences clustered together in a strongly supported (92%, 83%, 93% BV in ML, NJ, MP, respectively) monophyletic group. This

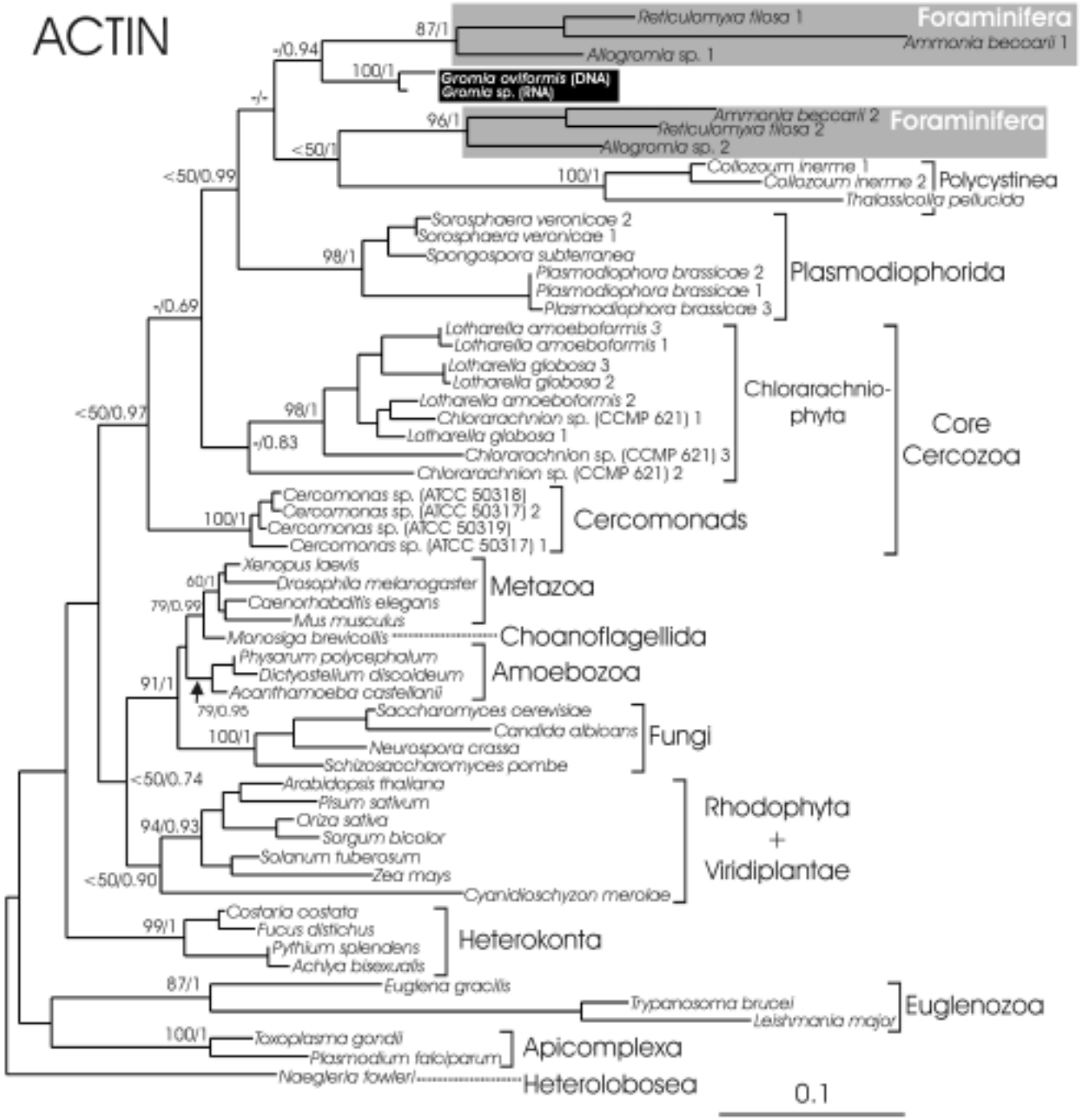

Fig. 1. Phylogenetic position of *Gromia* based on ML analysis of actin gene sequences. Values at nodes indicate bootstrap supports greater than 50% (left) calculated for a tree inferred with the Fitch-Margoliash distance method (see text) and posterior probability (right). Important nodes supported by less than 50% bootstrap valued are indicated by <50%. Except for the two foraminiferan actin families, the bootstrap supports for relations within major eukaryotic groups are omitted for clarity. For *Gromia*, the type of nucleic acid used to isolate actin sequences is indicated in brackets. Single digit numbers at the extreme right of Foraminifera, Polycystinea, Plasmodiophorida, Chlorarachniophyta, and Cercomonads species correspond to different actin gene homologs known. The scale bar represents 0.1 substitutions per site.

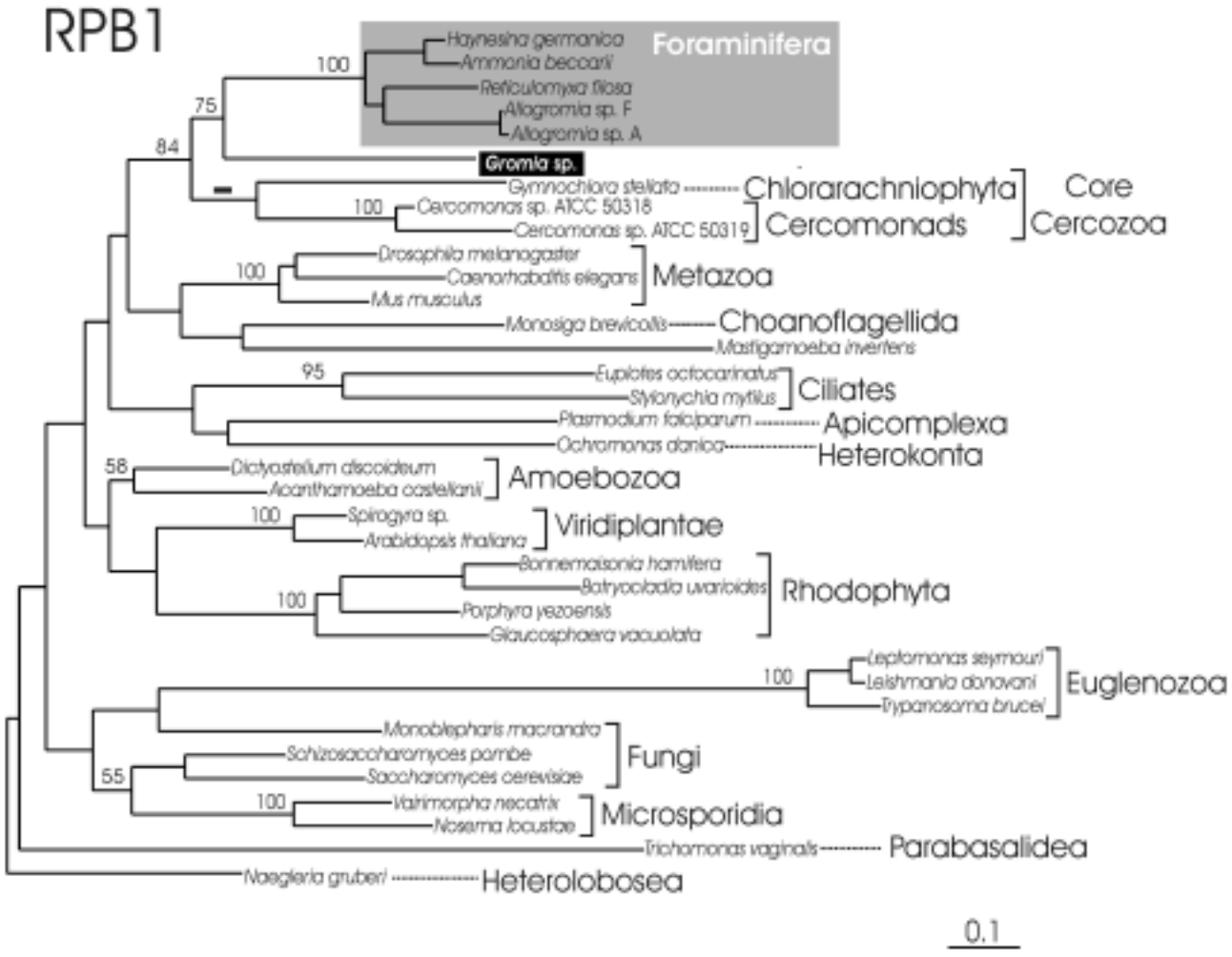

Fig. 2. Phylogenetic position of *Gromia* based on ML analysis of RPB1 sequences. Values at nodes indicate bootstrap supports greater than 50% calculated for a tree inferred with the Fitch-Margoliash distance method (see text). The bootstrap supports for relations within major eukaryotic groups are omitted for clarity. A dash on the branch leading to Core Cercozoa indicates that the topology shown is not supported in the Fitch-Margoliash distance method. The scale bar represents 0.1 substitutions per site.

clade included the chlorarachniophytes, the cercomonads, and the Euglyphida, along with the agglutinated testate amoeba *Pseudodifflugia*, the undefined filose "Nuclearia-like" strain N-por, *Massisteria*, *Cryothecomonas*, and *Thaumatomonas*. The grouping of this clade with Foraminifera, *Gromia*, Haplosporidia and Plasmodiophorida was supported by BV of 67%, 80% and 71% in ML, NJ and MP analyses, respectively. The general topology of our SSU trees was congruent with previous large-scale SSU rRNA phylogenies of eukaryotes, and all well recognised high-level taxa, including plants, red algae, alveolates, heterokonts, amoebae, animals and fungi were recovered with good statistical support.

Finally, sequencing of the monomer-monomer junction of the polyubiquitin gene of *G. oviformis* showed it being characterized by a single serine insertion. Similar insertions of one or two amino acids are observed in all Foraminifera and Cercozoa but not in any other eukaryotes (Fig. 4).

DISCUSSION

Phylogenetic analyses of three molecular markers (actin, RPB1 and SSU rRNA) support the close evolutionary relationship between *Gromia* and Foraminifera.

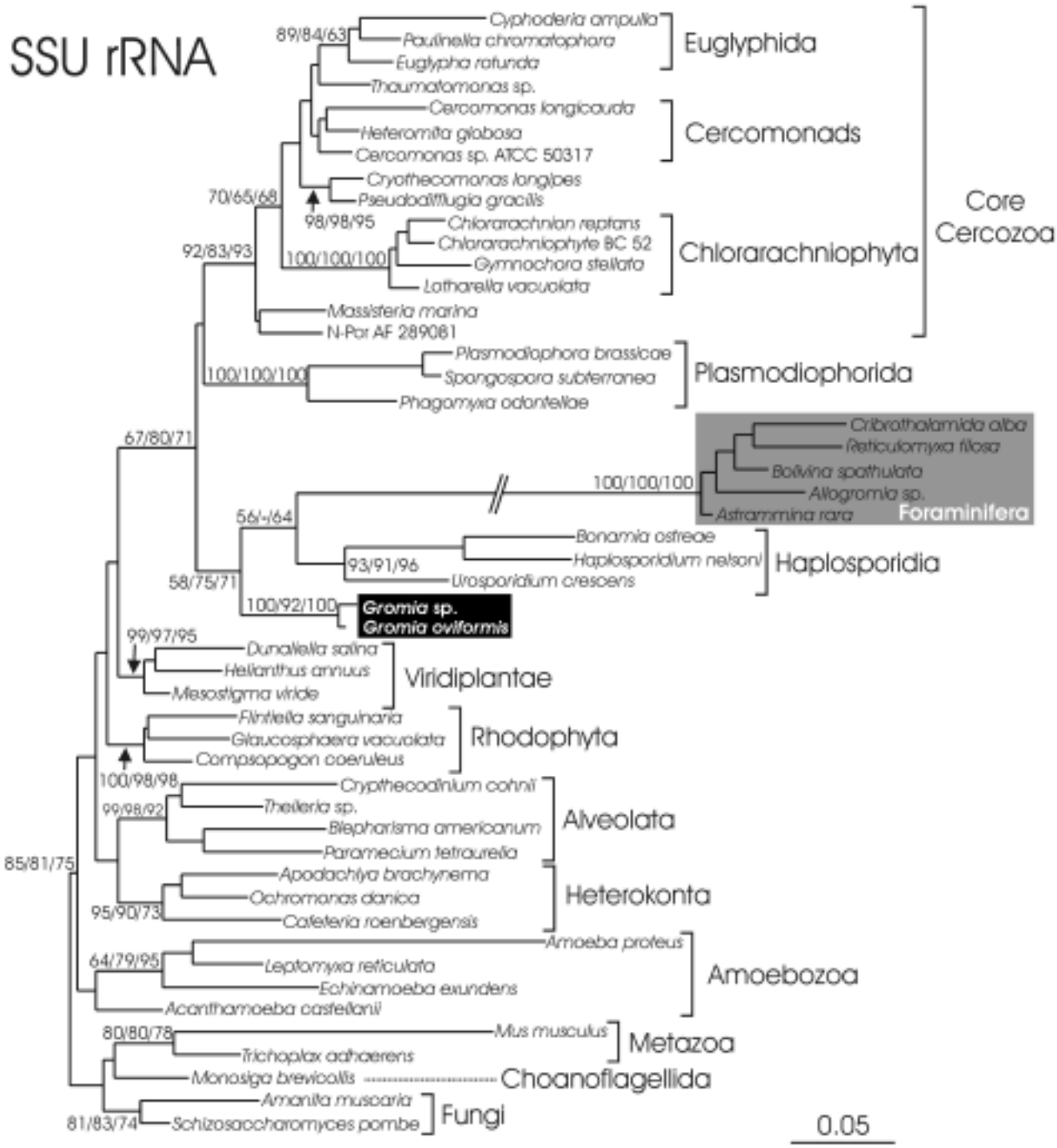

Fig. 3. Phylogenetic position of *Gromia* based on ML analysis of SSU rRNA sequences. Values at nodes indicate bootstrap supports greater than 50% calculated for the ML, NJ, and MP method, respectively. Except for Core Cercozoa, the bootstrap supports for relations within major eukaryotic groups are omitted for clarity. The branch leading to Foraminifera is not drawn to scale. The scale bar represents 0.05 substitutions per site.

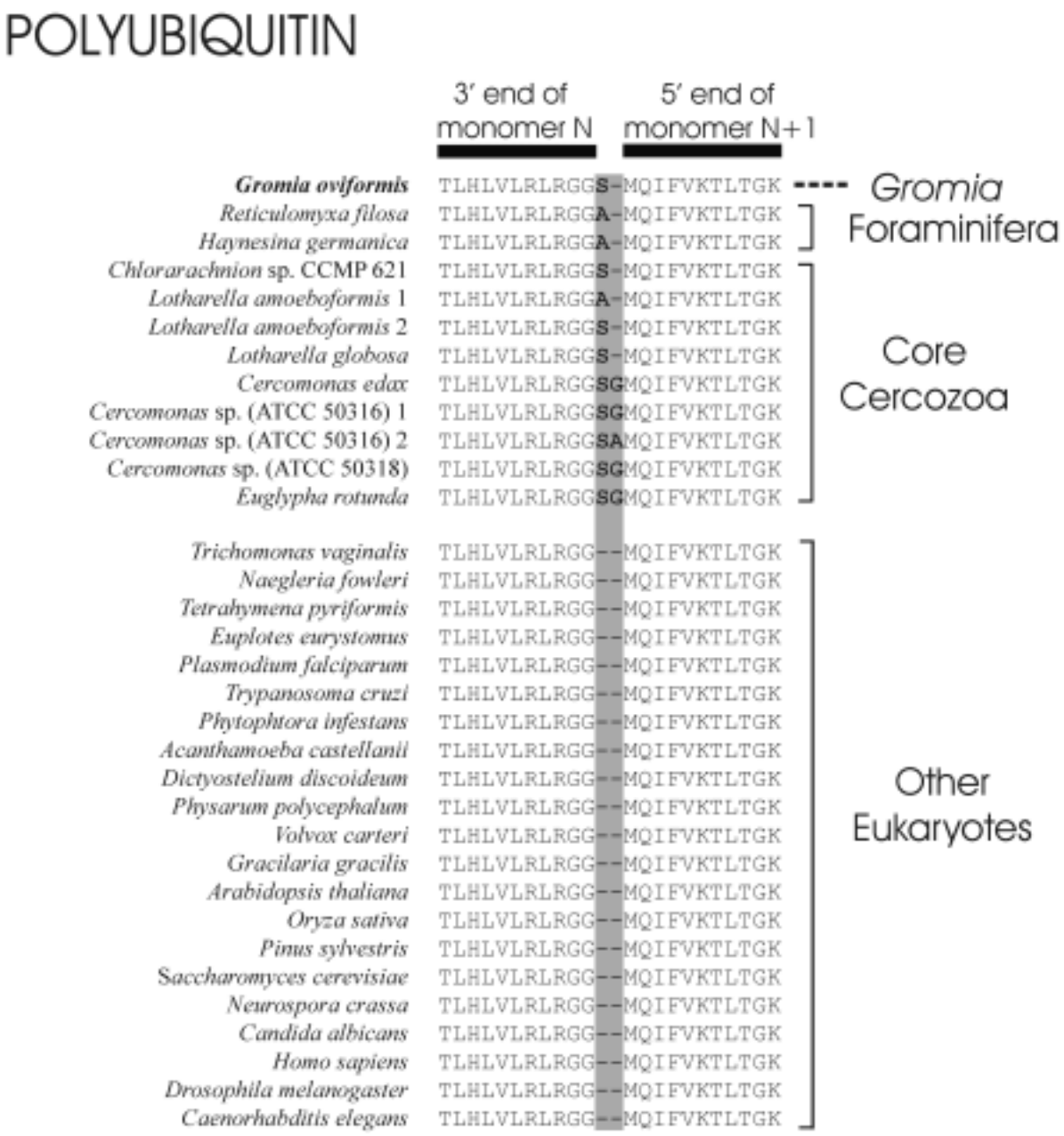

Fig. 4. Junction between two ubiquitin monomers in the polyubiquitin gene of *Gromia oviformis*, Foraminifera, Core Cercozoa and other eukaryotes. Single or double amino acid insertions are observed in *Gromia*, Foraminifera, and Cercozoa. Single digit numbers at the extreme right of chlorarachniophytes and cercomonads species correspond to different polyubiquitin gene homologs known.

However, each gene gives a slightly different image of this association.

The actin phylogeny shows two *Gromia* sequences as members of a clade comprising Foraminifera, Polycystinea, and Plasmodiophorida. Within this clade, both ML and Bayesian methods support the grouping of *Gromia* with the foraminiferan actin type 1 (Fig. 1). Polycystine radiolarians consistently branch with the type 2 and none of our analyses recovered the monophyly of the two foraminiferan paralogs, which was observed in earlier actin phylogenies (Pawlowski *et al*. 1999, Keeling 2001). The independent branching of the two foraminiferan actin paralogs in our trees likely results from discrepancies in their evolutionary rates. Indeed, a large taxonomic sampling of foraminiferan actin genes indicate higher evolutionary rates in type 2

compared to type 1 (unpublished data). Therefore, the grouping of the faster evolving type 2 with the fast-evolving polycystines can reasonably be regarded as a long branch attraction artefact.

Our study confirms the sister group relation between *Gromia* and Foraminifera suggested by earlier analysis of RPB1 gene sequences (Longet *et al.* 2003). Their close relationships are also indicated by analysis of SSU rRNA gene sequences, however, in this case Foraminifera appear more closely related to Haplosporidia than to *Gromia* (Fig. 3). The phylogenetic position of Haplosporidia as a sister group to Foraminifera in SSU trees is surprising since Haplosporidia, which are parasites of freshwater and marine invertebrates that form multinucleate plasmodia in host tissues and reproduce by spores (Perkins 2000), share no morphological features with Foraminifera. This can be explained by extreme simplification of haplosporidian cells adapted to the parasitic mode of life. Alternatively, the close relationships between both groups can be biased by the long branch attraction (LBA) phenomenon, which is very common in rRNA phylogenies (Philippe and Adoutte 1998). Close relationship between *Gromia* and Haplosporidia was earlier suggested by Cavalier-Smith and Chao (2003b), however, in the analyses performed by these authors, Foraminifera cluster with the Polycystinea, which constitutes another example of LBA phenomenon. Remarkably, in Bayesian analyses, which are much less sensitive to substitution rates heterogeneity, Foraminifera branch together with Haplosporidia and *Gromia*, while Polycystinea and other radiolarians form a separate clade (Nikolaev *et al*. 2004).

The principal difficulty in establishing the relations between *Gromia*, Foraminifera, Haplosporidia and other Cercozoa is a lack of broad taxonomic sampling of protein-coding genes. Further analyses of actin and RPB1 genes of Haplosporidia will be necessary to test their grouping with Foraminifera. Increased taxonomic sampling will also allow protein phylogenies to be constructed from concatenated datasets. Such approaches already proved successful in providing better resolution than single gene phylogenies both between and within major eukaryotic groups (e.g. Baldauf *et al.* 2000, Simpson and Rogers 2004). A generally congruent topology of actin and RPB1 trees suggests that both genes are good candidates for future concatenated phylogenies to be inferred.

The positioning of *Gromia* close to the Foraminifera in molecular phylogenies is congruent with several similarities between these organisms that go far beyond the superficial resemblance of gross test morphology and oral apparatus (Hedley and Bertaud 1962). The presence of similar laminated structures in the test wall of the single-chambered foraminifer *Allogromia laticollaris* and *Gromia oviformis* prompted Arnold (1982) to consider both species as an "isomorphic pair". Arnold (1982) also noticed the possibility of fundamental resemblance between shell formation *in G. oviformis* and the proloculus of many polythalamous Foraminifera. Moreover, *Gromia* and Foraminifera share a similar mode of life and resemble each other in having a complex life cycle with asexual and sexual phases. Arnold (1966) observed gametogenesis, fertilisation and production of amoeboid zygotes in plastogamic pairs of adult specimens of *G. oviformis* - a mode of reproduction that is strikingly reminiscent of that of some Foraminifera (Lee *et al.* 1992).

If the close relationship between *Gromia* and Foraminifera is confirmed by further phylogenetic studies, *Gromia* will become a key organism for understanding the origin of Foraminifera. It will be of great interest to compare more thoroughly the ultrastructure and the motility of their pseudopodia. Although *Gromia*'s pseudopodia are non-granular, they do anastomose and can form reticulate structures (Hedley 1962). They seem to move much slower than foraminiferan reticulopodia, but it is uncertain whether the movement is bidirectional or not (Bowser, personal comm.). The mechanisms responsible for the movement of *Gromia*'s pseudopodia are poorly known. More extensive studies of *Gromia*'s actin and tubulin genes may shed new light on genetic factors responsible for the evolution of foraminiferan granuloreticulopodia, and thus may lead to a better understanding of the exceptional success of this group.

Acknowledgements. The authors thank Sam Bowser and Tomas Cedhagen for comments on the manuscript. *Gromia* sp. was collected during the cruise of the RV *Jan Mayen*, funded by the University of Tromsø and by grants from the research Council of Norway (141050/730 to MH). This work was supported by the Swiss National Science Foundation grant 3100A0-100415.

REFERENCES

Archibald J. M., Keeling P. J. (2004) Actin and ubiquitin protein sequences support a cercozoan/foraminiferan ancestry for the plasmodiophorid plant pathogens. *J. Eukaryot. Microbiol.* **51:** 113-118

Archibald J. M., Longet D., Pawlowski J., Keeling P. J. (2003) A novel polyubiquitin structure in Cercozoa and Foraminifera:

evidence for a new eukaryotic supergroup. *Mol. Biol. Evol.* **20:** 62-66
Arnold Z. M. (1966) Observation on the sexual generation of *Gromia oviformis* Dujardin. *J. Protozool.* **13:** 23-27
Arnold Z. M. (1982) Shell-wall lamination in *Gromia oviformis* Dujardin. *J. Foraminiferal Res.* **12:** 298-316
Baldauf S. L., Roger A. J., Wenk-Siefert I., Doolittle W. F. (2000). A kingdom-level phylogeny of eukaryotes based on combined protein data. *Science* **290:** 972-977
Bhattacharya D., Helmchen T., Melkonian M. (1995) Molecular evolutionary analyses of nuclear-encoded small subunit ribosomal RNA indentify an independent Rhizopod lineage containing the Euglyphida and the Chlorarachniophyta. *J. Eukaryot. Microbiol.* **42:** 65-69
Berney C., Pawlowski J. (2003) Revised small subunit rRNA analysis provides further evidence that Foraminifera are related to Cercozoa. *J. Mol. Evol.* **57 (Suppl. 1):** 120-127
Bulman S. R., Kühn S. F., Marshall J. W., Schnepf E. (2001) A phylogenetic analysis of the SSU rDNA from members of the Plasmodiophorida and Phagomyxea. *Protist* **152:** 43-51
Burki F., Berney C., Pawlowski J. (2002) Phylogenetic position of *Gromia oviformis* inferred from nuclear-encoded small subunit ribosomal RNA. *Protist* **153:** 251-260
Cavalier-Smith T., Chao E. E. (1996/7) Sarcomonad phylogeny and the origin of euglyphid amoebae. *Arch. Protistenkd.* **147:** 227-236
Cavalier-Smith T., Chao E. E. (2003a) Phylogeny of Choanozoa, Apusozoa, and other Protozoa and early eukaryote megaevolution. *J. Mol. Evol.* **56:** 540-563
Cavalier-Smith T., Chao E. E. (2003b) Phylogeny and classification of phylum Cercozoa (Protozoa). *Protist* **154:** 341-358
Chomczynski P., Sacchi N. (1987) Single-step method of RNA isolation by guanidinium thiocyanate-phenol-chloroform extraction. *Anal. Biochem.* **162:** 156-159
Cifelli R. (1990) A history of the classification of Foraminifera (1826-1933). *Cushman Found. for Foraminiferal Res.* **Spec. Publ. 27:** 1-88
de Saedeleer H. (1934) Beitrag zur Kenntnis der Rhizopoden: morphologische und systematische Untersuchungen und eine Klassifikationsversuch. *Mém. Mus. Roy. d'Hist. Nat. Belgique* **60:** 1-112
Felsenstein J. (1981) Evolutionary trees from DNA sequences: a maximum likelihood approach. *J. Mol. Evol.* **17:** 368-376
Felsenstein J. (1985) Confidence limits on phylogenies: an approach using the bootstrap. *Evolution* **39:** 783-791
Felsenstein J. (1993) PHYLIP (Phylogeny Inference Package) J. Felsenstein, University of Washington, Seattle
Hedley R. H. (1958) Confusion between *Gromia oviformis* and *Allogromia ovoidea*. *Nature* **182:** 1391-1392
Hedley R. H. (1962) *Gromia oviformis* (Rhizopodea) from New Zealand with comments on the fossil chitinozoa. *N. Z. J. Sci.* **5:** 121-136
Hedley R. H., Bertaud W. S. (1962) Electron-microscopic observations of *Gromia oviformis* (Sarcodina). *J. Protozool.* **9:** 79-87
Keeling P. J. (2001) Foraminifera and Cercozoa are related in actin phylogeny: two orphans find a home? *Mol Biol. Evol*. **18:** 1551-1557
Lanave C., Preparata G., Saccone C., Serio G. (1984) A new method for calculating evolutionary substitution rates. *J. Mol. Evol.* **20:** 86-93
Larsen N., Olsen G. J., Maidak B. L., McCaughey M. J., Overbeek R., Macke T. J., Marsh T. L., Woese C. R. (1993) The ribosomal database project. *Nucleic Acids Res.* **21:** 3021-3023
Lee J. J., Faber W. W. Jr., Anderson R.O., Pawlowski, J. (1992) Life cycles of Foraminifera. In: Biology of Foraminifera (Eds J. J. Lee, Anderson R. O.). Academic Press, 285-334
Longet D., Archibald J. M., Keeling P. J., Pawlowski J (2003) Foraminifera and Cercozoa share a common origin according to RNA polymerase II phylogenies. *Int. J. Syst. Evol. Microbiol.* **53:** 1735-1739
Neef J. M., van de Peer Y., de Rijk P., Chapelle S., de Wachter R. (1993) Compilation of small ribosomal subunit structures. *Nucleic Acids Res.* **21:** 3025-3049
Nikolaev S. I., Berney C., Fahrni J. F., Bolivar I., Polet S., Mylnikov A. P., Aleshin V. V., Petrov N. B., Pawlowski J. (2004). The twilight of Heliozoa and rise of Rhizaria, an emerging supergroup of amoeboid eukaryotes. *Proc. Natl. Acad. Sci. USA* **101:** 8066-8071
Nyholm K.-G., Gertz I. (1973) To the biology of the monothalamous foraminifer *Allogromia marina* n. sp. *Zoon* **1:** 89-93
Patterson D. J., Simpson A. G. B., Rogerson A. (2000) Amoebae of uncertain affinities. In: An Illustrated Guide to the Protozoa (Eds J. J. Lee, G. F. Leedale, P. Bradbury). 2 ed., Society of Protozoologists, Lawrence, KS, 804-827
Pawlowski J., Bolivar I., Fahrni J. F., de Vargas C., Bowser S. S. (1999) Molecular evidence that *Reticulomyxa filosa* is a freshwater naked foraminifer. *J. Eukaryot. Microbiol.* **46:** 612-617
Perkins, F.O. (2000) Phylum Haplosporidia. In: An Illustrated Guide to the Protozoa (Eds J. J. Lee, G. F. Leedale, P. Bradbury). 2 ed., Society of Protozoologists, Lawrence, KS, 1328-1341
Philippe H., Adoutte A. (1998) The molecular phylogeny of eukaryotes: solid facts and uncertainties. In: Evolutionary Relationships among Protozoa. (Eds H. Coombs, K. Vickerman, M. A. Sleigh, A. Warren). Chapman and Hall, London, 25-56
Posada D., Crandall K. A. (1998) Modeltest: testing the model of DNA substitution. *Bioinformatics* **14:** 817-818
Rodrigez R., Olivier J. L., Marin A., Medina J. R. (1990) The general stochastic model of nucleotide substitution. *J. Theor. Biol.* **142:** 485-501
Saitou N., Nei M. (1987) The neighbor-joining method: a new method for reconstructing phylogenetic trees. *Mol. Biol. Evol.* **4:** 406-425
Simspson A. G., Roger A. J. (2004) Protein phylogenies robustly resolve the deep-level relationships within Euglenozoa. *Mol. Phylogenet. Evol.* **30:** 201-212
Strimmer K., von Haeseler A. (1996) Quartet puzzling: a quartet maximum-likelihood method for reconstructing tree topologies. *Mol. Biol. Evol.* **13:** 964-969
Swofford D. L. (1998) PAUP*: phylogenetic analyses using parsimony (*and other methods). Sinauer Associates, Sunderland, MA
Thompson J. D., Higgens D. G., Gibson T. J. (1994) CLUSTAL W: improving the sensitivity of progressive multiple sequence alignment through sequence weighting, position-pecific gap penalities and weight matrix choice. *Nucleic Acids Res.* **22:** 4673-4680
Wuyts J., de Rijk P., van de Peer Y., Pison G., Rousseeuw P., de Wachter R. (2000) Comparative analysis of more than 3000 sequences reveals the existence of two pseudoknots in area V4 of eukaryotic small subunit ribosomal RNA. *Nucleic Acids Res.* **28:** 4698-4708
Wylezich C., Meisterfeld R., Meisterfeld S., Schlegel M. (2002) Phylogenetic analyses of small subunit ribosomal RNA coding regions reveal a monophyletic lineage of euglyphid testate amoebae (Order Euglyphida). *J. Eukaryot. Microbiol.* **49:**108-118

Received on 22nd March, 2004; revised version on 25th June, 2004; accepted on 14th July, 2004

Acta Protozool. (2004) 43: 313 - 328

ACTA
PROTOZOOLOGICA

Considerations on the Systematic Position of *Uronychia* and Related Euplotids Based on the Data of Ontogeny and 18S rRNA Gene Sequence Analyses, with Morphogenetic Redescription of *Uronychia setigera* Calkins, 1902 (Ciliophora: Euplotida)

Weibo SONG[1], Norbert WILBERT[2], Zigui CHEN[1] and Xinlu SHI[3]

[1]Laboratory of Protozoology, KLM, Ocean University of China, Qingdao, China; [2]Institut für Molekulare Physiologie und Entwicklungsbiologie, Universität Bonn, Bonn, Germany; [3]Biological Department of the Hangzhou Normal University, Hangzhou, China

Summary. Characteristics found in morphogenetic process of the *Uronychia setigera* Calkins, 1902 during binary division and the molecular data of several euplotid genera inferred from 18S rRNA gene sequence analyses are compared and discussed. The results indicate that the traditional order Euplotida might comprise 3 paraphyletic groups: the eueuplotids, i.e. euplotids with a 5-cirral anlagen mode and a subcortical origin of the oral primordium during morphogenesis (we call them the "typical" euplotids in the text), gastrocirrhids (the pseudoeuplotids) and discocephalids, the last of which is possibly a convergent lineage. The results suggest also that *Uronychia* represents a primitive type within typical euplotids in phylogeny. Based on these analyses, a conclusion is suggested which consists of essentially the following points: (1) The traditional euplotids are likely a paraphyletic assemblage with differently originated groups. As a suggestion based on the new definition, the euplotids *s. l.* contains at least 2 subgroups: the eueuplotids and the sister group, gastrocirrhids (pseudoeuplotids) with multi-anlagen mode which is a divergent or apomorphic feature. (2) The systematic position of discocephaline remains unclear, but possibly an intermediate group between the euplotids *s. str.* and stichotrichs. We agree, however, that it is presently placed within the order Euplotida, as an outer group of other two assemblages. (3) The morphogenetic feature of 5-cirral-anlagen-mode is highly conservative and should be hence weighted with more phylogenetic value(s) in systematic analysis. (4) We suppose that some features like the origin mode of the leftmost frontal (formed from the UM-anlage), the situation of undulating membranes (e.g. two in number, curved in appearance) represent apomorphic features, and should not be over-evaluated, which caused often the diverse structures of the phylogenetic trees. (5) Euplotids *s. str.* might be derived from the 5-anlagen ancestor-type of hypotrichs *s. l.*, which is possibly also the ancestor of the current stichotrichs.

Key works: 18S rDNA gene sequences, Ciliophora, euplotids, morphogenesis and phylogeny, *Uronychia setigera.*

INTRODUCTION

Typical euplotid ciliates, as widely accepted for a long time, are regarded as a monophyletic lineage and a sister group with other traditional hypotrichs *s. l.* (or stichotrichs), which contains several well-known taxa, e.g. *Euplotes, Diophrys, Uronychia, Aspidisca, Gastrocirrhus, Discocephalus* (Deroux and Tuffrau 1965, Hartwig 1973, Curds and Wu 1983, Small and Lynn 1985, Song and Wilbert 2000). However, evidence (accumulated recently from molecular investigations) suggests that these ciliates might be a paraphyletic assemblage (Chen and Song 2001, 2002). This result is also partly supported by the interpretation derived from

Address for correspondence: Weibo Song, Laboratory of Protozoology, KLM, Ocean University of China, Qingdao 266003, China; Fax: +86 532 203 2283; E-mail: wsong@ouc.edu.cn

non-molecular phylogenetic analyses, which indicate that the highly specialized *Uronychia* branches very early from the main cluster, and represents possibly a marginalized lineage against other euplotids (Song 1995).

The small *Uronychia* species, *U. setigera* Calkins, 1902, is commonly found in littoral biotopes (Calkins 1902, Kahl 1932, Bullington 1940, Song and Wilbert 1997). Its morphology and infraciliature were recently redefined by Song and Wilbert (1997), albeit it is often confused with its congener, *Uronychia binucleata* (under various names, details see Song and Wilbert 1997). To unravel the phylogenetic position and the systematic relationships of *Uronychia* among related taxa, the 18S rRNA gene data based on several euplotid genera and morphogenetic characteristics revealed in *U. setigera* have been re-examined/re-analyzed and, as a new contribution, more detailed descriptions for this species are presented as well in the current paper.

Thus, our paper has two main aims: (1) we will check again the morphogenetical data obtained in those well-known genera of euplotids to find/question hiatuses which are seemingly ignored in last time; (2) Based on both ontogenetical and DNA sequence data, to address the systematic relationships between/among the taxa which are traditionally arranged in euplotids.

MATERIALS AND METHODS

Morphological and morphogenetical studies

Population of *Uronychia setigera* used for morphogenetic studies was collected from coastal waters near Qingdao (36°08' N; 120°43' E), China. After isolation, pure cultures were kept in the Laboratory of Protozoology, OUC. For molecular work, clonal cultures were established and maintained in sterilized seawater at room temperature with rice grains as food source to enrich bacteria. Cells in division were impregnated using protargol method (Wilbert 1975). Drawings were made with the help of a camera lucida at 1250× magnification. For clarity, parental cirri are shown in diagrams of morphogenetic stages only by outline, whereas new ones are shaded black.

Genomic DNA extraction, PCR amplification, sequencing and phylogenetic analyses

Nine species with original sequence data are concerned in the present studies, which were identified based on both *in vivo* observation and silvered (protargol and silver nitrate methods) specimens. DNA extraction, isolation and PCR reaction were performed as previously described (Chen *et al*. 2002).

Sequences analyzed are accessible at GenBank/EMBL with the following codes: *Aspidisca steini* AF305625 (Chen and Song 2002), *Diophrys appendiculata* AY004773 (Chen and Song 2001), *Euplotidium arenarium* Y19166 (Petroni *et al*. 2000), *Euplotes charon* AF492705 (Chen and Song, unpubl), *E. crassus* AJ310492 (Bernhard *et al*. 2001), *E. eurystomus* AF452707 (Chen and Song, unpubl), *E. magnicirratus* AJ549210 (Petroni *et al*. 2002), *E. minuta* AJ310490 (Bernhard *et al*. 2001), *E. parawoodruffi* AF452708 (Chen and Song, unpubl), *E. rariseta* AF492706 (Chen and Song, unpubl), *E. vannus* AY004772 (Chen and Song 2002), *E. woodruffi* AF492707 (Chen and Song, unpubl), *E. raikovi* AJ305251 (Petroni *et al*. 2002), *Holosticha multistylata* AJ277876 (Shin *et al*. 2000), *Laboea strobila* AF399151 (Snoeyenbos-West *et al*. 2002), *Oxytricha ferruginea* X53486 (Chen and Song, unpubl), *Phacodinium metchnikoffi* AJ277877 (Shin *et al*. 2000), *Protocruzia* sp. AF194409 (Shin *et al*. 2000), *Sterkiella nova* (= *Oxytricha nova*) X03948 (Elwood *et al*. 1985), *Strombidium purpureum* U97112 (Hirt *et al*. unpubl), *Stylonychia lemnae* AJ310497 (Bernhard *et al*. 2001), *Uronychia transfuga* AF260120 (Chen and Song 2001).

The 18S rRNA gene sequences were aligned with a computer assisted procedure, Clustal W (Version 1.80) (Thompson *et al*. 1994), and refined by considering the conservation of both primary and secondary structures (Elwood *et al*. 1985). PHYLIP (Phylogeny Inference Package, Version 3.57) (Felsenstein 1995) was used to calculate the sequence similarity and evolutionary distances between pairs of nucleotide sequences using the Kimura (1980) two-parameter model. Distance-matrix trees were then constructed using the Fitch and Margoliash (1967) least-squares (LS) method and the neighbor-joining (NJ) method (Saitou and Nei 1987). PAUP v4.0b1 was used for the maximum parsimony (MP) analysis (Swofford 1998). Of the 2037 aligned sites, 540 phylogenetically informative characters were used to find the most parsimonious tree using the heuristic search method. Both parsimony and distance data were bootstrap resampled 1,000 times (Felsenstein 1985).

Terminology and systematics

Basically, the terminology and systematics used in the present paper are according to Corliss (1979) and Lynn and Small (2002). However, the higher systematic classification or contents have changed greatly since Corliss' review and are still in argument. Thus we use mainly a vernacular terminology in the text, e.g. stichotrichs, euplotids, hypotrichs or add *sensu lato* (*s. l.*) *stricto* (*s. str.*) to the taxa. Some terms are recalled to avoid possible confusion:

Cirral anlagen. This word is used basically for stichotrichs and euplotids to describe the primordia which will generate late frontoventral transverse cirri, including the undulating membrane anlage (UM-anlage) and streaks which appear ventrally to the right of buccal field. In these primordia, the UM-anlage usually gives rise to one leftmost frontal cirrus. However, this is not the case at least in several euplotids, e.g. *Uronychia*, *Aspidisca* and *Euplotes*, in which the left most cirrus is formed *de novo* either near the UM-anlage (in the opisthe), or completely isolated (in the proter); hence, this term is defined in the present work, only for these 5 streak-like primordia (the UM-anlage is excluded). The cirral anlagen I-V here are equivalent to the anlagen II-VI by some other researchers (i.e., UM-anlage is the No. 1) (Foissner 1996, Eigner 1997, Berger 1999).

Epicortical (opposite to **subcortical**). This term refers to the most common mode of primordia formation in morphogenesis, of which the basal bodies of primordia occur on the cell surface rather than subsurface (beneath the cortex).

Eueuplotids (opposite to **pseudoeuplotids**). This term indicates euplotids with a 5-cirral anlagen mode and subcortical origin of the oral primordium during morphogenesis; it excludes the pseudoeuplotids which do not have such features.

RESULTS

Morphology and infraciliature of *Uronychia setigera* (Figs 1-7, 9-10)

The morphology of living cells is slightly different from that previously described (Song and Wilbert 1997, Chen *et al*. 2003); hence it is only briefly redescribed here.

Newly sampled cells show about the same size, *ca* 50-60 × 40-50 µm *in vivo*, while after culture for weeks their size becomes rather variable; from 50 to maximum 90 µm in length with body shape generally oval (as shown in Fig. 1). Buccal field enormous, extending over 60% of body length. Lateral spur-like protrusions on left margin often less conspicuous in this population than the forms described by Song and Wilbert (1997) and Chen *et al*. (2003) (Fig. 2, arrow). Ventrally 2 concaves in posterior portion of cell, where transverse (TC) and left marginal (MC) cirri insert, whereas on dorsal side, a third depression corresponding position of caudal cirri (Fig. 3, CC). Cytoplasm colourless to greyish, usually comprising many to numerous granules (2-8 µm across). No food vacuoles detected (Fig. 1). Two macronuclear nodules (Ma), connected by funiculus (Figs 2-4). Micronucleus not observed. Movement typical of *Uronychia*: rapidly jumping sideways or backwards, swimming very fast while rotating around its longitudinal axis. During pause, all cirri stiffly spread as shown in Fig. 1.

Structure of adoral zone of membranelles (AZM) genus typical (Figs 2, 3, 6, 7). Invariably 11 adoral membranelles in anterior part (AZM_1); cilia of membranelles about 15 µm long. Posterior part (AZM_2) composed always of 4 membranelles (bases about 10 µm in length; Fig. 7, arrowhead), in which basal bodies are irregularly arranged (not in rows) like those in primordia. One small cirrus-like membranelle (named buccal cirrus here, BC) apart from AZM_2 and inconspicuous, with the base about 3 µm long (Figs 2, 7). Paroral membrane (PM) mighty and surrounding buccal field, with right end near buccal cirrus, often slightly crook-like (Fig. 2); cilia of PM about 30 µm long (Fig. 1).

Somatic ciliature as described before (Song and Wilbert 1997) except the number of basal body pairs in

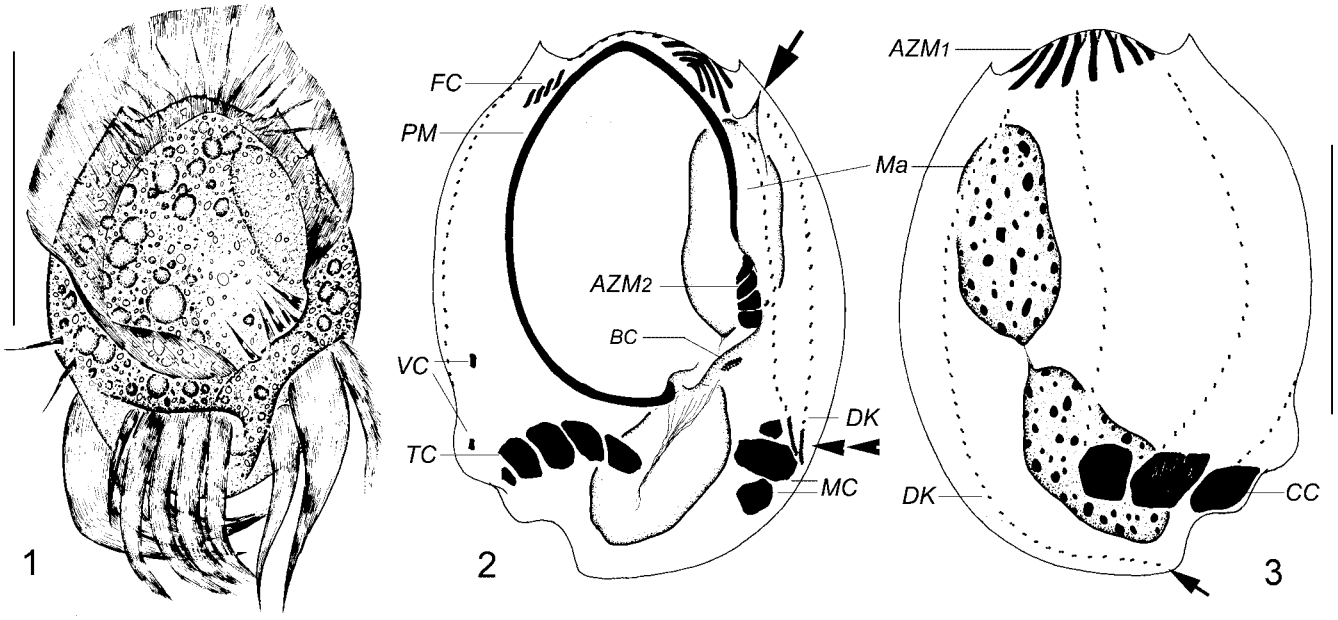

Figs 1-3. *Uronychia setigera in vivo* (**1**) and after protargol impregnation (**2, 3**). **1** - ventral view of a typical individual; **2** - ventral view, to show the general infraciliature; arrow marks the spine which is often lower positioned, whereas double-arrowheads indicate the fragment-like part at the posterior end of the leftmost two dorsal kineties; **3** - dorsal view of the same specimen as in Fig. **2**, to show the dorsal kineties and the nuclear apparatus; arrow marks the 3rd kinety which curves and extends to the posterior margin. $AZM_{1,2}$ - anterior and posterior parts of the adoral zone of membranelles, BC - buccal cirrus, CC - caudal cirri, DK - dorsal kinety, FC - frontal cirri, MC - marginal cirri, Ma - macronuclei, PM - paroral membrane, TC - transverse cirri, VC - ventral cirri. Scale bars - 40 µm.

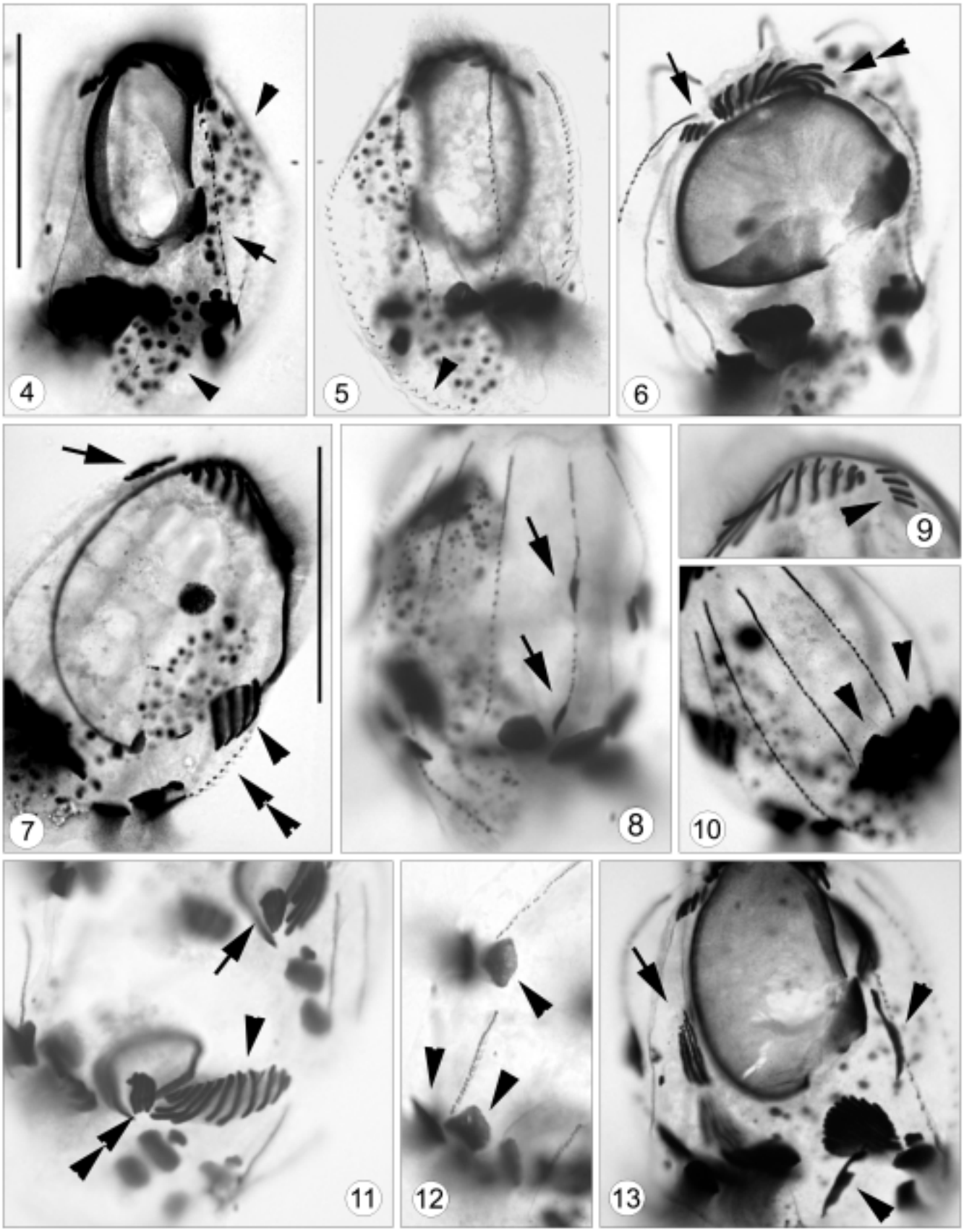
4
5
6
7
8
9
10
11
12
13

the leftmost kinety (Fig. 4, arrow), which is slightly higher than that previously reported (17-25 *vs. ca* 15). Invariably 4 membranelle-like frontal (FC), 2 inconspicuous ventral (VC), 5 strong transverse (TC) and 3 left marginal cirri (MC), while on dorsal side 3 mighty caudal cirri on right margin (Figs 3, 5-7, 9, 10). Totally 6 dorsal kineties, of them 2 to 3 on margin or ventrally positioned, in which basal bodies at the post ends of the leftmost 2 kineties are always densely packed (Fig. 2, double-arrowhead).

Morphogenesis in binary fission (Figs 8, 11-36)

Morphogenesis of *Uronychia* species in binary division was studied by many authors, which repeatedly confirmed that the developmental pattern of cortical structure as well as nuclear apparatus within congeners exhibit extremely similar mode (Dembowska 1926, Taylor 1928, Fauré-Fremiet 1964, Hill 1990, Wilbert 1995, Song 1996). Hence only the important events and some details which were insufficiently described in previous investigations are documented here.

Stomatogenesis. Morphogenesis starts with the appearance of a small patch of kinetosomes, the opisthe's oral primordium (POP), within a subsurface or subcortical pouch positioned between cytostome and left marginal cirri (Fig. 23). Slightly later, the proter's oral primordium (AOP) appears, also subcortically, anterior to the parental AZM_2 (Fig. 24), in this stage, membranelles in the POP begin to align (Fig. 24, double-arrowhead). Both the POP and AOP develop then by rapid proliferation of kinetosomes (Fig. 26), and soon an additional anlage, the primordium for paroral membrane (UM-anlage), appears within the subcortical pouch, which is located opposite to the posterior end of the AOP and POP, respectively (Fig. 28, arrowheads; 30). Subsequently, two groups in the POP, each with 11 and 5 membranelles, and two groups both with 5 membranelles in the AOP are differentiated and finally migrate onto the surface of cell (Figs 11, 14, 15, 17, 32, 34). Meanwhile, the UM-anlage begins to lengthen and then develops along the right edge of each opening pouch, at mid portion of which one short anlage (for the leftmost frontal cirrus) occurs *de novo* in both proter and opisthe (Figs 15; 32, arrowheads). In late stages, two groups of membranelles in both oral primordia are separated, and among them the first one migrates anteriorly. As in its congeners, the first part in the proter will replace the posterior 5 membranelles of AZM_1, while the anterior (parental) 6 are retained (Fig. 35, arrow). In the second group of AZM in both dividers, the most posterior membranelle (the smallest one) moves apart from the other 4 and then to the final position as the "buccal cirrus" (Figs 34, 35).

Development of the somatic ciliature. At about the same time as the oral primordia are formed, basal bodies for FVT-cirral primordia (CA) develop on the cell surface as first 4, and then 5 streaks (anlagen I-V) anterior to the transverse cirri (Figs 19, 23, 24). Clearly no parental ciliary organelles are involved in the formation of these new primordia. Then each of 5 anlagen extends to its maximum length before they divide into two sets (Figs 19, arrow; 26, double-arrowheads). Subsequently, the later events within the cirral anlagen in both dividers undergo in the same mode as in previous descriptions (Song 1996, Shi and Song 1999): streaks broaden, break apart and then migrate developing as distinct cirri (Figs 18, 20, 22, 30, 32, 34, 35).

According to the segmentation of cirri, the cirral anlagen I-V give rise to the pattern of 3:3:2:2:3, respectively, while the leftmost cirrus is formed *de novo* near the UM-anlage as described above. Nevertheless, only 11 cirri in total are formed in non-divisional stage following the pattern of 3:2:1:1:3, that is, one segment from each of anlagen II-IV will be resorbed before/after cell division is finished.

The anlagen of left marginal cirri for proter and opisthe are formed also *de novo* and separately on the cell surface near the old AZM_2 and the marginal cirri (Figs 13, arrowheads; 24, arrows), which are then enlarge and segmented to form the cirri for daughter cells (Fig. 28, double-arrowheads).

On dorsal side, the proliferation of new basal bodies occurs at two levels within each of the six old kineties. The development of these anlagen seems to follow a

Figs 4-13. Photomicrographs of *Uronychia setigera*, to show the non-divisional (**4-7, 9, 10**) and divisional stages (**8, 11-13**). **4** - ventral view, arrow points the leftmost kinety, arrowheads mark the macronuclei; **5** - dorsal view of the same specimen as in Fig. 4, arrowhead indicates the long 3rd dorsal kinety; **6** - anterior view, to show the first part of AZM (AZM_1, double-arrowheads) and the frontal cirri (arrow); **7** - ventral view, arrowhead marks the 2nd part of AZM (AZM_2), double-arrowheads indicate the leftmost kinety, arrow indicates the frontal cirri; **8** - dorsal view, arrows mark the newly formed caudal cirri; **9** - dorsal view of anterior portion, arrowhead marks the frontal cirri; **10** - dorsal view, arrowheads indicate the dominant caudal cirri; **11** - ventral view, arrow and double-arrowheads mark the newly formed AZM_2 in both proter and opisthe, respectively, while arrowhead indicates the AZM_1 in the opisthe; **12** - dorsal view, arrowheads mark the caudal cirri in both dividers; **13** - ventral view, arrowheads mark the new marginal cirri, arrow indicates the FVT-cirral anlagen (only 4 are recognized in this specimen). Scale bars - 50 μm.

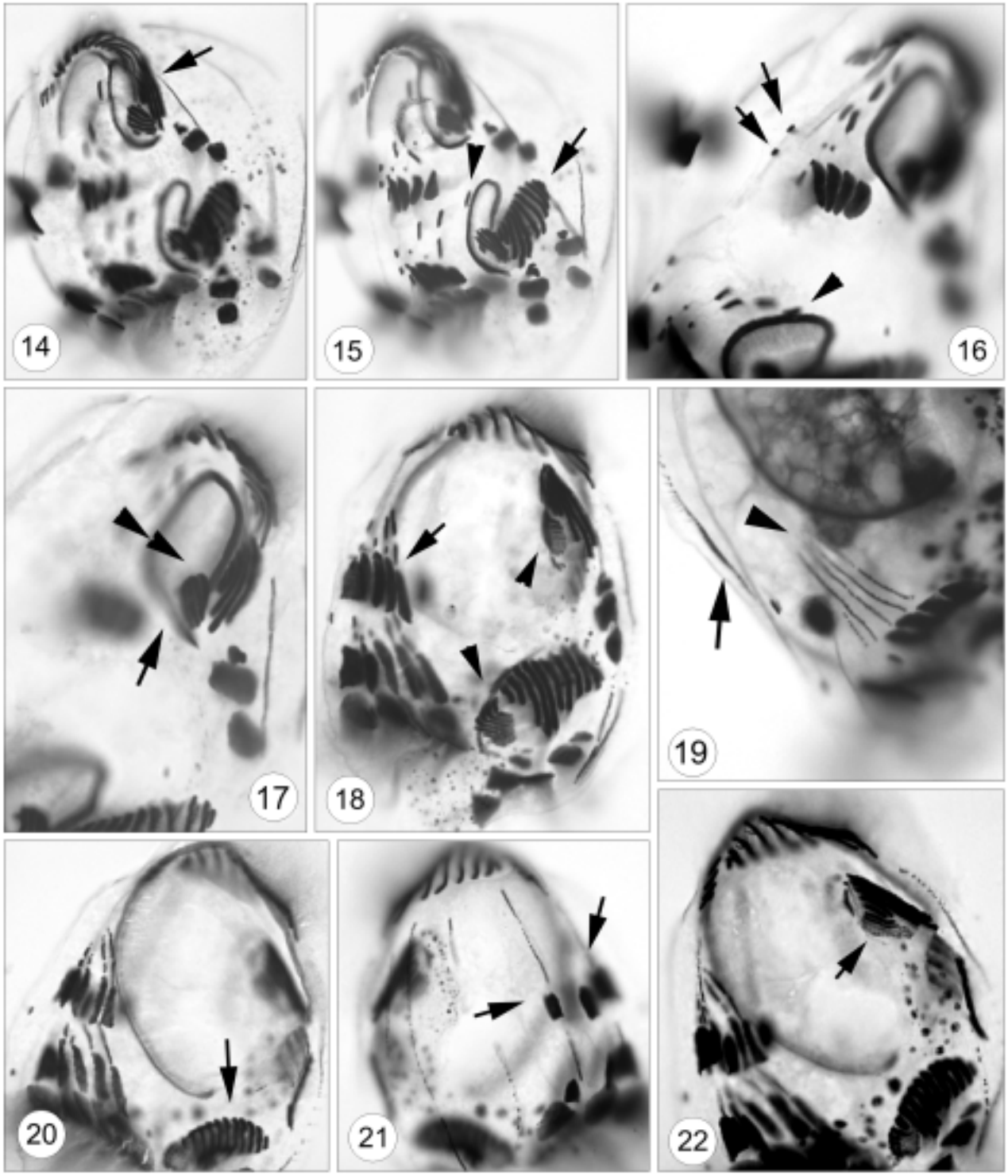

Figs 14-22. Photomicrographs of *Uronychia setigera* in morphogenesis. **14, 15** - ventral views of the same specimen focusing on different levels; arrow in Fig. 14 marks the newly build AZM_1 which just replaces the old structure, arrow in Fig. 15 marks the AZM_1 of the opisthe, while arrowhead indicates the leftmost frontal cirrus derived from the paroral membrane anlage; **16, 17** - ventral views of the same specimen at different focus levels; arrows in Fig. 16 indicate the two inconspicuous ventral cirri, double-arrowheads in Fig. 17 mark theAZM_2 of the proter (note that the paroral membrane, arrow, is positioned at different level); **18** - ventral view, arrowheads mark the AZM_2 in both dividers, whereas arrow indicates the segmented cirral anlagen; **19** - ventral view, arrow marks the newly formed caudal cirrus in the rightmost dorsal kinety, which is just as a slender patch of kinetosomes, while arrowhead indicates the 5 "primary" cirral anlagen; **20** - ventral view, arrow marks the AZM_1 in the opisthe; **21** - dorsal view, arrows mark the caudal cirri of the proter; **22** - ventral view, arrow marks the posterior portion of the oral primordium in the proter, where the last membranelles of the AZM_2 are still in formation.

Table 1. Summary of data on morphogenesis in five well-known typical euplotid genera, with emphasis on the features excluding other non-euplotidous spirotrichs. (AZM - adoral zone of membranelles, FVT - frontoventral transverse, UM - undulating membrane).

Characters	*Uronychia*	*Aspidisca*	*Euplotes*	*Diophrys*	*Certesia*
FVT-cirral anlagen	5 primary streaks	5 primary streaks	5 primary streaks	5 primary streaks	5 primary streaks
Oral primordium in the proter	present	absent	absent	absent	absent
Origin of the oral primordium in the opisthe	subcortically	subcortically	subcortically	subcortically	subcortically
Fate of the parental adoral zone of membranelles during division	invariably 5 proximal membranelles will be replaced by the OP in the proter	completely retained will be renewed by de-differentiating and rebuilding mode	completely retained	proximal portion	completely retained
Formation of the 2nd part of AZM	present	present	absent	absent	absent
Undulating membrane in the proter	rebuilt by the *de novo* newly-formed UM-anlage	old one retained no UM-anlage	old one retained, no UM-anlage	completely renewed the new UM-anlage*	completely renewed by the new UM-anlage*
Formation of the par- and endoral membranes from the UM-anlage	no	no	no	yes	no
Origin of the leftmost frontal cirrus	*de novo*, near the UM-anlage	*de novo*	*de novo*	derived from the UM-anlage	derived from the UM-anlage
Formation of the left marginal cirri	*de novo*, from MC-anlage	absent	*de novo*, from MC-anlage	*de novo*, from MC-anlage	from MC-anlage, *de novo*
No. of membranelles formed by oral primordia	invariable	variable	variable	variable	variable
Origin of dorsal kinety anlagen	intrakinetally, secondary**	as left	as left	as left	as left
Formation of caudal cirri	from rightmost two anlagen, with a complex mode***	no caudal cirri formed	from rightmost one anlage, with a complex mode	from rightmost two anlagen, with a complex mode	no caudal cirri formed
Arrangement of basal bodies in cirri/membrane/ membranelles in non-division stage	irregular and anarchic, in “anlage” state	well-developed, in rows	well-developed, in rows	well-developed, in rows	well-developed, in rows
Data sources	Hill 1990, Song 1996, Shi and Song 1999, Present work	Diller 1975, Hill 1979, Song 2003, Deroux and Tuffrau1965	Bonner 1954, Tuffrau *et al*. 1976, Washburn and Borror 1972	Hill 1981, Song and Packroff 1993, Song and Wilbert 1994	Wicklow 1983

* This process is undertaken yet not *de novo*, but by a “de-differentiating and then rebuilding *in situ*” mode, basal bodies of old structures join the formation of the new anlage;
** Sometimes inconspicuously or difficult to outline the new anlagen because newly proliferated basal bodies appear within the parental strucutures; *** In this mode, two or more caudal cirri are developed from the posterior end of the rightmost anlage.

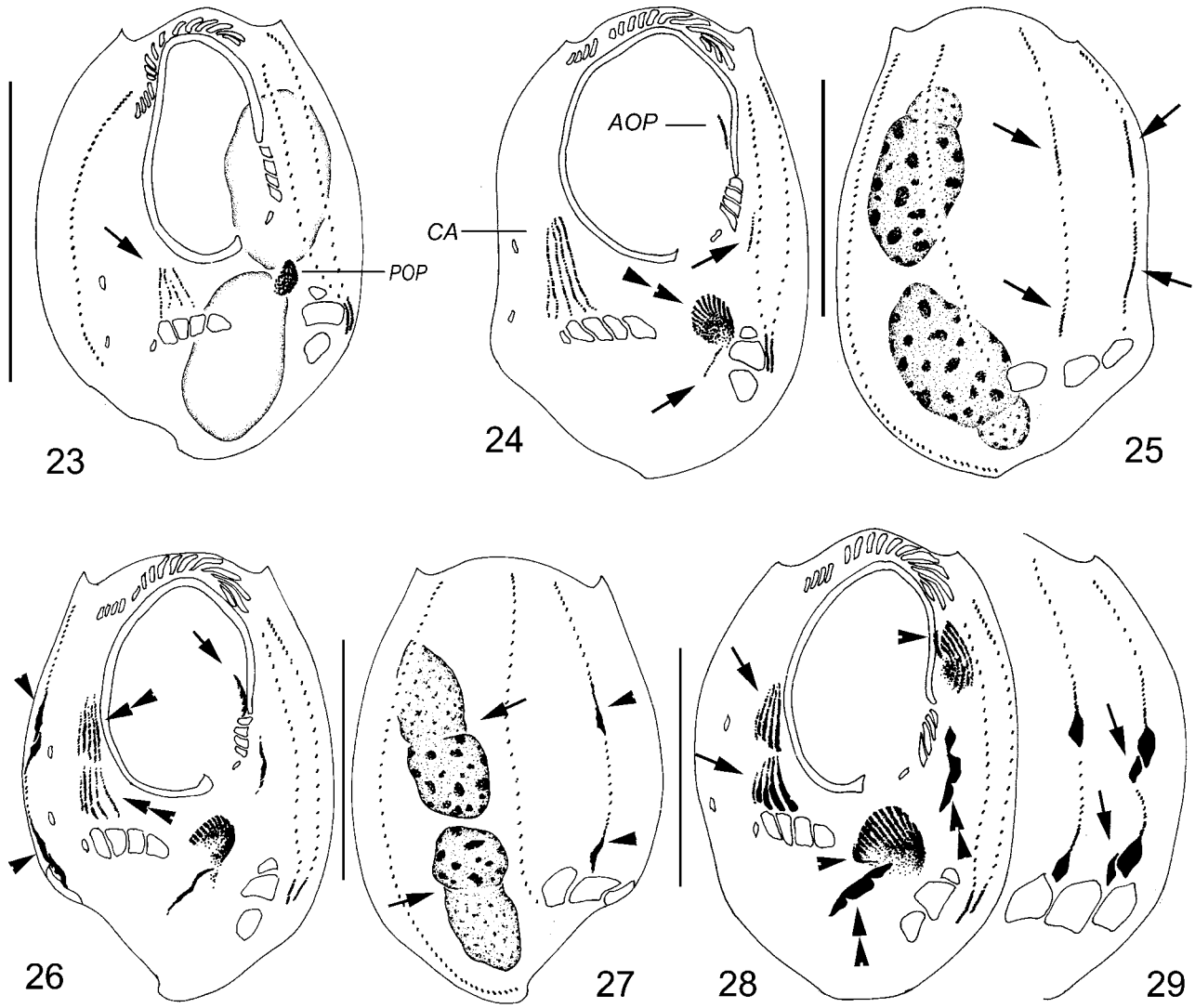

Figs 23-29. *Uronychia setigera* in morphogenesis. **23** - ventral view of an early divider, arrow marks the cirral anlagen (note that there are only four streaks at this stage); **24** - ventral view (note that the membranelles begin to generate, double-arrowheads), arrows mark the anlagen of the marginal cirri; **25** - dorsal view of the same specimen as Fig. 24, arrows mark the new caudal cirri formed within the 2 rightmost dorsal kineties; **26, 27** - ventral and dorsal views, arrowheads in mark the newly formed caudal cirri, double-arrowheads indicate the cirral anlagen (note they are in 2 groups); arrows in Fig. 26 marks the oral primordium of the proter, while in Fig. 27 mark the macronuclear replication bands; **28, 29** - ventral and dorsal views of the same specimen, to show the newly formed paroral membrane anlage (arrowheads), anlagen of marginal cirri (double-arrowheads) and 2 groups of cirral anlagen (arrows in Fig. 28); arrows in Fig. 29 mark the 2nd caudal cirrus generated from the rightmost dorsal kinety anlage in both dividers, respectively. AOP - anterior oral primordium, CA - cirral anlagen, POP - posterior oral primordium. Scale bars 50 μm.

gradient from right to left (Figs 25, 31, 33, arrows). Caudal cirri are generated as in other congeners (and even as in *Diophrys*)(Song and Packroff 1993): two caudal cirri are formed at the posterior end of the rightmost anlage in both proter an opisthe, while the second primordium (from right) gives rise to the third one (Figs 8, 12, 21, 27, 29, 36).

As a conclusion, the morphogenesis in *Uronychia setigera*, as in its congeners, can be summarized as follows: (1) The oral primordium (OP) in both proter and opisthe develops *de novo* in a subcortical pouch, respectively, in which the new membranelles formed in the proter's OP will replace the leftmost 5 parental ones; 6 old membranelles will be retained for the proter. (2)

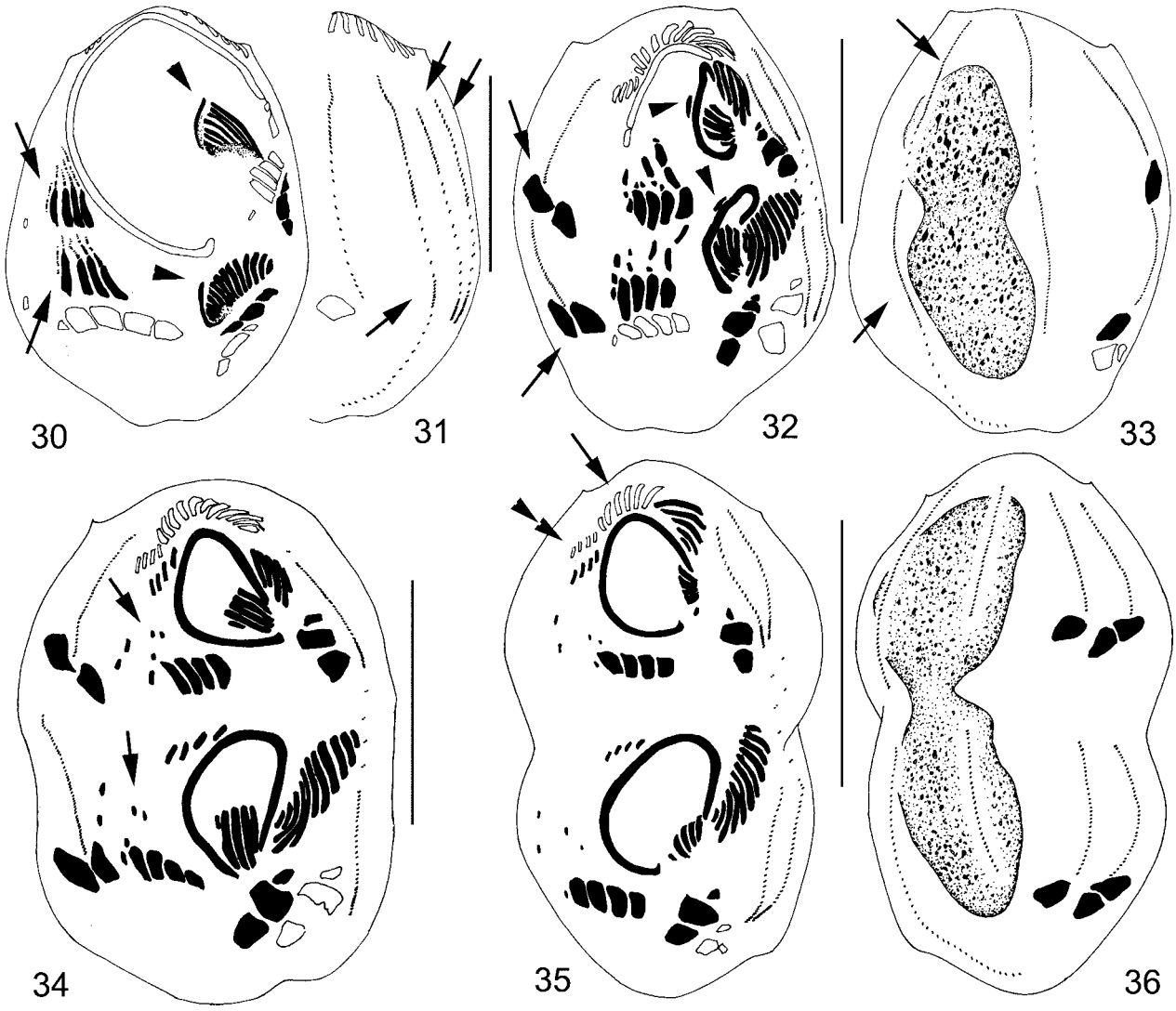

Figs 30-36. *Uronychia setigera* in morphogenesis. **30** - ventral view, arrows mark the thread-like cirral anlage, arrowheads indicate the short paroral membrane anlage in both dividers; **31** - dorsal-to-ventral view of the same specimen, to show the leftmost 3 dorsal kineties, note kinetosomes in some portions are arranged more densely due to the proliferation of basal bodies in order to form the "anlagen" for the dorsal kineties; **32** - ventral view, arrows mark the new caudal cirri; **33** - dorsal view of the same specimen as in Fig. 32, arrows refer the 3rd kinety anlage in both proter and opisthe; **34** - ventral view, arrows mark ventral cirri; **35** - ventral view, arrow marks the old membranelles which will retain for the proter, while double-arrowheads indicate the old frontal cirri; **36** - dorsal view of the same specimen as in Fig. 35, to show that the fused macronuclear mass is in division. Scale bars 50 μm.

Highly specialized undulating membrane generates from the isolated UM-anlage which is formed and develops independently from the OP within the same subcortical pouch. (3) Five primary FVT-cirral anlagen appear *de novo* on the cell surface, which divide and give rise to 2 sets of cirral anlagen for the proter and opisthe. (4) Three frontal, 2 ventral and 5 transverse cirri derive from the 5 FVT-cirral anlagen in both daughter cells, usually 2 to 3 extra ventral cirri generated from these anlagen will be resorbed; the left marginal cirri develop from the marginal-anlage; all these primordia are formed *de novo*. (5) The leftmost frontal cirrus develops *de novo* on the cell surface in both dividers, and has no connection with the UM-anlage. (6) Origination of 3 caudal cirri is involved in the 2 rightmost dorsal kineties with a multi-segmentation mode.

Molecular phylogenetic trees constructed from complete 18S rRNA gene sequences

The bootstrap trees constructed from 18S rRNA sequences are demonstrated in Figs 37, 38. The maximum-parsimony analyses in our work provide strong

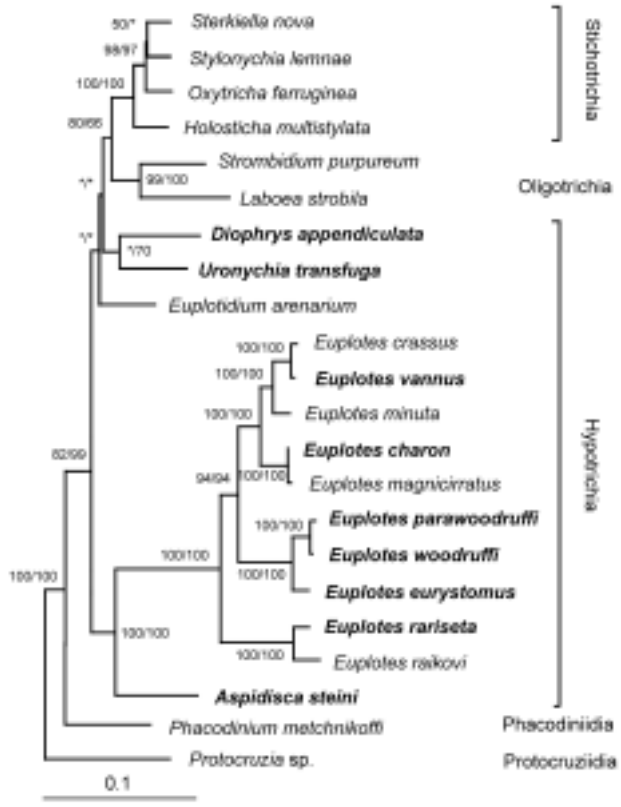

Fig. 37. Distance tree of the spirotrichous ciliates inferred from complete 18S-like, small subunit ribosomal RNA gene sequences. Evolutionary distances were calculated by the Kimura (1980) two-parameter correction model and constructed by the Fitch and Margoliash (1967) least-squares [LS] method. The numbers at the nodes represented the bootstrap percentages of 1,000 for the LS method followed by the bootstrap values for the Saitou and Nei (1987) neighbor-joining [NJ] method. Asterisks indicate bootstrap values less than 50%. Evolutionary distance is represented by the branch length to separate the species in the figure. The scale bar corresponds to 10 substitutions per 100 nucleotide positions. The euplotid species sequenced by the present authors are represented in **boldface**.

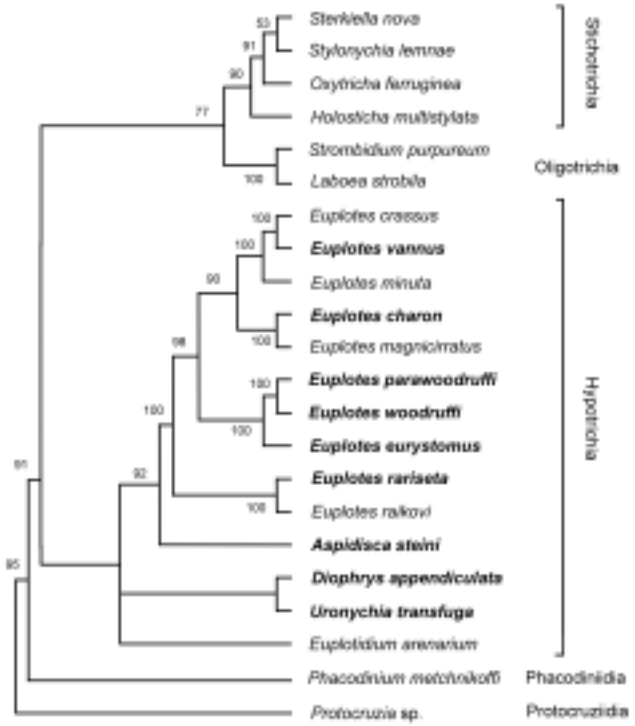

Fig. 38. A maximum-parsimony tree of the spirotrichous ciliates constructed from complete 18S-like small subunit ribosomal RNA gene sequences. The numbers at the forks exhibit the percentage of times the group occurred out of the 1,000 trees. No significance is placed on branch lengths connecting the species. The euplotid species sequenced by the present authors are represented in **boldface**.

support for the monophyly of typical taxa in Euplotina while the genus *Euplotidium*, the only Gastrocirrhidae, of which the sequences data are available, branches from them at low level (Fig. 38). The distance-matrix tree gives slightly different result (Fig. 37), i.e. the 18S rRNA data locate *Uronychia* and *Diophrys* within the Stichotrichia clade (the hypotrichs *s. l.*) though with very lower (lower than 50%) bootstrap support. *Euplotidium* is also grouped with them. All *Euplotes* species and *Aspidisca* are clustered together in a separate clade. In agreement with Borror and Hill (1995) who concluded that *Diophrys* and *Uronychia* are more closely related to each other than to *Euplotes* (hence as a different family, Uronychiidae), both trees support this arrangement and indicate also that the genus *Aspidisca* might separate from them at family level as well. All results obtained reflect consistently that *Euplotidium* (or Gastrocirrhidae) is a sister group to all of them.

DISCUSSION

Identification of *Uronychia setigera*

According to the morphological redescription by Song and Wilbert (1997), the well-known genus *Uronychia* contains now 3 valid morphospecies, *U. transfuga*, *U. binucleata*, and *U. setigera* with numerous synonyms, hence considerably fewer in number than previously believed (Taylor 1928, Kahl 1932, Bullington 1940, Fenchel 1965, Agamaliev 1971, Dragesco and Dragesco-Kernéis 1986, Valbonesi and Luporini 1990, Petz *et al.* 1995). Shortly later, one more species with beaded macronuclei and a long row of ventral cirri on the right

Table 2. Comparison of groups among traditional euplotids *s. l.* and oxytrichids (outer group).

Characters	eueuplotids	gastrocirrhids	discocephaline*	oxytrichids**
Cirral anlagen, number	invariably 5 in number	non-5, usually more than 6	non-5, usually more than 6	invariably 5 in number
Type of development of FVT-cirral anlagen	primary, *de novo*	primary, *de novo*	primary, possibly *de novo* ?	secondary, non-*de novo*
Origin of the oral primordium	within a subsurface pouch	on cell surface, *de novo*	on cell surface, *de novo*	on cell surface, *de novo*
Body shape	generally flattened and oval	subconical, non-oval	cephalized, elongated	typically elongated
Marginal cirri	absent, or only on left side	absent, or only on left side	on both left and right sides	on both sides or only on left side, grouped
Distribution of the frontoventral cirri	usually non-grouped***, reduced in number	non-grouped, in rows	grouped, like that in oxytrichids	characteristically grouped
Caudal cirri	present (few) or absent	absent	present and many, usually in several longitudinal rows	usually present, 3 in number
Origin of caudal cirri	(if present) generated from leftmost 2 dorsal kinety anlagen when present	-	formed as that mode in eueuplotids (from leftmost kinety anlagen)	one formed at posterior end of each kinety
Cilia in dorsal kineties	very short, stub-like	very short, stub-like	often very long, bristle-like	long or short
Adoral zone of membranelles	dominant, *ca* 1/2 or more of cell length	dominant, as in left	less than 1/3, like in other oxytrichids	generally less than 1/3 of cell length
Undulating membranes	mostly single, two in *Diophrys*	single	well-developed two	well-developed two
Origin of the leftmost frontal cirrus	*de novo* except in *Diophrys*****	from anterior end of UM-anlage	from anterior end of UM-anlage	from anterior end of UM-anlage
Macronuclear apparatus	beaded or in 1-2 segments, (band- or sausage-like in the latter)	as in eueuplotids number, sparsely distributed within the cell	numerous in	mostly two, oval in shape
Data sources	original	Hu and Song 2003	Wicklow 1982	Berger 1999

* This type is represented by *Discocephalus ehrenbergi*; ** Based largely on *Oxytricha*-complex; *** Frontal and ventral cirri in some genera (e.g. *Diophrys, Uronychia*) are in two groups; **** This cirrus in *Diophrys* derives from the UM-anlage.

cell margin, *Uronychia multicirrus*, was added (Song 1997).

The small form, *Uronychia setigera*, as defined by Song and Wilbert (1997), differs from the closely-related *U. binucleata* in lower number of basal bodies in the leftmost dorsal kineties (*ca* 20 *vs*. *ca* 30), conspicuously smaller size in natural water (*ca* 60 μm *vs*. about 100 μm in length) and presence of the lateral spur or spine at

about anterior 2/3 of cell on left margin (*vs*. absent or inconspicuous in *U. binucleata*) (Calkins 1902, Kahl 1932, Curds and Wu 1983, Song and Wilbert 1997). This conclusion was recently confirmed by researches using DNA-fingerprinting and ARDAR riboprinting methods (Chen *et al*. 2003).

Some noticeable morphogenetic features in *Uronychia*

The morphogenesis in all three well-known morphospecies of *Uronychia, U. transfuga, U. binucleata* and *U. setigera* has been repeatedly investigated even in last decades using silver methods. Among them, the largest form with beaded macronuclei, *U. transfuga* was studied by Wilbert and Kahan (1981) and Wilbert (1995), although only the main stages were documented. The species described by Hill (1990) under the name *Uronychia transfuga* and by Song (1995) under the name of *U. uncinata* would be populations of *U. binucleata* (see Song and Wilbert 1997). The small one, *U. setigera* was likely only once described (Shi and Song 1999), which matches completely the results of the present work.

All the hitherto data demonstrate that fissional events in this genus are highly stable and conservative, hence, the general morphogenetic pattern is shared by all known congeners. These data also suggest that *Uronychia*, compared with other related taxa, e.g. *Euplotes, Aspidisca, Diophrys*, possesses more primitive features: (1) UM-primordium forms only a single anlage-like membrane; (2) all ciliary organelles are present, and (3) most ciliary organelles appear to be at early developing stage considering the arrangement of basal bodies which are uniquely distributed in an anarchic mode. In addition, 2 caudal cirri developing from the posterior end of a single kinety anlage (the leftmost one) is possibly also a plesiomorphic characteristic, for the anterior one might represent the non-loosened kinety corresponding to some oxytrichids, in which the rightmost DK-anlage (of the dorsal group) is usually segmented to form the 4th kinety and the newly formed kinety bears the caudal cirrus (Eigner 1997, Foissner 1996, Berger 1999). This mode is seen also in *Euplotes* and *Diophrys* (Tuffrau *et al*. 1976, Hill 1981, Song and Packroff 1993, Song and Wilbert 1994), and implying that it is a conservative feature having a long evolutionary history.

Considering the general process of the development of the oral apparatus, *Uronychia* exhibits the combination of 3 unusual stomatogenetic characteristics: (1) oral primordium in the proter develops *de novo* and subcortically as well; (2) AZM divided into 2 parts, and (3) the piece-together-mode of the AZM_1 in the proter. Among these, the most noticeable event is the point 3, namely the formation of AZM_1 in the proter: it is (invariably !) composed of 6 parental (retained) and 5 newly formed membranelles. This phenomenon is unique even in all spirotrichids, though a "similar" process is seen also in several other non-euplotids, e.g. *Hemigastrostyla* and some urosylids. In these taxa, nevertheless, the proter's oral primordium develops unexceptionally on the cell surface (epicortically) and forms a variable number of membranelles (Hemberger 1982, Song and Hu 1999), i.e. very likely a convergent similarity.

As given in the morphogenetic descriptions (see Results), some newly formed ventral cirri will be resorbed before/after cell division is completed, i.e. one cirrus from the each of cirral anlagen II-IV will be dissolved. Clearly, this process might be individual-dependent: in some cases, those to-be-dissolved cirri could be retained for a short time after division as we observed in some individuals.

Another event needs to be clarified: the leftmost frontal cirrus in both proter and opisthe is formed *de novo* rather than generated from the UM-primordium like that in most hypotrichs *s. l.* This situation is seen also in at least two other morphologically rather specialized genera, *Aspidisca* (Diller 1975, Hill 1979, Song 2003) and *Euplotes* (Washburn and Borror 1972, Tuffrau *et al*. 1976), this implys that this might be a plesiomorphic character.

Hill (1990) described that the paroral membrane in *Uronychia binucleata* (called *U. transfuga*) divides and overlaps at the anterior end before completion of division, thus forming the right and left oral membranes. This description is, however, neither supported by the morphological (Song and Wilbert 1997) nor by the morphogenetic observations (Song 1996, called *U. uncinata*). In *U. setigera,* the present work and a previous report (Shi and Song 1999) substantiate the same conclusion: UM-primordium gives rise to only a single structure. Similar results are also obtained in *U. transfuga* (Wilbert and Kahan 1981, Wilbert 1995).

Systematic relationships and position of *Uronychia* and related euplotids

Euplotids traditionally comprise of at least 12 traditional genera assigned by Corliss (1979) to 3 families, Aspidiscidae, Euplotidae and Gastrocirrhidae. They are characterized by reduced somatic ciliature, rigid body and mostly oval/flattened shape, absence of right mar-

ginal cirri, dominant AZM, and subcortical mode of stomatogenesis (Borror 1972, Tuffrau *et al*. 1976, Corliss 1979, Curds and Wu 1983, Dragesco and Dragesco-Kernéis 1986). This classification is generally accepted by most taxonomists, though some related or "sister groups" were subsequently added into this increasingly comprehensive complex, and its systematic arrangement was often slightly redefined (Small and Lynn 1985, Hill and Borror 1992, Borror and Hill 1995). The updated system is suggested by Lynn and Small (2002), in which the order Euplotida consists of 2 suborders: the Euplotina with "typical" euplotids (5-anlagen-mode) plus gastrocirrhids, while another suborder, Discocephalina, is composed of some cephalized marine groups (Wicklow 1982).

In euplotids *s. l.*, most genera in Aspidiscidae and Euplotidae belong to the type of 5-cirral anlagen (5 transverse cirri in non-dividing stage) or "typical" euplotids (eueuplotids, see terminology) though only 5 of them, *Aspidisca, Euplotes, Certesia, Diophrys* and *Uronychia,* have been both morphologically and morphogenetically studied (Washburn and Borror 1972, Wicklow 1983, Hill 1990, Song and Packroff 1993, Song and Wilbert 1994). Different from these eueuplotids, the discocephalins with the representative genus *Discocephalus,* demonstrates distinctly diverse morphology and a highly different mode with multi-cirral anlagen and epicortical stomatogenesis (Wicklow 1982) (Table 2). In Gastrocirrhidae, the genus *Gastrocirrhus* is likely the only one, in which the morphogenesis is partly known (Hu and Song 2003). Based on the description by Hu and Song, 5 features can be recognized: (1) the oral primordium develops on cell surface; (2) FVT-cirri generate from many (more than 5) cirral anlagen; (3) no marginal and caudal cirri are formed; (4) paroral membrane is a single structure, (5) one streak-like UM-anlage develops *de novo* in both proter and opisthe, from which the leftmost frontal cirrus is generated. This reflects that *Gastrocirrhus* is an intermediate type between *Discocephalus* and other typical euplotids mentioned above (Table 2).

The main morphogenetic features found in 5 "typical" euplotid genera are tabulated (Table 1). Among these, the most significant characters are: (1) oral primordium develops subcortically; (2) five *de novo* formed primary FVT-cirral anlagen; (3) single undulating membrane generates from the isolated UM-anlage (yet presence of two membranes in *Diophrys* is clearly an apomorphic character); (4) the leftmost frontal cirrus develops completely separated from the UM-anlage (again, it is exceptional in *Diophrys* which exhibits a stichotrichous mode); (5) multi-segmentation of caudal cirri (when present); (6) no right marginal cirri generated. Considering so many morphological and morphogenetical features shared by diverse taxa, it is unlikely that these euplotids develop from different ancestors convergently, so that combination of these characters should be, in our opinion, regarded to be critical criteria for a monophyletic complex. The multi-anlagen-mode (non-5-cirral anlagen) is seemingly an apomorphic character, which derives divergently from (?) the 5-anlagen type as revealed by investigations on *Amphisiella annulata* by Berger (2004). The morphogenesis of this stichotrich ciliate supports that, apart from 5 normal cirral streaks, there is always an inconspicuous, extra anlage being formed which develops to the 6th transverse cirrus. The epicortical origin of the oral primordium is definitely a primary character (vs. subcortical mode) for it occurs in numerous highly diverse stichotrichs/ hypotrichs, which indicates it is impossible due to convergent evolution. Hence a reasonable surmise is that, within the order Euplotida, the gastrocirrhids are indeed a closely related group to the eueuplotids, which are as pseudoeuplotids belonging to the same suborder as suggested by Lynn and Small (2002). This view is basically supported also by molecular data (Chen and Song 2001, 2002; Chen *et al*. 2002), based on which gastrocirrhids are almost always clustered with other eueuplotid clade (Figs 37, 38). As to the discocephalids/discocephaline, they could be, considering their morphological and morphogenetic features (no molecular data in this group available yet), possibly a marginalized or even a paraphyletic group to the euplotine, which are even more closely related to oxytrichids, e.g. grouped frontoventral cirri, 2 UM-membranes, epicortical origin of oral primordium, elongated body shape and generally presence of both marginal rows (Table 2). Nevertheless, further evidences are needed to indicate in which position this group should be placed.

With reference to the AZM in the proter, at least 4 basic patterns can be recognized in all spirotrichs (Hemberger 1982, Foissner 1996, Eigner 1997, Berger 1999, Hu *et al*. 2003): (1) The parental structure is intact and retained for the proter, e.g. in many euplotids, oxytrichids, many amphisiellids, discocephalids and kahliellids. (2) Posterior portion of AZM is partly renewed after de-differentiation of old membranelles and then a re-building process, in which no new OP is involved, e.g. *Diophrys* and some urostylids. (3) The old AZM will be completely replaced by a new one which

is formed by a *de novo* appeared OP, like in most urostylids. (4) (Only in the posterior portion) partly renewed by the newly formed structure, hence piecing together with the retained old part (the distal part), e.g. *Uronychia, Hemigastrostyla*. Thus, euplotids (both eueuplotids and pseudoeuplotids) exhibit 3 different patterns of the formation/rebuild of the oral structure. This suggests that this diversity is likely due to divergent evolution (from an ancestor type) though evidence could not be traced in the morphogenesis.

Finally, an interesting point of discussion is the relationship between euplotids and hypotrichs *s. l.* (stichotrichs) or the origin of the euplotids if we consider that two assemblages have close connection as most hitherto information has revealed. Our opinion is that the euplotids are not the most primitive forms, though there is still no firm evidence showing that stichotrichs is the forerunner of euplotids. The most "critical" reasons are from morphogenetic data, e.g. 5-anlagen pattern and the subcortical origin of the oral primordium. The former feature is shared by both euplotids and many highly dedifferentiated stichotrichs (e.g. oxytrichids, kahliellids *vs*. the primitive *Kiitricha*), hence not the most primitive taxa. This indicates clearly that this similarity does not derive from parallel evolution. Whereas the latter feature, the oral primordium originating subcortically, should be also an apomorphic characteristic because in most other lower ciliates (non-spirotrichs) oral primordium develops on the cell surface (Foissner 1996). Other evidence comes from the morphological features: (1) many euplotids have only left marginal cirri or simply absent (divergent from predecessors with both left and right ones); (2) presence of bipartite AZMs is surely an apomorphic feature. However, considering some primitive characteristics in euplotids, e.g. most genera have only a single undulating membrane, 2 caudal cirri develop from a single dorsal kinety anlage, the ancestor of euplotids is also less likely any current type of stichotrichs. We presume that, especially because of the fact that 5-anlagen pattern is widely seen in many taxa in oxytrichids as well, euplotids (at least the eueuplotids) derive from a forerunner possessing the 5-anlagen mode, which might be also the predecessor of many present hypotrichs *s. l.*

In conclusion, our new points of views on taxonomy of euplotids are: (1) The traditional euplotids could be a paraphyletic assemblage consisting of "true" and outer groups. As a suggestion based on the new definition, the order Euplotida *s. l.* contains at least 2 subgroups: the eueuplotids or "typical" euplotids, a monophyly consisting of the taxa with the pattern of 5-cirral-anlagen as well as the subcortical origin of the oral primordium, and the sister group, gastrocirrhids (or pseudoeuplotids), with multi-anlagen feature which is a divergent, or apomorphic feature. (2) The systematic position of discocephaline remains unclear, but possibly an intermediate group between the euplotids *s. str.* and stichotrichs; However, we agree that it is presently placed within the order Euplotida, as an outer group of other two assemblages. (3) The morphogenetic feature of 5-cirral-anlagen-mode is highly conservative and should be hence weighted with more phylogenetic value(s) in systematic analysis. (4) We suppose that some features like the origin mode of the leftmost frontal (formed from the UM-anlage), and the situation of undulating membranes (e.g., two in number and curved in appearance) represent apomorphic features, and should not be over-evaluated. (5) Euplotids *s. str.* might be derived from the 5-anlagen ancestor-type of hypotrichs *s. l.*, which is possibly also the ancestor of the current stichotrichs.

Acknowledgements. This study was mainly supported by "the Natural Science Foundation of China" (project No. 40376045). We gratefully acknowledge the "Deutsche Forschungsgemeinschaft" (DFG), Germany, for providing a visiting grant to the senior author to finish the writing work.

REFERENCES

Agamaliev F. G. (1971) Complements to the fauna of psammophilic ciliates of the Western coast of the Caspian Sea. *Acta Protozool.* **8:** 379-407 (in Russian with English summary)

Berger H. (1999) Monograph of the Oxytrichidae (Ciliophora, Hypotrichia). *Monographiae Biol.* **78:** 1-1080

Berger H. (2004) *Amphisiella annulata* (Kahl, 1928) Borror, 1972 (Ciliophora: Hypotricha) morphology, notes on morphogenesis, review of literature, and neotypification. *Acta Protozool.* **43:** 1-14

Bernhard D., Stechmann A., Foissner W., Ammermann D., Hehn M., Schlegel M. (2001) Phylogenetic relationships within the class Spirotrichea (Ciliophora) inferred from small subunit rRNA gene sequences. *Mol. Phyl. Evol.* **21**: 86-92

Bonner J. T. (1954) The development of cirri and bristles during binary fission in the ciliate *Euplotes eurystomus*. *J. Morph.* **95:** 95-107

Borror A. C. (1972) Revision of the order Hyportyichida (Ciliophora, Protozoa). *J. Protozool.* **19:** 1-23

Borror A. C., Hill B. F. (1995) The order Euplotida (Ciliophora): taxonomy, with division of Euplotes into several genera. *J. Eukaryot. Microbiol.* **42:** 457-466

Bullington W. E. (1940) Some ciliates from Tortugas. *Pap. Tortugas Lab.* **32**: 179-221

Calkins C. N. (1902) Marine protozoa from Woods Hole. *Bull. U. S. Fish Comm.* **21:** 413-468

Chen Z., Song W**.** (2001) Phylogenetic positions of *Uronychia transfuga* and *Diophrys appendiculata* (Euplotida, Hypotrichia, Ciliophora) within hypotrichous ciliates inferred from the small subunit ribosomal RNA gene sequences. *Europ. J. Protistol.* **37:** 291-301

Chen Z., Song W. (2002) Phylogenetic positions of *Aspidisca steini* and *Euplotes vannus* within the order Euplotida (Hypotrichia: Ciliophora) inferred from complete small subunit ribosomal RNA gene sequences. *Acta Protozool.* **41:** 1-9

Chen Z., Shang H., Song W. (2002) Phylogenetic studies on *Uronychia transfuga* (Protozoa, Ciliophora, Hypotrichida) inferred from its small subunit rRNA gene sequence. *High Techn. Letters* **10:** 98-102 (in Chinese with English summary)

Chen Z., Song W., Warren A. (2003) Species separation and identification of *Uronychia* spp. (Hypotrichia: Ciliophora) using RAPD fingerprinting and ARDAR riboprinting. *Acta Protozool.* **42:** 83-90

Corliss J. O. (1979) The Ciliated Protozoa: Characterization, Classification and Guide to the Literature. 2nd ed. Pergamon Press, New York

Curds C. R., Wu I. C. H. (1983) A review of the Euplotidae (Hypotrichida, Ciliophora). *Bull. Br. Mus. Nat. Hist. (Zool.)* **44:** 191-247

Dembowska W. S. (1926) Studies on the regeneration of Protozoa. II. Regeneration of the ciliary apparatus in some marine Hypotricha. *J. exp. Zool.* **43:** 485-504

Deroux G., Tuffrau M. (1965) *Aspidisca orthopogon* n. sp. Révision de certains mécanismes de la morphogenèse a l'aide d'une modification de la technique au protargol. *Cah. Biol. Mar.* **6:** 293-310

Diller W. F. (1975) Nuclear behavior and morphogenetic changes in fission and conjugation of *Aspidisca costata* (Dujardin). *J. Protozool.* **22:** 221-229

Dragesco J., Dragesco-Kernéis A. (1986) Ciliés libres de l'Afrique intertropicale. *Faune Tropicale,* **26:** 1-559

Eigner P. (1997) Evolution of morphogenetic processes in the Orthoamphisiellidae n. fam., Oxytrichidae, and Parakahliellidae n. fa., and their depiction using a computer method (Ciliophora, Hypotrichida). *J. Euk. Microbiol.* **44:** 553-573

Elwood H. J., Olsen G. J., Sogin M. L. (1985) The small-subunit ribosomal RNA gene sequences from the hypotrichous ciliates *Oxytricha nova* and *Stylonychia pustulata*. *Mol. Biol. Evol.* **2:** 399-410

Fauré-Fremiet E. (1964) Les ciliés hypotrichs retrocursits. *Arch. Zool. Exp. Gen.* **104:** 65-74

Felsenstein J. (1985) Confidence limits on phylogenies: An approach using the bootstrap. *Evolution* **39:** 783-791

Felsenstein J. (1995) "PHYLIP: Phylogeny Inference Package," Version 3.57c. Department of Genetics, University of Washington, Seattle

Fenchel T. (1965) Ciliates from scandinavian molluscs. *Ophelia* **2:** 71-174

Fitch W. M., Margoliash E. (1967) Construction of phylogenetic trees. *Science* **155:** 279-284

Foissner W. (1996) Ontogenesis in ciliated protozoa, with emphasis on stomatogenesis. In: Ciliates, Cells as Organisms (Eds. K. Hausmann and P. C. Bradbury), 95-177. Gustav Fischer, Stuttgart

Hartwig E. (1973) Die Ciliaten des Gezeiten-Sandstrandes der Nordssinsel Sylt. I. Systematik. *Abh. math-naturw. Kl Akad. Wiss. Mainz. Mikrofauna Meer.* **18:** 1-69

Hemberger H. (1982) Revision der Ordnung Hypotrichida Stein (Ciliophora, Protozoa) an Hand von Protargolpräparaten und Morphogenesedarstellungen. PhD Thesis, University of Bonn, Germany

Hill B. F. (1979) Reconsideration of cortical morphogenesis during cell division in *Aspidisca* (Ciliophora, Hypotrichida). *Trans. Am. Microsc. Soc.* **98:** 537-542

Hill B. F. (1981) The cortical morphogenesis cycle associated with cell division in *Diophrys* Dujardin, 1841 (Ciliophora, Hypotrichida). *J. Protozool.* **28:** 215-221

Hill B. F. (1990) *Uronychia transfuga* (O. F. Müller, 1786) Stein, 1859 (Ciliophora, Hypotrichida, Uronychidae): cortical structure and morphogenesis during division. *J. Protozool.* **37:** 99-107

Hill B. F., Borror A. C. (1992) Redefinition of the genera *Diophrys* and *Paradiophrys* and establishment of the genus *Diophryopsis* n. g. (Ciliophora, Hypotrichida): Implication for the species problem. *J. Protozool.* **39:** 144-153

Hu X., Song W. (2003) Redescription of two known species, *Gastrocirrhus monilifer* (Ozaki et Yagiu, 1942) and *Gastrocirrhus stentoreus* Bullington, 1940, with reconsideration of the genera *Gastrocirrhus* and *Euplotidium*. *Acta Protozool.* **42:** 345-355

Hu X., Song W., Suzuki T. (2003) Morphogenesis of *Holosticha braduryae* (Protozoa, Ciliophora) during asexual reproduction cycle. *Europ. J. Protistol.* **39:** 173-181

Kahl A (1932) Urtiere oder Protozoa. I: Wimpertiere oder Ciliata (Infusoria), 3. Spirotricha. *Tierwelt Dtl* **25:** 399-650

Kimura M. (1980) A simple method of estimating evolutionary rates of base substitutions through comparative studies of nucleotide sequences. *J. Mol. Evol.* **16:** 111-120

Lynn D. H., Small E. B. (2002) Phylum Ciliophora Doflein, 1901. In: The Illustrated Guide to the Protozoa (Eds. J. J., Lee, G.. F. Leedale, P. C. Bradbury), 2nd ed, Society of Protozoologists, Allen Press, Lawrence, Kansas, 371-656

Petroni G., Spring S., Schleifer K. H., Verni F., Rosati G. (2000) Defensive extrusive ectosymbionts of *Euplotidium* (Ciliophora) that contain microtubule-like structures are bacteria related to Verrucomicrobia. *Proc. Natl. Acad. Sci. USA* **97:** 1813-1817

Petroni G., Dini F., Verni F., Rosati G. (2002) A molecular approach to the tangled intrageneric relationships underlying phylogeny in *Euplotes* (Ciliophora, Spirotrichea). *Mol. Phylogen. Evol.* **22:** 118-130

Petz W, Song W, Wilbert N (1995) Taxonoy and ecology of the ciliate fauna (Protozo, Ciliophora) in the endopagial and pelagial of the Weddell Sea, Antarctica. *Stapfia* **40:** 1-223

Saitou N., Nei M. (1987) The neighbor-joining method: a new method for reconstructing phylogenetic trees. *Mol. Biol. Evol.* **4:** 406-425

Shi X., Song W. (1999) On morphology and morphogenesis of *Uronychia setigera* during asexual division. *Acta Hydrobiol. Sin.* **23:** 146-150 (in Chinese with English summary)

Shin M. K., Hwang U. W., Kim W., Wright A.-D. G., Krawczyk C., Lynn D. H. (2000) Phylogenetic position of the ciliates *Phacodinium* (order Phacodiniida) and *Protocruzia* (subclass Protocruziidia) and systematics of the spirotrich ciliates examined by small subunit ribosomal RNA gene sequences. *Europ. J. Protistol.* **36:** 293-302

Small E. B., Lynn D. H. (1985) Phylum Ciliophora. In: An Illustrated Guide to the Protozoa (Eds. J. J. Lee, S. H. Hutner, E. C. Bovee), Lawrence press, Kansas, 393-575

Snoeyenbos-West O. L. O., Salcedo T., McManus G. B., Katz L. A. (2002) Insights into the diversity of choreotrich and oligotrich ciliates (Class: Spirotrichea) based on genealogical analyses of multiple loci. *Int. J. Syst. Evol. Microbiol.* **52:** 1901-1913

Song W. (1995) Preliminary studies on the phylogenetic relationship of genera within the family Euplotidae (Ciliophora, Hypotrichida). *Oceanol. Limnol. Sin.* **26:** 527-534 (in Chinese with English summary)

Song W. (1996) Morphogenetic studies on *Uronychia uncinata* (Protozoa, Ciliophora) during its asexual division. *Acta Oceanol. Sin.* **15:** 93-99

Song W. (1997) On the morphology and infraciliature of a new marine hypotrichous ciliate, *Uronychia multicirrus* sp. n. (Ciliophora, Hypotrichida). *Acta Protozool.* **36:** 279-285

Song W. (2003) Reconsideration of the morphogenesis in the marine hypotrichous ciliate, *Aspidisca leptaspis* Fresenius, 1865 (Protozoa, Ciliophora). *Europ. J. Protistol.* **39:** 53-61

Song W., Hu X. (1999) Divisional morphogenesis in *Hemigastrostyla enigmatica* (Dragesco & Dragesco-Kernéis), with discussion of its systematic position (Protozoa, Ciliophora). *Hydrobiologia* **391:** 249-257

Song W., Packroff G. (1993) Beitrag zur Morpphogenese des marinen Ciliaten *Diophrys scutum* (Dujardin, 1841). *Zool. Jb. Anat.* **123:** 85-95

Song W., Wilbert N. (1994) Morphogenesis of the marine ciliate *Diophrys oligothrix* Borror, 1965 during the cell division (Protozoa, Ciliophora, Hypotrichida). *Europ. J. Protistol.* **30:** 38-44

Song W., Wilbert N. (1997) Morphological investigation on some free living ciliates (Protozoa, Ciliophora) from China Sea with description of a new *Hypotrichous* genus, *Hemigastrostyla* nov. gen. *Arch. Protistenkd.* **148:** 413-444

Song W., Wilbert N. (2000) Ciliates form Antarctic sea ice. *Polar Biol* **23:** 212-222

Swofford D. L. (1998) Phylogenetic Analysis Using Parsimony, version 4. Sinauer, Sunderland

Taylor C. V. (1928) Protoplasmic reorganization in *Uronychia uncinata* n. sp., during binary fission and regeneration. *Physiol. Zool.* **1:** 1-26

Thompson J. D., Higgins D. G., Gibson T. J. (1994) CLUSTAL W: improving the sensitivity of progressive multiple sequence alignment through sequence weighting, positions-specific gap penalties and weight matrix choice. *Nucleic Acids Res.* **22:** 4673-4680

Tuffrau M., Tuffrau H., Genermont J. (1976) La réorganisation infraciliaire au cours de la conjugaison et l'origine du primordium buccal dans le genre *Euplotes*. *J. Protozool.* **23:** 517-523

Valbonesi A., Luporini P. (1990) A new marine species of *Uronychia* (Ciliophora, Hypotrichida) from Antarctica: *Uronychia antarctica*. *Boll. Zool.* **57:** 365-367

Washburn E. S., Borror A. C. (1972) *Euplotes raikovi* Agamaliev, 1966 (Ciliophora, Hypotrichida) from New Hampshire: description and morphogenesis. *J. Protozool.* **19:** 604-608

Wicklow B. J. (1982) The Discocephalina (n. subord.): ultrastructure, morphogenesis and evolutionary implications of a group of endemic marine interstitial hypotrichs (Ciliophora, Protozoa). *Protistologica* **18:** 299-330

Wicklow B. J. (1983) Ultrastructure and cortical morphogenesis in the eupotine hypotrichs *Certesia quadrinucleata* Dabre-Domergue, 1885 (Ciliophora, Protozoa). *J. Protozool.* **30:** 256-266

Wilbert N. (1975) Eine verbesserte Technik der Protargolimprägnation für Ciliaten. *Mikrokosmos* **64:** 171-179

Wilbert N. (1995) Benthic ciliates of salt lakes. *Acta Protozool.* **34:** 271-288

Wilbert N., Kahan D. (1981) Ciliates of Solar Lake on Red Sea shore. *Arch. Protistenk.* **124:** 70-95

Received on 5th March, 2004; revised version on 8th June, 2004; accepted on 18th June, 2004

Acta Protozool. (2004) 43: 329 - 336

ACTA
PROTOZOOLOGICA

Ultrastructural Description of the Life Cycle of *Nosema diphterostomi* sp. n., a Microsporidia Hyperparasite of *Diphterostomum brusinae* (Digenea: Zoogonidae), Intestinal Parasite of *Diplodus annularis* (Pisces: Teleostei)

Céline LEVRON[1], Sonia TERNENGO[1], Bhen Sikina TOGUEBAYE[2] and Bernard MARCHAND[1]

[1]Laboratoire Parasites et Ecosystèmes Méditerranéens, Faculté des Sciences et Techniques, Université de Corse, Corte, France; [2]Laboratoire de Parasitologie, Département de Biologie Animale, Faculté des Sciences et Techniques Université C.A. Diop, Dakar, Sénégal

Summary. The life cycle of a new microsporidium, *Nosema diphterostomi* sp. n. is described. This parasite infects the epithelial gut and connective tissue of a trematode *Diphterostomum brusinae* (Digenea: Zoogonidae), intestinal parasite of *Diplodus annularis* (Pisces: Teleostei). All development stages are in close contact with the host cell cytoplasm and have paired nuclei (diplokaryon). Matures spores measure about 2.1 × 1.4 µm. They possess a polar filament with 6-7 coils, a posterior vacuole and a polaroplast made up of an outer part of dense and closely spaced lamellae encircling an inner part of widely spaced lamellae. All morphological and ultrastructural features indicate that the described microsporidium belongs to the genus *Nosema*. In comparison with the other *Nosema* of trematodes, this parasite is a new species. We propose the name *Nosema diphterostomi* sp. n. according to the generic name of its host.

Key words: *Diphterostomum brusinae*, *Diplodus annularis*, hyperparasite, Microsporidium, *Nosema diphterostomi* sp. n., Nosematidae.

INTRODUCTION

Diphterostomum brusinae (Stossich, 1888) Stossich, 1903 (Digenea, Zoogonidae) is a parasite of the digestive tract of the Sparid fish *Diplodus annularis* (Linnaeus, 1758). During an ultrastructural study of this platyhelminth, we discovered a microsporidium which develops in different tissues of this parasite.

Hyperparasite microsporidia of trematodes have been reported on numerous occasions. They belong to the genus *Nosema* Naegeli, 1857, *Pleistophora* Gurley, 1893 and *Unikaryon* Canning, Lai *et* Lie, 1974 as well as to the collective group of *Microsporidium* Balbiani, 1884 (Canning 1975, Canning and Madhavi 1977, Sprague 1977, Canning and Olson 1980, Canning *et al.* 1983, Azevedo and Canning 1987). The species, found in *D. brusinae*, belongs to the genus *Nosema*. In this study, the development cycle of this new species is described

Address for correspondance: Céline Levron, Laboratoire Parasites et Ecosystèmes Méditerranéens, Faculté des Sciences et Techniques, Université de Corse, Campus Grossetti, B.P. 52, F-20250 Corte, France; Fax: + 33 4 95 45 00 29; E-mail: levron@univ-corse.fr

and compared with that of the other *Nosema* from trematodes.

MATERIALS AND METHODS

Several teleostean specimens *Diplodus annularis* (Linnaeus, 1758) (Sparidae) were collected in the "Bonifacio Strait Marine Reserve" (Mediterranean Sea, France) during 2001 and 2002 summers. After necropsy and extraction, the specimens of the trematode *Diphterostomum brusinae* (Stossich, 1888) Stossich, 1903 (Zoogonidae) were kept alive in a 0.9 % NaCl solution. Different adults specimens were fixed in cold (4°C) 2.5 % glutaraldehyde in a 0.1 M sodium cacodylate buffer at pH 7.2, rinsed for one night in a 0.1 M sodium cacodylate buffer at pH 7.2, postfixed in cold (4°C) 1 % osmium tetroxide in the same buffer for 1 h, dehydrated with ethanol and propylene oxide, embedded in Epon and then polymerised at 60°C for 48 h. Ultrathin sections (60 to 90 nm thick) were cut on a LKB 8800A ultramicrotome, placed on copper grids, and stained with uranyl acetate and lead citrate according to Reynolds (1963).

The grids were examined in a Hitachi H600 electron microscope at 75 kV in the laboratory "Parasites and Mediterranean Ecosystems" in the University of Corsica (Corte, France).

During examination of sections of *D. brusinae*, hyperparasite microsporidia were found in connective tissue and intestinal cells.

RESULTS

Site of infection (Figs 1, 2)

The microsporidium infects intestinal cells (Fig. 1) and connective tissue (Fig. 2). All development stages are in close contact with the cytoplasm of the host cell.

Development stages (Figs 3-14)

Meronts (Fig. 3): They are more or less spherical cells with two or four nuclei in diplokaryotic arrangement. The meronts are surrounded by a single plasma membrane. Their cytoplasm is electron-light and contains some endoplasmic reticulum cisternae and free ribosomes. In longitudinal section, the diplokaryon occupies three quarters of the cell. The nuclear envelope is rather difficult to observe. Mostly, the nuclear envelope appears clearly only where the two nuclei of the diplokaryon are adjacent. However, the nucleoplasm, electron-dense, always allows us to distinguish the diplokaryon of the cytoplasm which surrounds it.

During the meront division, both nuclei constituting the diplokaryon divide simultaneously. The first demonstration of this division is the appearance of one then two spindle plaques on the surface of the nuclear envelopes (Fig. 3). These spindle plaques appear in the shape of a superficial depression of the nuclear envelope underlined by an internal layer of electron-dense material. Prior to the division of the cytoplasm, the spindle plaques migrate bringing about the elongation then the division of diplokaryon. So, it appears temporarily meronts with two diplokarya.

Sporonts (Figs 4, 5): The transformation of meronts into sporonts is realized by the appearance of a wall outside the plasma membrane. The sporonts are thus recognizable by an electron-dense thick envelope (≈ 300 Å) and an elongated shape. They always contain reticulum endoplasmic cisternae, free ribosomes and one or two diplokarya.

The division process of sporonts is similar to that of the meronts. Two spindles plaques appear on the nuclear envelope of each nucleus (Fig. 4). Nucleus elongates simultaneously then divides by central constriction prior to the cytoplasm division (Fig. 5). So, it forms in a moment sporonts with two diplokarya.

Sporoblasts (Figs 6-8): The division of sporonts gives rise to two sporoblasts. Each sporoblast, like the other stages of development, possesses a diplokaryon. They are elongated and surrounded by a thick envelope of about 350 Å. Their cytoplasm is electron-dense. The evolution of the sporoblast begins with the genesis of the polar filament and with the appearance of a vacuole, in contact to a dictyosome. This vacuole serves as matrix for the internal parts of the polar filament (Fig. 6). In transverse section, the young polar filament presents a thick envelope, a clear layer and an electron-dense central axis. In longitudinal section, the old sporoblasts possess a polar filament with 7 to 8 coils around the diplokaryon (Fig. 7). However, some abnormal sporoblasts are observed with a polar filament arranged in 13 to 16 coils (Fig. 8).

Spores (Figs 9-14): Fresh spores are not observed. Our study was exclusively realized in electron microscopy. Spores appear ovoid in shape and possess a diplokaryon (Fig. 9). On 28 spores measured in cross and longitudinal sections, the average size is 2.1 ± 0.3 µm with a minimum of 1.4 µm and a maximum of 2.6 µm in length and 1.4 ± 0.2 µm with a minimum of 1.1 µm and a maximum of 2.1 µm in width. The spore envelope is composed of an electron-dense exospore of 220 ± 80 Å thick and an electron-lucent endospore of 475 ± 225 Å thick. Several elements are recognizable inside the spore: a diplokaryon, a polar filament with an anchoring disc, a polaroplast and a posterior vacuole (Figs 9-11).

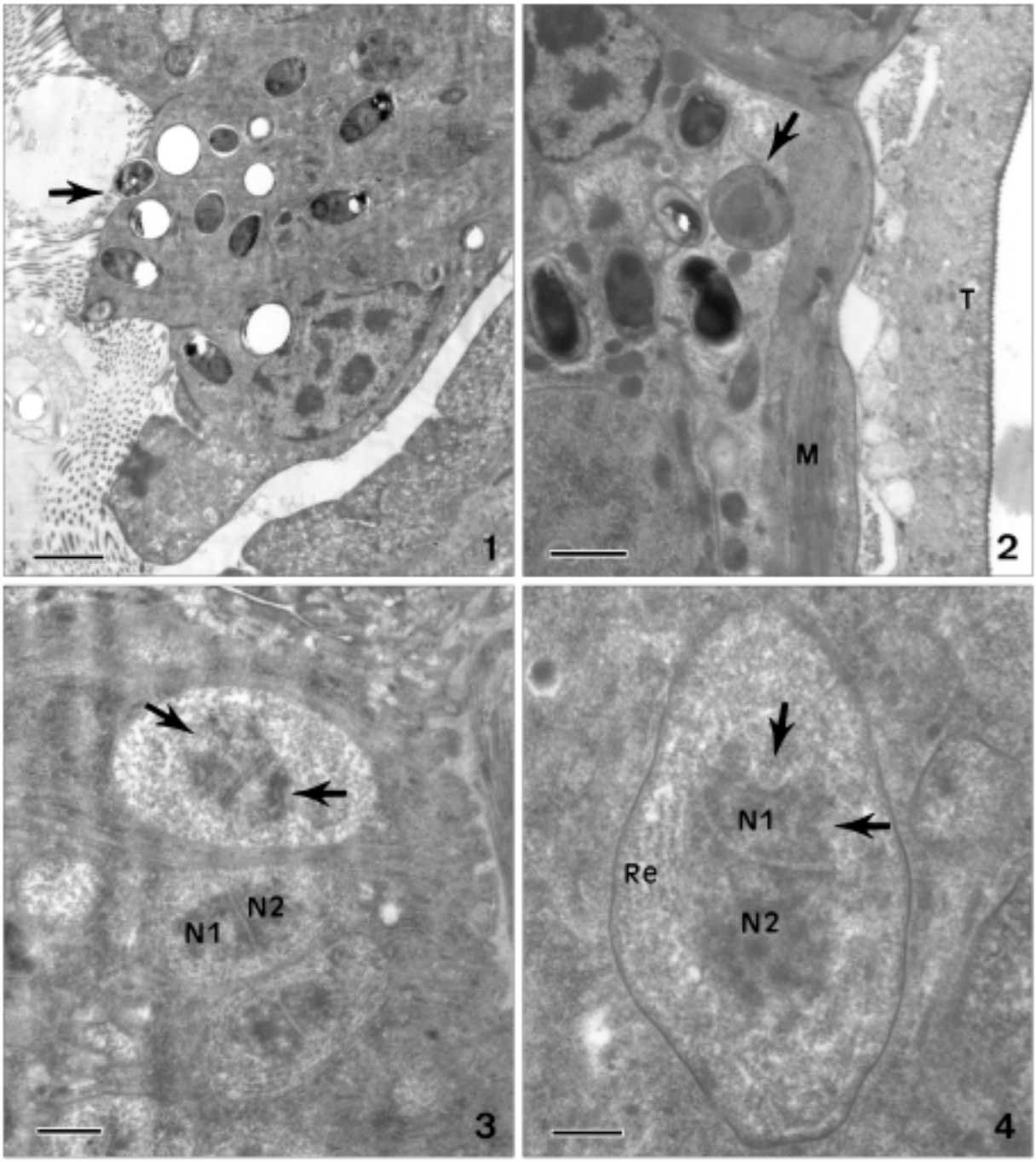

Figs 1-4. Electron micrographs of *Nosema diphterostomi* sp. n. **1** - gut epithelial cells of *D. brusinae* infested by *N. diphterostomi* (arrow); **2** - connective tissues containing *N. diphterostomi* (arrow); **3** - meronts showing the spindle plaques (arrows) and diplokaryon (N1 and N2); **4** - sporont with the electron-dense membrane and the spindle plaques (arrows). M - muscle, N1, N2 - diplokaryon, Re - endoplasmic reticulum, T - tegument. Scale bars 2.5 µm (1); 1.5 µm (2); 1 µm (3); 0.5 µm (4).

The polar filament is about 100 nm in diameter. It is isofilar, possesses a short rectilinear proximal part followed by an important helical distal part describing 6 to 7 coils around the diplokaryon. In its proximal part, the polar filament expands slightly before fusing with the anchoring disc (Fig. 10).

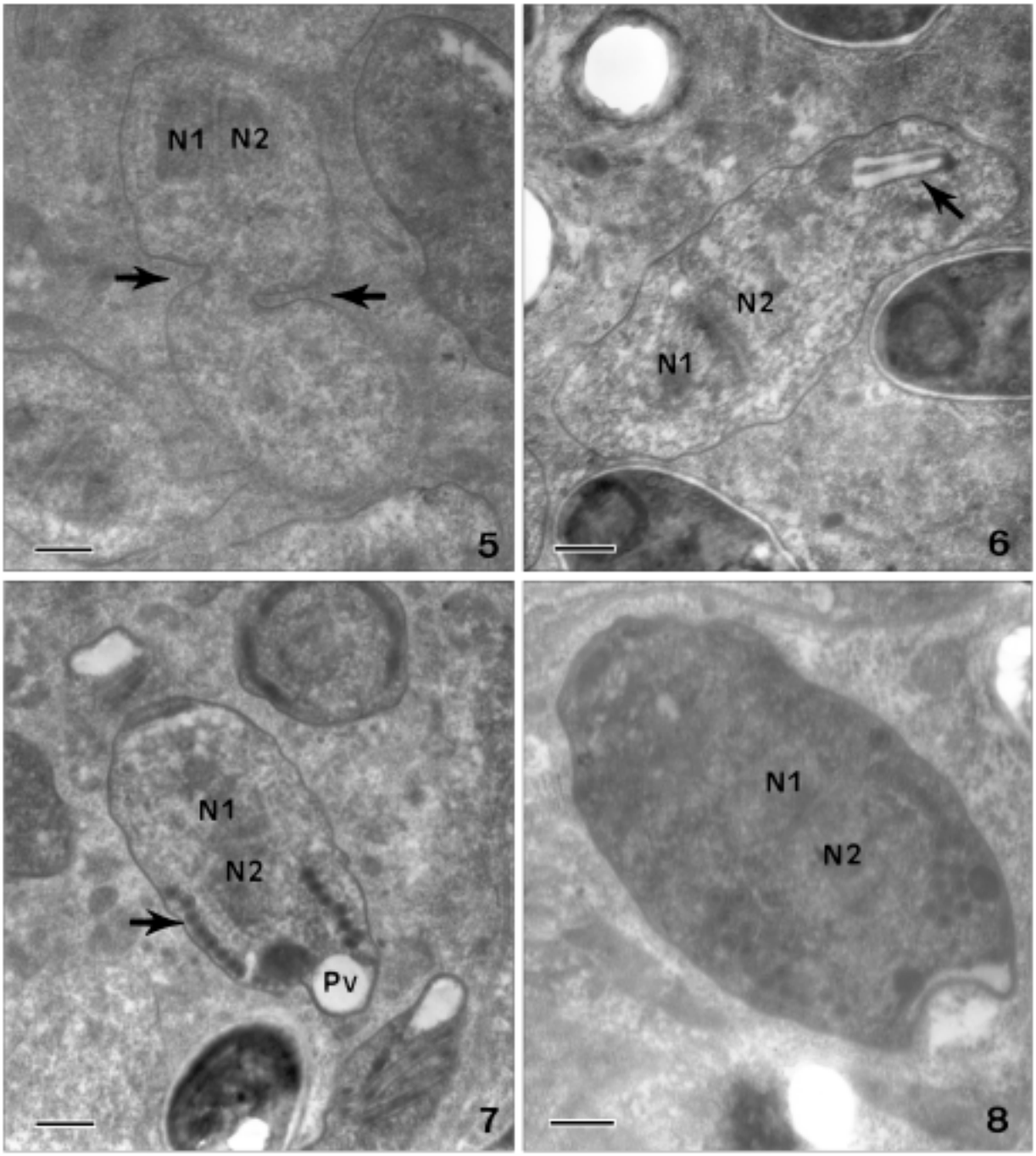

Figs 5-8. Electron micrographs of sporogony and sporogenesis of *N. diphterostomi* sp. n. **5** - division of sporonts with the strangulation of the cytoplasm (arrows); **6** - young sporoblast showing the formation of the polar filament (arrow); **7** - mature sporoblast containing polar filament with 7 to 8 coils (arrow); **8** - abnormal sporoblast with 13 to 16 coils of polar filament. N1, N2 - diplokaryon, Pv - posterior vacuole. Scale bars 0.5 µm.

The polaroplast (Figs 10-12) presents two lamellar parts: an outer electron-dense part made up of closely arranged membranes encircling a less electron-dense inner part constituted of more loosely arranged membranes.

An electron-lucent vacuole occupies the posterior end of the spore (Fig. 13). A few spores, in the process of emergence, were observed emptying of their content (Fig. 13). In this case, the envelope, which conserved its initial organization, presents a distinct fusion between its

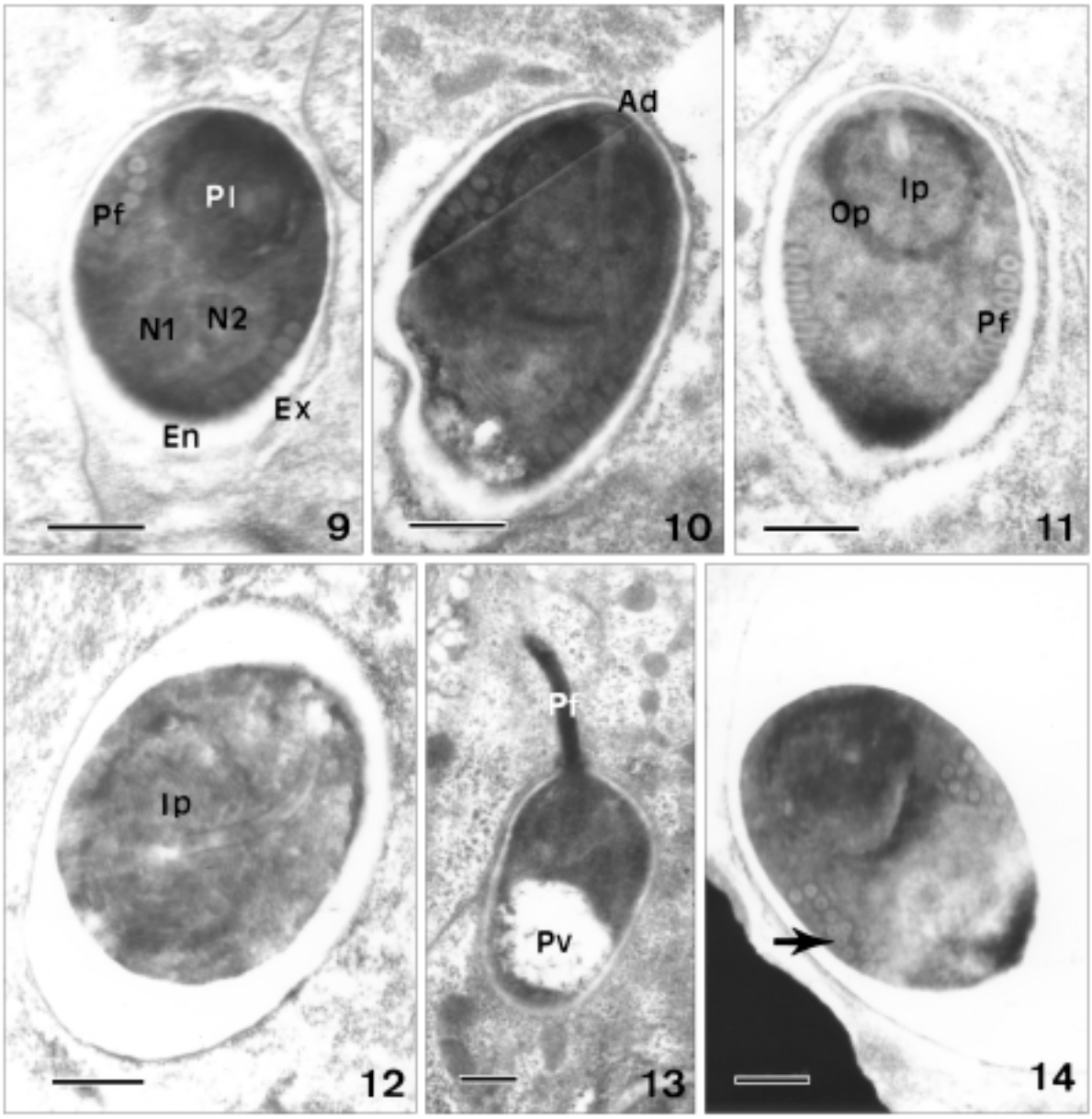

Figs 9-14. Electron micrographs of spores of *N. diphterostomi* sp. n. **9** - spore showing the diplokaryon (N1, N2), the exospore (Ex), the endospore (En), the polar filament (Pf) and the polaroplast (Pl); **10** - mature spore with anchoring disc (Ad); **11** - spore showing the inner (Ip) and the outer parts (Op) of the polaroplast. Pf: polar filament; **12** - section of the spore showing the lamellae of the inner (Ip) part of the polaroplast; **13** - extrusion of the polar filament (Pf) in the host cell. Pv - posterior vacuole; **14** - abnormal spore with 13 to 14 polar tube coils (arrow). Scale bars 0.5 µm.

endospore and its exospore at the spore opening level. The polar filament, turned like a finger glove, is then observed in the cytoplasm of the host cell. Inside the spore, the posterior vacuole swells, causing the extrusion of the spore content along the canal formed by the polar filament.

Abnormal spores presenting a polar filament with 13 to 14 coils were observed (Fig. 14). These spores are bigger than the most numerous spores considered as normal. They measure 3.5×2.2 µm.

DISCUSSION

The ultrastructural characteristics and the developmental cycle of the microsporidium, parasite of the

Table 1. *Nosema* species hyperparasites of trematodes.

Species	Type host	Hyperparasite	Spore mesurations	Localities	References
Nosema dollfusi	*Bucephalus cuculus*	*Crassostrea virginica*	3 × 1.7 µm	Maryland USA	Sprague 1964
Nosema eurytremae	*Eurytrema pancreaticum*; *Postharmostomum gallinum*	*Bradybaena similaris*	3.94 × 2.26 µm	Malaysia	Colley *et al.* 1975
Nosema gigantica	*Allocreadium fasciatusi*	*Aplocheilus melastigma*	7.9 × 4.9 µm	India	Canning and Madhavi 1977
Nosema xiphidiocercariae	Plagiorchiidae	*Lymnae palustris*	4.5 × 2.3 µm	Moscow Russia	Sprague 1977
Nosema lepocreadii	*Lepocreadium manteri*	*Leuresthes tenuis*	3.5 × 1.5 µm	San Diego USA	Canning and Olson 1980; Canning *et al.* 1983
Nosema diphterostomi sp. n.	*Diphterostomum brusinae*	*Diplodus annularis*	2.1 × 1.4 µm	Corsica, France	Present study

trematode *D. brusinae*, present all criteria of the genus *Nosema* Naegeli, 1857 described by Sprague (1977). All ultrastructural features of spores of the genus *Nosema* were specified by Sato *et al.* (1982) and Canning and Vavra (2000).

To our knowledge, 16 microsporidia species were described in trematodes, but among these species, only five belong to the genus *Nosema* (Table 1). They are *Nosema dollfusi* Sprague, 1964, *Nosema eurytremae* Canning, 1972, *Nosema xiphidiocercariae* Voronin, 1974, *Nosema gigantica* Canning *et* Madhavi, 1977, and *Nosema lepocreadii* Canning *et* Olson, 1980.

Nosema dollfusi was described in the sporocysts of *Bucephalus cuculus*, parasite of the oyster *Crassostrea virginica* from Maryland in USA. These spores are binucleate and measure 3 × 1.7 µm in stained preparations (Sprague 1964). The merogony and the sporogony were not described. This *Nosema* differs from the present species by the spore size and by its host which, in larval stage, parasitizes a mollusc. Nevertheless, this trematode, in adult stage, parasitizes a fish (Gibson *et al.* 2001). Thus, it is very likely that this microsporidium is also present in adult trematode when it is parasite of fish. Probably, there is a transovarial transmission.

Nosema eurytremae presents a wide host spectrum, but was first described as a hyperparasite of larvae of the trematodes *Eurytrema pancreaticum* and *Postharmostomum gallinum* in the land snail *Bradybaena similaris* in Malaysia. It was studied in electron microscopy by Colley *et al.* (1975). According to these authors, fresh spores measure 3.94 × 2.26 µm. The spore wall is about 250 nm thick except at the level of the anchoring disc where it is approximately 80 nm thick. The polar filament makes 11 to 12 coils. The polaroplast presents an anterior part composed of laminated and dense membranes and a posterior part formed by flattened sacs. This *Nosema* is different from the present species by the size and ultrastructure of its spores but also by the fact that it lives in larva parasite of land snail. It must be also present in adult parasites of land animals (birds, mammals).

Nosema xiphidiocercariae is hyperparasite of sporocyst, cercaria, metacercaria in Plagiorchiidae parasite of *Lymnaea palustris*, freshwater mollusc in Russia. These fresh spores measure 4.5 × 2.3 µm and the spores, stained with Giemsa, measure 4.0 × 2.3 µm (Sprague 1977). This *Nosema* differs from the present species by the spore size and by the fact that its host lives in a freshwater mollusc. The microsporidium must be present in the adult trematode, parasite of freshwater fish.

Nosema gigantica infests adult of *Allocreadium fasciatusi*, parasite of *Aplocheilus melastigma* a freshwater fish in India. The ultrastructural data of its devel-

opment stages are not available. Its spores stained with Giemsa measure 7.9 × 4.9 µm (Canning and Madhavi 1977). It differs from the present species by the spore size and by the fact that its host lives in a freshwater animal.

Nosema lepocreadii was described in adult of *Lepocreadium manteri*, parasite of *Leuresthes tenuis* a marine fish in San Diego (USA). It was studied in electron microscopy by Canning *et al.* (1983). Its sporogony is disporoblastic but sometimes polysporoblastic. Its fresh spores measure 3.5 × 1.5 µm, possess a polar filament with 10 coils and a polaroplast with an anterior granular part and a lamellar posterior part (Canning and Madhavi 1977, Canning *et al.* 1983). It is different from our species by its sporogony, the size and the ultrastructure of its spores.

Other microsporidia, initially classified in the genus *Nosema* and living in adult trematodes parasites of marine animals, were described. There are *Microsporidium distomi* Lutz *et* Splendore, 1908 (Canning 1975) and *Microsporidium spelotremae* Guyénot, Naville *et* Ponse, 1925 (Canning 1975).

Microsporidium distomi was described in adult trematode *Distomum lingulata*, parasite of the amphibian *Bufo marinus*. These spores measure 2.0 × 0.8-1µm (Sprague 1977). It was transferred by Canning (1975) in the *Microsporidium* group because it forms cysts and its development stages were not described.

Microsporidium spelotremae is hyperparasite of *Spelotrema carcini* parasite of the crab *Carcinus maenas*. Its fresh spores measure 3.5 × 1.5 µm and fixed measure 2.6-3 × 1.3-1.5 µm (Sprague 1977). It was moved by Canning (1975) in the *Microsporidium* group because its spores are sometimes grouped and its development stages were not described.

The present *Nosema* parasitizes essentially the epithelial gut. According to Larsson (1999), the digestive tissue is the first reached by the microsporidia. Next, the spores are going to extrude their polar filament to infect new tissues (Berrebi 1978). This polar filament extrusion is possible by an osmotic pressure increase inside the spore (Lom and Vavra 1963, Weidner and Byrd 1982). This hatching process of the spore was described at length by Toguebaye and Marchand (1987) in *Nosema couilloudi*.

An ultrastructural peculiarities of this new *Nosema* is the polaroplast organization. Such a polaroplast was observed in *Ameson atlanticum* parasite of the crab *Cancer pagurus* (Vivares and Azevedo 1988).

The *Nosema*, described here, differs from all *Nosema* species known in the trematodes. This species is new and we name it *Nosema diphterostomi* sp. n. after the type host, *Diphterostomum brusinae*.

Taxonomic summary

Type host: *Diphterostomum brusinae* (Digenea, Zoogonidae).

Type locality: Bonifacio Strait Marine Reserve, Corsican Mediterranean Coast.

Sites of infection: Intestinal cells and connective tissue.

Life cycle stages: Diplokaryotic. In close contact with the host cell cytoplasm.

Spores: Ovoid. 2.1 × 1.4 µm. Isofilar polar filament with 6-7 coils. Polaroplast with an outer part and a lamellar inner part. Posterior vacuole with amorphous electron-dense content.

Material deposited: In the laboratory "Parasites and Mediterranean Ecosystems" in the University of Corsica (France) No 72928, 10/03.

Etymology: Specific name alludes to the host genus.

Remarks: *N. diphterostomi* is a hyperparasite of the fish *Diplodus annularis* (Sparidae).

Acknowledgements. The study was partially supported by the "Bonifacio Strait Marine Reserve" and by a grant of INTERREG III. We thank the fishermen of the "Bonifacio Strait Marine Reserve" for biological material.

REFERENCES

Azevedo C., Canning E. U. (1987) Ultrastructure of a microsporidian hyperparasite, *Unikaryon legeri* (Microsporida), of trematode larvae. *J. Parasitol.* **73:** 214-223

Berrebi P. (1978) Contribution à l'étude biologique des eaux saumâtres du littoral méditerranéen français. Biologie d'une microsporidie: *Glugea atherinae* n. sp., parasite de l'athérine *Atherina boyeri* Risso, 1810 (Poisson, Téléostéen) des étangs côtiers. Thèse de 3ème cycle U.S.T.L., Montpellier, 1-196

Canning E. U. (1975) The microsporidian parasites of Plathelminthes: their morphology, development, transmission and pathogenicity. Commonwealth Institute of Helminthology, Misc. Publi. N°2, 1-32

Canning E. U., Madhavi R. (1977) Studies on two new species of Microsporidia hyperparasitic in adult *Allocreadium fasciatusi* (Trematoda, Allocreadiidae). *Parasitology* **75:** 293-300

Canning E. U., Olson A. C. (1980) *Nosema lepocreadii* sp. n., a parasite of *Lepocreadium manteri* (Digena: Lepocreadiidae) from the gut of the California Grunion, *Leuresthes tenuis*. *J. Parasitol.* **66:** 154-159

Canning E. U., Vavra J. (2000) Phylum Microsporidia. In: The Illustrated Guide to the Protozoa. 2nd edition, Society of Protozoologists, Allen Press Inc., Lawrence, USA, 39-126

Canning E. U., Olson A. C., Nicholas J. P. (1983) The ultrastructure of *Nosema lepocreadii* Canning and Olson, 1979 (Microspora, Nosematidae) and its relevance to the generic diagnosis of *Nosema* Nägeli, 1857. *J. Parasitol.* **69:** 143-151

Colley F. C., Lie K. J., Zaman V., Canning E. U. (1975) Light and electron microscopical study of *Nosema eurytremae*. *J. Invert. Pathol.* **26:** 11-20

Gibson D. I., Jones A., Bray R. A. (2001) Keys to the Trematoda. CABI Publishing and the Natural History Museum, 1-521

Larsson J. I. R. (1999) Identification of Microsporidia. *Acta Protozool.* **38:** 161-197

Lom J., Vavra J. (1963) The mode of sporoplasm extrusion in microsporidian spores. *Acta Protozool.* **1:** 81-89

Reynolds E. S. (1963) The use of lead citrate at high pH as an electron-opaque stain in electron microscopy. *J. Cell Biol.* **17:** 208-212

Sato R., Kobayashi M., Watanabe H. (1982) Internal structure of spores of microsporidians isolated from the silkworm, *Bombyx mori*. *J. Invert. Pathol.* **40:** 260-265

Sprague V. (1964) *Nosema dollfusi* n. sp. (Microsporidia, Nosematidae), a hyperparasite of *Bucephalus cuculus* in *Crassostrea virginica*. *J. Protozool.* **11:** 381-385

Sprague V. (1977) Annotated list of species of Microsporidia. In: Comparative Pathobiology, Vol. 2, Systematics of the Microsporidia, (Eds. Lee A. Bulla Jr and Thomas C. Cheng.). Plenum Press, New York, 31-334

Toguebaye B. S., Marchand B. (1987) Intracellular emergence of the microsporidian sporoplasm as revealed by electron microscopy in *Nosema couilloudi* (Microspora, Nosematidae). *Arch. Protistenk.* **134:** 397-407

Vivares C. P., Azevedo A. (1988) Ultrastructural observations of the life cycle stages of *Ameson atlanticum* sp. nov., a microsporidian parasitizing *Cancer pagurus* L. J. *Fish Diseases* **11:** 379-387

Weidner E., Byrd W. (1982) The microsporidian spore invasion tube. II. Role of calcium in activation of tube discharge. *J. Cell Biol.* **93:** 970-975

Received on 12th February, 2004; revised version on 31st May, 2004; accepted version on 1st June, 2004

Acta Protozool. (2004) 43: 337 - 343

ACTA
PROTOZOOLOGICA

Description of Three New Myxosporean Species (Myxozoa: Myxosporea: Bivalvulida) of the Genera *Myxobilatus* Davis, 1944 and *Myxobolus* Bütschli, 1882

Saugata BASU[1, 2] and Durga P. HALDAR[1]

[1]Protozoology Laboratory, Department of Zoology, University of Kalyani, Kalyani; [2]Department of Biology, Uttarpara Govt. High School, Uttarpara, Hooghly, West Bengal, India

Summary. The present communication describes three new species of myxosporeans (Myxozoa: Myxosporea: Bivalvulida), *Myxobilatus odontamblyopusi* sp. n., *Myxobolus catmrigalae* sp. n. and *M. buccoroofus* sp. n. from *Odontamblyopus rubicundus* (Hamilton- Buchanan), Catla-Mrigal hybrid carp [male parent fish *Catla catla* (Hamilton-Buchanan) × female parent fish *Cirrhinus mrigala* (Hamilton-Buchanan)] and *Labeo bata* (Hamilton-Buchanan) of West Bengal, India, respectively. Spores of the new myxobolid species are resolved by LM and SEM.

Key words: *Myxobilatus odontamblyopusi* sp. n., *Myxobolus buccoroofus* sp. n., *M. catmrigalae* sp. n., Myxozoa, India.

Abbreviations: LCP - length of caudal filament, LP - length of polar capsule, LPC - larger polar capsule, LS - length of spore, LSCP - length of spore with caudal prolongation, PC - polar capsule, SP - spore, SPC - smaller polar capsule, WP - width of polar capsule, WS - width of spore.

INTRODUCTION

Myxobilatus odontamblyopusi sp. n., *Myxobolus catmrigalae* sp. n. and *M. buccoroofus* sp. n. from *Odontamblyopus rubicundus* (Hamilton-Buchanan), Catla-Mrigal hybrid carp [male parent fish *Catla catla* (Hamilton-Buchanan) × female parent fish *Cirrhinus mrigala* (Hamilton-Buchanan)] and *Labeo bata* (Hamilton-Buchanan) of West Bengal, India, respectively, are described in the present study. The descriptions of these three myxosporeans are in accordance with the guidelines of Lom and Arthur (1989) and Lom and Dyková (1992).

MATERIALS AND METHODS

Host fishes (total number of host fishes examined are mentioned separately in taxonomic summary) were collected alive from the local fish markets (type locality mentioned separately in taxonomic summary) and brought to the laboratory and necropsied immediately. Sporogonic plasmodia, when found, were carefully removed with sterile forceps, smeared on clean grease-free slides with drops of 0.5% NaCl solution, covered with cover slips and sealed with bee's

Address for correspondence: Durga P. Haldar, Protozoology Laboratory, Department of Zoology, University of Kalyani, Kalyani-741235, West Bengal, India; Fax: 91-33-2582 8282; E-mail: saugata4070@vsnl.net

wax for examination under the oil immersion lens of Olympus CH-2 phase contrast microscope. Some of the fresh smears were treated with various concentrations (2-10%) of KOH solution for the extrusion of polar filaments. The India ink method of Lom and Vavrá (1963) was employed for observing the mucous envelope of spores. For permanent preparations, air-dried smears were stained with Giemsa after fixation in acetone-free absolute methanol. Measurements (based on twenty fresh spores treated with Lugol's iodine) were determined with aid of a calibrated ocular micrometer. All measurements are presented in µm as mean ± SD followed in parentheses by the range. Drawings were made on fresh / stained materials with the aid of a camera lucida (mirror type) and computer programme Corel Draw 9.0. Spore surface was visualized by means of SEM.

RESULTS AND DISSCUSION

Myxobilatus odontamblyopusi sp. n. (Figs 1-8)

Plasmodia: Sporogonic plasmodia encased within hosts' cells appearing as 'cysts' are yellowish-white in colour, elongately ellipsoidal in shape and measure 0.77-1.56 mm × 0.66-1.44 mm. They are attached to almost all the gill filaments in heavily infected fishes.

In the early developmental stages the uninucleate pansporoblasts are scanty. Uninucleate stages (Fig. 1) range from 2.5 to 3.4 in diameter. The nuclei are karyosomatic. With Giemsa the karyosome appears as a small central or eccentric body staining deep red. Binucleate forms (Fig. 2) have a large and a small nuclei and measure 3.7 by 2.9. Tetranucleate ones (Fig. 3), ranging from 5.7 to 6.8 in diameter, possess two large and two small nuclei. Spore forming pansporoblasts (Fig. 4) measure 16 by 12. These have twelve karyosomatic generative nuclei and four somatic residual nuclei which are not, however, always apparent. Developing spores are aligned either posterior end to anterior end or anterior end to anterior end in disporous pansporoblasts.

Spore: Spores are histozoic. Developing spores (Fig. 5) are round to oval in shape, are devoid of caudal filaments, have 3 or 4 filament coils with each polar capsule. Developed spores (Figs 6-8) are 9.0 ± 0.49 (8.1-10.3) × 5.2 ± 0.41 (4.8-6.3) and are lanceolate in valvular view with pointed anterior and posterior ends (Figs 6, 8). The broadest biconvex point lies at or just anterior to posterior end of polar capsules. Spores are oval with one side convex and other flat as seen in sutural plane (Fig. 7). The spore body is divided into two nearly equal halves by straight sutural ridge (~ 0.4 in width) (Figs 6, 8). Spore valves are moderately thick. Surface of valves are with faint longitudinal striations (Fig.7). The spore valves extend posteriorly into two long [length 20.6 ± 1.85 (17.9-24.9)] equal tapering processes (Figs 6, 8) which are separate throughout the entire length, thereby clearly fulfiling the character of the genus *Myxobilatus* as proposed by Davis (1944). These caudal prolongations are transparent in fresh condition and take deep blue colour when stained in giemsa.

Two equal pyriform polar capsules [3.4 ± 0.29 (3.0-3.9) × 2.1 ± 0.14 (1.9-2.5)] are situated in a plane perpendicular to that of suture (Figs 6, 8). In some cases almost completely extruded polar filaments have been seen (Fig. 8), in others the filaments form 5-6 spiral coils in each polar capsule (Fig. 6).

The granular homogenous mass of sporoplasm occupies the space between and behind the polar capsules but does not extend on the sides of the polar capsules (Figs 6, 8). Iodinophilous vacuole is absent. There are two oblong sporoplasmic nuclei [diameter 1.3 ± 0.12 (1.2-1.7)], lying side by side in the sporoplasm (Figs 6, 8).

Spore index:

LS: WS = 1: 0.578
LSCP: LS = 1: 0.436
LSCP: LCP = 1: 0.558
LP: WP = 1: 0.618
LS: LP = 1: 0.378
WS: WP = 1: 0.404

Taxonomic affinities: Davis (1944) has revised the genus *Henneguya* and proposed to divide it into three genera i.e. (1) *Henneguya*, (2) *Unicauda* and (3) *Myxobilatus*. In India, this is the third record of the genus *Myxobilatus* and the first from the gills of any estuarine fish. The other two species are *Myxobilatus mastacembeli* Qadri *et* Lalitha Kumari, 1965 from the intestine of the fresh water fish, *Mastacembelus armatus* (Lacépèdes) and *Myxobilatus fossilis* Susha *et* Janardanan, 1994 from the urinary bladder of *Heteropneustus fossilis* (Bloch).

The present species of *Myxobilatus* resembles, in size and/or in shape, *M. legeri* Cépède, 1905; *M. wisconsinensis* Mavor *et* Strasser, 1916; *M. sinipercae* Dogiel *et* Akhmerov, 1960; *M. pseudorasborae* Shulman, 1962; *M. varicorhini* Kandilov, 1963; *M. noturi* Guilford, 1965; *M. cotti* Guilford, 1965; and *M. yukonensis* Arthur *et* Margolis, 1975.

Of these *Myxobilatus* species the spores of *M. sinipercae* (LSCP: 45-50); *M. varicorhini* (LSCP: 28-31); *M. cotti* (LSCP: 30.0-98.4); *M. yukonensis* (LSCP: 16.7-36.2) are larger than the present species. Spores of *M. pseudorasborae* closely resemble the spores of present species in the spore length (length

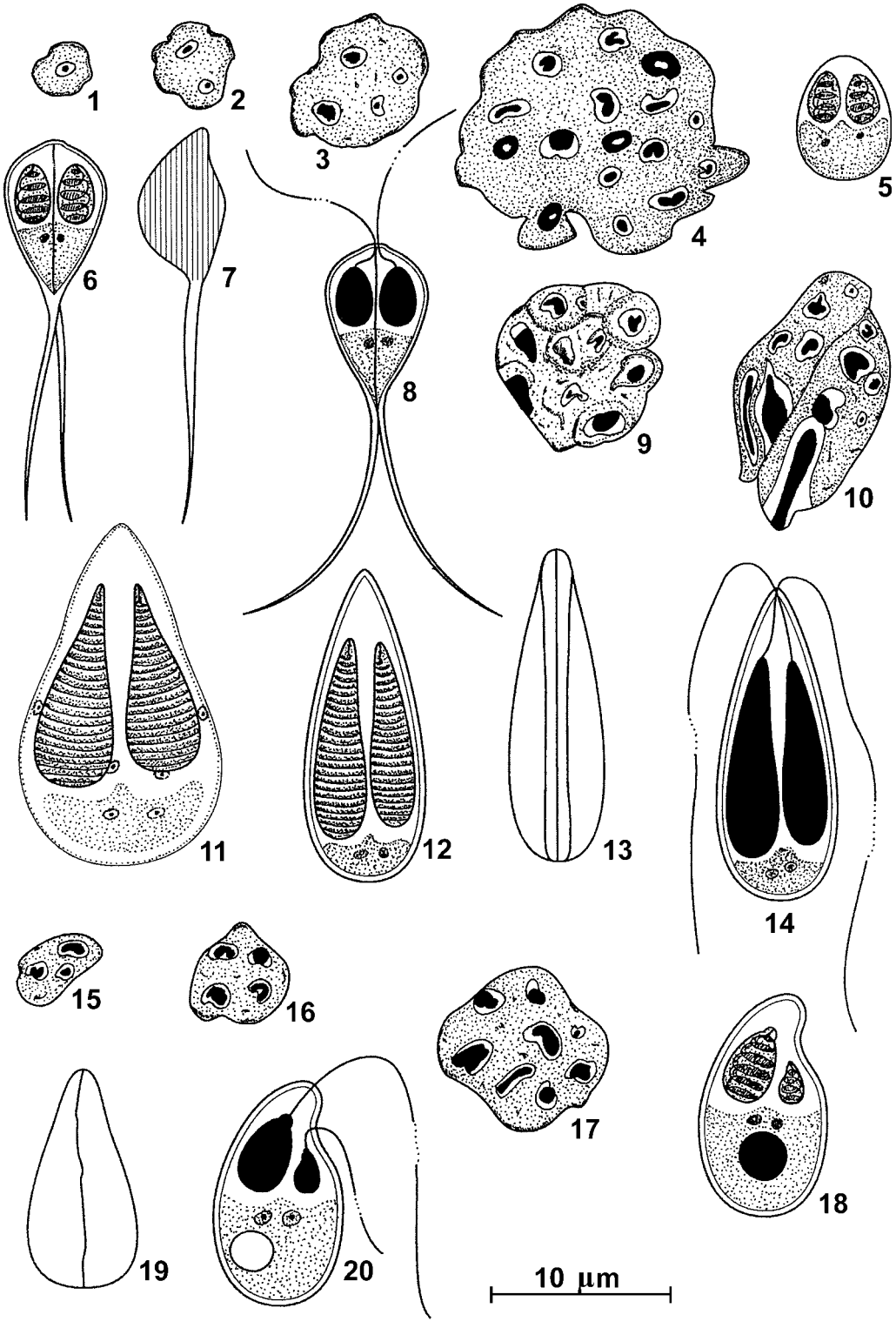

Figs 1-20. Camera lucida drawings of plasmodia and spores. **1-8** - *Myxobilatus odontamblyopusi* sp. n.; **1-4** - pansporoblasts; **5** - fresh developing spore in valvular view; **6** - fresh developed spore in valvular view; **7** - fresh developed spore in sutural view; **8** - fixed developed spore in valvular view with extruded polar filaments. **9-14** - *Myxobolus catmrigalae* sp. n.; **9-10** - late developmental stages; **11**- fresh developing spore in valvular view; **12** - fresh developed spore in valvular view; **13** - fresh developed spore in sutural view; **14** - fixed developed spore in valvular view with extruded polar filaments. **15-20** - *Myxobolus buccoroofus* sp. n.; **15-17** - pansporoblasts; **18** - fresh developed spore in valvular view; **19** - fresh developed spore in sutural view; **20** - fixed developed spore in valvular view with extruded polar filaments. Lugol's iodine: 1-7, 9-13, 15-19; Giemsa: 8, 14, 20. Scale bar 10 µm.

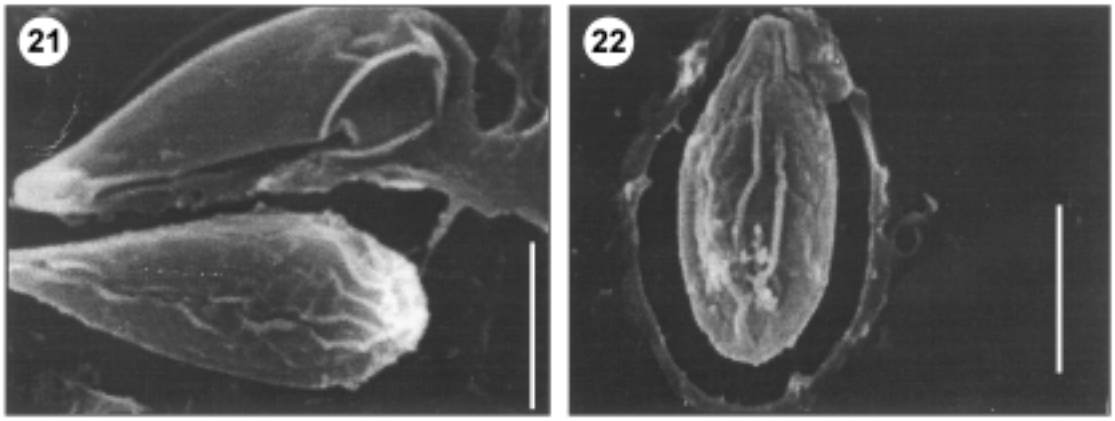

Figs 21, 22. 21 - *Myxobolus catmrigalae* sp. n. spore; **22 -** *Myxobolus buccoroofus* sp. n. spore. SEM. Scale bars 10 µm.

range in *M. pseudorasborae* is 9.8-12). But the caudal processes and polar capsule dimensions are much smaller in the latter species (in *M. pseudorasborae* caudal processes and polar capsule dimensions are 19.5-22.5 and 5.0-6.5 × 2.6 respectively). Polar capsule dimensions in *M. wisconsinensis* (3.5 × 2.5) closely resemble to that of present species under discussion. But the shape and dimensions of the spore of former species is different (spore dimension in *M. wisconsinensis* is 11.5 × 7.0). The spores of *M. legeri* (LSCP: 19.5-22.5, SP: 8.5-11 × 6-8, PC: 2.8-3.5 × 2.0) and *M. noturi* (LSCP: 18.6-28.0, SP: 7.2-10.8 × 6.0-7.2, PC: 4.2-5.4 × 2.5) show much similarity with the present species. However, spore width in both of the former two species is distinctly larger than the species under study. Furthermore, the oval spores of *M. legeri* with slightly tapered anterior end lack any valvular striations which are present in the lanceolate anteriorly pointed spores of the present species. Although spores of *M. noturi* have valvular striations, but the shape of the spore (oval with rounded anterior end) is strongly different from the species under discussion. Moreover, the present species is histozoic (all other species referred to above are coelozoic) and its site of infection is not associated with urinary tract which is typical of all species described above.

The present species is also compared with the first Indian described species of *Myxobilatus, M. mastacembeli* Qadri *et* Lalitha Kumari, 1965 described from a fresh water fish *Mastacembelus armatus* (Lacépèdes). The spore dimensions (SP: 8.5-12.5 × 4.6-6.2; LCP: 15-28) and the shape and dimensions of polar capsule (PC: 3.1-3.9 × 1.5-1.9) of *M. mastacembeli* closely resemble the present species. But the flattened and elongated spores of *M. mastacembeli* with rounded anterior end is distinctly different from the present one (present spores are lanceolate with pointed anterior and posterior extremities). In addition, the valvular striations are lacking in the former species which is a taxonomically important character of *M. odontamblyopusi* sp. n. Furthermore, the host range, site of infection and the geographical location of the host are different.

According to Lom and Dyková (1992), histozoic myxobilatid spp. may also be found as in the present instance although majority described species are coelozoic in nature.

After careful comparison with all species described so far, it is proposed to establish a new species for this myxozoan and the name *Myxobilatus odontamblyopusi* sp. n. is assigned to it in this communication.

Taxonomic summary

Type host: *Odontamblyopus rubicundus* (Hamilton-Buchanan). Host family: Gobioididae.

Type locality: Canning (Latitude: 22°20´ N, Longitude: 88°40´ E), 24 Parganas (South), West Bengal, India.

Type specimens: Paratypes are spores stained in Giemsa, in the collection of Harold W. Manter Laboratory of Parasitology, Nebraska, USA, No. HWML 16704.

Prevalence of infection: 44/254 (17.32 %).

Etymology: The species epithet *odontamblyopusi* is from the name of its type host *Odontamblyopus rubicundus* (Hamilton-Buchanan).

***Myxobolus catmrigalae* sp. n. (Figs 9-14, 21)**

Plasmodia: Fully developed creamy white coloured plasmodia appear on the gill lamellae as spherical 'cyst', contain few late developmental stages (Figs 9-10), developing spores (Fig. 11) and developed spores (Figs 12-14, 21).

Spore: Developing spores (Fig. 11) are elongately pyriform or large tear shaped bodies in valvular view with broadly rounded posterior end. These measure 20.4 ± 0.38 (20.0-21.8) × 16.3 ± 0.29 (15.7-17.1). Two unequal polar capsules are also elongated and pyriform. The dimension of larger polar capsule is 14.7 ± 0.42 (12.9-15.3) × 7.1 ± 0.25 (5.2-8.1) and that of smaller polar capsule is 11.8 ± 0.18 (10.2-12.7) × 5.6 ± 0.31 (4.8-5.9). All the six nuclei (i.e., two each of valvogenic, capsular and sporoplasmic) are seen in Giemsa stain preparation.

Developed spores (Figs 12-14) are 18.8 ± 0.47 (17.8-19.5) × 5.9 ± 0.16 (5.7-6.2) are elongated and pyriform in valvular view (Figs 12, 14) and lenticular in sutural view (Fig.13) with a straight thin sutural line. The spore is bluntly pointed anteriorly with a rounded posterior end (Figs 12, 14). The two shell valves are smooth, symmetrical and thin-walled (Fig.13). Two anteriorly situated pyriform polar capsules run parallel to each other but sometimes converge slightly towards the anterior end (Figs 12-14). One polar capsule is slightly larger [11.9 ± 0.25 (11.6-12.4) × 2.5 ± 0.13 (2.2-2.7)] than the other [11.0 ± 0.16 (10.7-11.3) × 2.3 ± 0.13 (2.0-2.5)] and they occupy almost 4/5th part of the spore cavity. Polar filaments make 22-25 and 21-23 coils in the larger and smaller polar capsules respectively (Fig. 12). When extruded, the polar filaments always cross at the tip of the spore (Fig. 14). Granular homogeneous binucleate sporoplasm fills the extracapsular space of the spore cavity. There is no iodinophilous vacuole and mucus envelope around the spore is also absent.

The spore surface is smooth and devoid of mucous (Fig. 21). The sutural line, formed by the fused thick edges of each valve, is generally straight or slightly curved. Preparation technique apparently caused shrinkage of the valves along both sides of the sutural line.

Spore index:

LS: WS = 1: 0.314
LLPC: WLPC = 1: 0.210
LSPC: WSPC = 1: 0.209
LLPC: LSPC = 1: 0.924
WLPC: WSPC = 1: 0.92

Taxonomic affinities: The present myxozoan species resembles *Myxobolus* (=*Myxosoma*) a*nurus* (Cohn, 1895) Lom *et* Noble, 1984 reported from gills and fins of *Esox* spp. and *Perca fluviatilis*; *M.* (=*M.*) *dujardini* (Thélohan, 1899) Lom *et* Noble, 1984 reported from the gill lamellae, fins, kidneys, gonads and pancreas of *Rutilus* spp., *Leuciscus* spp., *Abramis* spp. etc.; *M.* (=*M.*) *andhrae* (Lalitha Kumari, 1969) Lom *et* Noble, 1984 reported from the intestinal wall of *Ophicephalus punctatus*; *M. punctatus* Roychaudhuri *et* Chakravarty, 1970 reported from the spleen and pharyngeal epithelium of *Ophicephalus punctatus*; *M. bhadrensis* Seenappa *et* Manohar, 1981 from the muscles of *Labeo rohita*; *M. hosadurgensis* Seenappa *et* Manohar, 1981 from the gills and muscles of *Cirrhinus mrigala*; *M. iranicus* Molnár, Masoumian *et* Abasi, 1996 from the spleen of *Barbus luteus* and *M. orissae* Haldar, Samal *et* Mukhopadhyay, 1996 reported from the gills of *Cirrhinus mrigala.*

Off these myxosporidan species, spores of *M.* (=*M.*) *anurus* (12.0-13.0 × 7.0-8.0), *M.* (=*M.*) *dujardini* (11.0-13.0 × 5.0-8.0), *M. bhadrensis* (8.0-11.0 × 7.0-8.0), *M. hosadurgensis* (9.0-11.0 × 5.0-8.0) and *M. iranicus* (13.2-14.0 × 7.5-9.2) have smaller and broader spores and thus these are different from the present species under study. The pyriform spores of *M.* (=*M.*) *andhrae* with 3-6 prominent parietal folds are different from the spores of the present species devoid of parietal folds or markings.

Further, the pyriform spore of *M. punctatus* closely resembles the shape of the present species, but polar capsules are equal in the former species. Moreover, glycogen containing iodinophilous vacuole is very much prominent in the former one which is lacking in the latter species. Furthermore, *M. orissae* shows similarity with the present species in having closer dimension of spore and the inequality of polar capsules, but the larger dimensions of two polar capsules, absence of iodinophilous vacuole and intercapsular appendix have made the present species distinct from *M. orissae.*

These features justify the establishment of this myxozoan as a new species for which it is designated as *Myxobolus catmrigalae* sp. n. in the paper.

Taxonomic summary

Type host: Catla-Mrigal hybrid carp [male parent fish *Catla catla* (Hamilton-Buchanan) × female parent fish *Cirrhinus mrigala* (Hamilton-Buchanan)].

Type locality: Kalna (Latitude: 23°13´ N, Longitude: 88°22´ E), Burdwan, West Bengal, India.

Type specimens: Paratypes are spores stained in Giemsa, in the collection of Harold W. Manter Laboratory of Parasitology, Nebraska, USA, No. HWML 16711.

Prevalence of infection: 182/277 (65.70 %).

Etymology: The species epithet *catmrigalae* is given after its type host Catla-Mrigal hybrid carp [male parent fish *Catla catla* (Hamilton-Buchanan) × female parent fish *Cirrhinus mrigala* (Hamilton-Buchanan)].

***Myxobolus buccoroofus* sp. n. (Figs 15-20, 22)**

Plasmodia: Very minute oval 'cyst' like plasmodia attached to the roof of the buccal cavity (i.e. anterior part of palate). Mechanical rupture of plasmodium shows some trinucleate (Fig. 15), tetranucleate (Fig. 16) and eight nucleated pansporoblasts (Fig. 17), and many developed spores (Figs 18-20).

Spore: Mature histozoic spores [12.1 ± 0.33 (11.6-12.7) × 7.1 ± 0.45 (6.4-8.1)] appear pyriform in valvular view (Figs 18, 20). The anterior end of the spore is narrow and bends on one side, usually towards the smaller polar capsule; while the posterior end becomes broad and rounded (Figs 18, 20). The two shell valves are smooth, uniformly thick and devoid of any parietal folds. In sutural view, the spore is lenticular with slightly undulating median sutural line (Fig. 19). Sutural ridge is indistinct.

Two polar capsules are unequal in shape and size (Figs 18, 20). The larger one is 4.9 ± 0.26 (4.5-5.3) × 2.9 ± 0.12 (2.7-3.0), elongately oval and oblique in position. A very small knob like structure is present at the anterior extremity of the larger polar capsule (Figs 18, 20). In some spores, it bears a short neck or duct through which polar filament extrudes. Usually, the polar filament makes 6-8 spiral coils inside the larger polar capsule (Fig. 18). The smaller polar capsule [2.5 ± 0.24 (2.0-2.9) × 1.5 ± 0.12 (1.3-1.7)] lies a little distance down, near the anteromiddle part of the spore. Hence the smaller polar capsule does not open anteriorly but laterally (Fig. 20). It is mostly pyriform in shape, either with very short duct or pointed anterior end or slightly notched anterior end and its posterior end is broadly rounded (Figs 18, 20). 4-5 loose coils form inside the smaller polar capsule (Fig. 19).The extruded polar filaments are unequal (Fig. 20). The ratio of the length of the two filaments is approximately 1: 3. The intercapsular ridge is absent. A thick mucus envelope covers the spore.

The sporoplasm is granular and homogenous and occupies the whole extracapsular space behind the polar capsules (Figs 18, 20). There is a large [diameter 2.9 ± 0.11 (2.7-3.1)] centrally placed iodinophilous vacuole (Fig. 18), but in a few forms it is lateral (Fig. 20). The two karyosomatic sporoplasmic nuclei of 1.2 ± 0.11 (1.0-1.3) diameter are always situated above the iodinophilous vacuole (Figs 18, 20).

Spore valves are generally smooth and the thick edges of each valve are fused to form a straight or slightly curved or undulated sutural line (Fig. 22). Two lateral ridges are seen in some spores separated from each other by a gap of 1.07.

Spore Index:

LS: WS = 1: 0.587
LLPC: WLPC = 1: 0.592
LSPC: WSPC = 1: 0.6
LLPC: LSPC = 1: 0.510
WLPC: WSPC = 1: 0.517

Taxonomic affinities: The *Myxobolus* species under consideration shows similarity with the spores of *M. toyami* Kudo, 1915; *M. calbasui* Chakravarty, 1939; *M. catlae* Chakravarty, 1943; *M. barbi* Tripathi, 1952; *M. drjagini* Akhmerov, 1954; *M. chondrostomi* Donec, 1962; *M. infundibulatus* Donec *et* Kulakowskaja, 1962; *M. anisocapsularis* Shulman, 1962; *M. osmaniae* Lalitha Kumari, 1969; *M. attui* Sarkar, 1984; *M. inaequus* Kent *et* Hoffman, 1984; and *M. undasuturae* Sarkar, 1994. Of these *Myxobolus* species spores of *M. barbi* and *M. attui* are much wider (WS in *M. barbi* is 9.0 and that in *M. attui* is 7.5-9.6) than in the present species. Further, the spores of *M. toyami* (LS: 14.0-15.0), *M. catlae* (LS: 14.5-16.5) and *M. anisocapsularis* (LS: 15.0-15.5) are larger than those in the species under study.

Similarly, besides the shape and inequality of polar capsules roughly oval spores of *M. calbasui* (SP: 12.4-15.0 × 8.2-10.0); elongated oval spores of *M. drjagini* (SP: 10-11 × 9-10), ovate spores of *M. chondrostomi* (SP: 13.5-17.0 × 10.0-11.7) and oval spores of *M. infundibulatus* (SP: 13.4-15.4 × 11.0-13.0) are morphometrically different from the pyriform spores of the present myxosporidan species. In addition spores of *M. osmaniae* are larger in dimension (SP: 12.0-15.0 × 8.2-10.0) than the present species. Moreover, the shell valves, in former species, have 8-10 parietal folds which is absent in the latter species under report.

The spore and polar capsules of *M. inaequus* are nearly similar in shape with this *Myxobolus* species.

However, the spores (19.8 × 8.6) in the former are much larger and possess small, rod-like intercapsular spine. Although the shape of the spore of *M. undasuturae* is almost identical with that of present species, the former species with smaller spore (SP: 10.0-11.0 × 5.0-6.0) and larger polar capsules (LPC: 5.0-6.5 × 2.0-2.5; SPC: 3.0-3.5 × 1.0-1.2) are distinctly different from the present species under consideration.

Considering the differences with the related species, the myxozoan in study is regarded as a new species and we designate the present species as *Myxobolus buccoroofus* sp. n. in this communication.

Taxonomic summary

Type host: *Labeo bata* (Hamilton-Buchanan).

Type locality: Hooghly (Latitude: 22°54´ N, Longitude: 88°24´ E), Hooghly (Dist.), West Bengal, India.

Type specimens: Paratypes are spores stained in Giemsa, in the collection of Harold W. Manter Laboratory of Parasitology, Nebraska, USA, No. HWML 16712.

Prevalence of infection: 59/296 (19.93 %).

Etymology: The species name *buccoroofus* is given to stress the infestation site (roof of the buccal cavity) of spores.

Acknowledgements. The senior author is thankful to the Director of School Education (Secondary Branch), Govt. of West Bengal and Sri Pannalal Purkait, W.B.E.S., Headmaster, Uttarpara Govt. High School for giving permission to continue the research work. Sincere thanks are also expressed to Mrs. Tinku Basu, for her active participation during the preparation of this manuscript.

REFERENCES

Davis H. S. (1944) A revision of the genus *Henneguya* (Myxosporidia) with description of two new species. *Trans. Amer. Micr. Soc.* **63:** 311-320

Lom J., Arthur J. R. (1989) A guideline for the preparation of species descriptions in Myxosporea. *J. Fish Dis.* **12:** 151-156

Lom J., Dyková I. (1992) Protozoan Parasites of Fishes. Development in Aquaculture and Fisheries Science, 26. Elsevier, Amsterdam

Lom J., Vavrá J. (1963) Mucous envelope of spores of the subphylum Cnidospora (Deflein, 1901). *Vest. Cs. Spol. Zool.* **27:** 4-6

Received on 11th February, 2004; revised version on 6th May, 2004; accepted on 12th May, 2004

Acta Protozool. (2004) 43: 345 - 349

ACTA
PROTOZOOLOGICA

Description of *Cochliopodium spiniferum* sp. n., with Notes on the Species Identification within the Genus *Cochliopodium*

Alexander KUDRYAVTSEV

Department of Invertebrate Zoology, Faculty of Biology and Soil Sciences, St. Petersburg State University, St. Petersburg, Russia

Summary. The new species named *Cochliopodium spiniferum* was isolated from a low-saline habitat at the White Sea (north-western Russia). It is identical in the light-microscopical features to *Cochliopodium* sp. 3 described by Bark in 1973. In contrast, the scales comprising the tectum of these amoebae are different. This is the first evident case when two cochliopodiums are identical in LM, but differ in the scale structure, emphasizing the necessity of both LM and EM study for precise species identification within the genus *Cochliopodium*.

Key words: *Cochliopodium spiniferum* sp. n., scales, species identification, systematics, ultrastructure.

Abbreviations: EM - electron microscopy, GA - "Golgi attachment", LM - light microscopy, MT - presumed microtubule, MTOC - microtubule organizing center, S - spines of the scales in the cross-section.

INTRODUCTION

The genus *Cochliopodium* comprises lens-shaped, flattened lobose amoebae bearing a tectum - a monolayer of scales covering the dorsal surface of the cell. Traditionally, the structure of the scales was considered to be the most reliable feature for characterizing *Cochliopodium* species (Bark 1973). However, recently Kudryavtsev *et al*. (2004) have shown that there is a group of *Cochliopodium* species, which differ in LM features but have very similar scales. In this paper, I describe an opposite situation, when two species of the genus *Cochliopodium* are similar in the LM features, but differ in the structure of scales. These species are "*Cochliopodium* sp. 3", an unnamed strain studied by Bark (1973), and *Cochliopodium spiniferum* sp. n., described in the present paper.

Address for correspondence: Alexander Kudryavtsev, Dept. of Invertebrate Zoology, Fac. of Biology and Soil Sci., St. Petersburg State University, Universitetskaya nab. 7/9, 199034 St. Petersburg, Russia; Fax: +7-812-3289703; E-mail: aak@ak14261.spb.edu

MATERIALS AND METHODS

Cochliopodium spiniferum was isolated from the bottom sediments of a stream flowing through a periodically flooded marsh near the Marine Biological Station of the St. Petersburg University at Srednii Island (Chupa Inlet, Kandalaksha Bay, the White Sea). Salinity of the site of sampling varies from freshwater to 10-15 ‰, depending on the tidal cycle. It was 6 ‰ at the moment of sampling. Amoebae were cloned and maintained on 1.5% NN agar prepared

with 6 ‰ artificial seawater (Wiegandt GmbH, Germany). For EM, amoebae were fixed with 1% phosphate-buffered OsO_4 for 30 min, dehydrated and embedded in Epon 812 resin. Whole mounts of scales were prepared according to the protocol of Sadakane *et al*. (1996) and stained with a 2 % solution of uranylacetate in 70 % ethanol.

RESULTS

Cochliopodium spiniferum sp. n.

Diagnosis: Length in locomotion, 18-39 μm (mean, 27 μm), breadth, 22-50 μm (mean, 32 μm), L:B ratio, 0.62-1 (mean, 0.84). Fan-shaped, oval or triangular, with numerous subpseudopodia and trailing filaments. One vesicular nucleus 5-7 μm in diameter, large central nucleolus 1.7-3 μm in diameter, with small lacunae. Five-rayed scales composed of a circular base plate, a central column of 5 stalks and a complex top part consisting of a central cone, a peripheral disc and a vertical striated spine. Diameter of the base plate, 0.8-1 μm; of the top disc, 0.6-0.8 μm; height of a scale, 0.8-0.9 μm; diameter of a spine, 0.04-0.07 μm, length of a spine, 1.7-2.2 μm.

Type material: Type strain is deposited with the Culture Collection of Algae and Protozoa (IFE, UK; accession No, CCAP 1537/3).

Habitat: Bottom sediments of a marsh with varying salinity at Srednii Island (Chupa Inlet, Kandalaksha Bay, the White Sea).

Differential diagnosis: Differs from the only named species similar in LM features, *C. bilimbosum*, in the scale structure. Identical in LM features to the unnamed strain "*Cochliopodium* sp. 3 " (Bark 1973) but differs from it in the structure of the scales.

Description: During locomotion the amoebae were oval, fan-shaped or, more rarely, broadly triangular with the base directed anteriorly (Figs 1-4). The leading edge of the hyaloplasm was irregular and very dynamic (Figs 1, 3). The anterior and lateral parts of the hyaloplasm extended far beyond the border of the tectum (Fig. 4). Often, the cell formed several short conical subpseudopodia directed anteriorly. Sometimes, the anterior and antero-lateral hyaloplasm was deeply cleft into a few separate lobes (Fig. 3). These lobes moved posteriorly along the lateral margins of the cell, and retracted after they reached the posterior edge. Sometimes, the tips of these lobes remained adhered to the substratum, leaving trailing filaments behind the moving cell after the retraction of the entire lobe. Besides, numerous trailing filaments were formed along the posterior margin of hyaloplasm, producing a "brush-like" appearance of the rear edge of an amoeba (Fig. 1). The posterior margin of the hyaloplasm was very narrow and often hidden beneath the granuloplasmic hump.

During non-directed movement, the amoebae were irregularly triangular, with numerous long hyaline subpseudopodia (Fig. 5). Some cells were rounded, with a narrow hyaloplasmic veil, but without any subpseudopodia or lobes (Fig. 6). Stationary amoebae were rounded and flattened. Their hyaloplasmic veil was very narrow, sometimes almost completely retracted. Amoebae never floated spontaneously. When detached artificially from the substratum, they adopted a spherical shape and settled down quickly. Sometimes, the cells remained spherical for a while after making contact with the substratum. In this case, the amoeba sometimes formed several long, narrow hyaline pseudopodia, penetrating the tectum.

The scales comprising the tectum were clearly seen as fine granules distributed over the dorsal surface of the cell (Figs 4, 6). The optical profile of the tectum was distinctly visible as a cross-striated double line along the margin of the granuloplasmic mass (Fig. 7). When the tectum was observed tangentially at high magnification (1250x) using DIC optics, very short, indistinct "rays" were seen radiating from the surface.

The nucleolus in the living cells (Fig. 7) appeared to be slightly "granulated". A layer of tiny, non-refractile granules could be observed along the periphery of the nucleus. No contractile vacuole was observed. The granuloplasm contained numerous yellowish refractile bipyramidal crystals, 1-3 μm in size (Figs 1-7) and a number of vacuoles of various sizes. Amoebae fed on bacteria and particles of non-living organic matter of similar size. At room temperature, amoebae began to encyst after 2-3 weeks in culture. Cysts (Fig. 8) were spherical or slightly ovoid, 10-20 μm in diameter, with a distinct inner wall. The outer wall was formed by the scales comprising the tectum, and it was not always clearly visible under LM.

The base plate of a scale had a distinct outer rim and appeared to be amorphous both in the whole mounts (Fig. 9) and in the sections (Fig. 10). At the bases of the stalks of the vertical column there were bird-foot-like structures with 3 or 4 digits, one digit being opposed to the others. The top part of the scale consisted of a peripheral funnel, formed by five radial spokes corresponding to the stalks, a fine networked disc, and a central cone 0.25-0.28 μm in height, formed by five

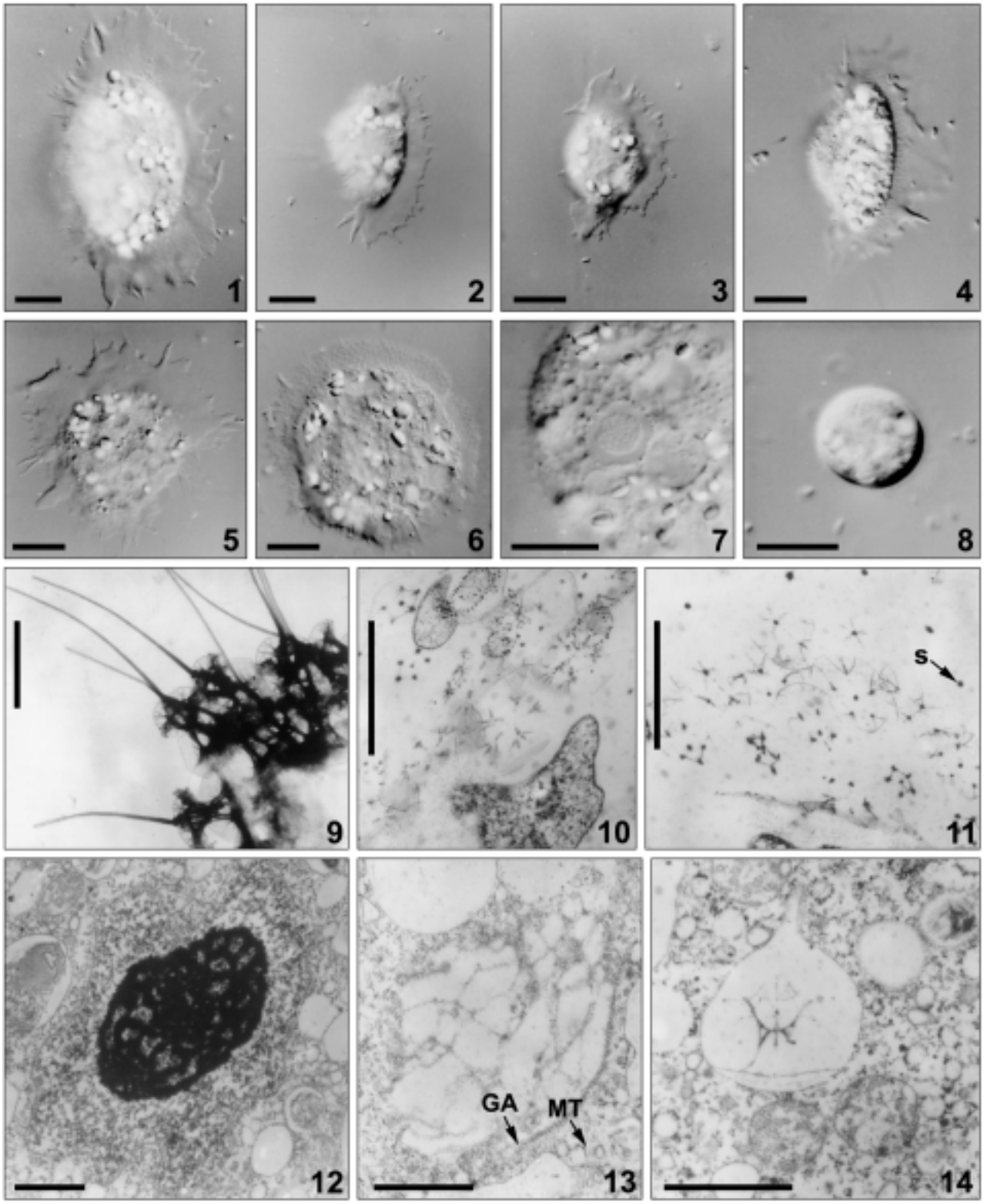

Figs 1-14. *Cochliopodium spiniferum* sp. n. **1-8 -** LM photographs, **9-14 -** EM photographs. **1-4 -** locomotive forms; **5-6 -** non-directly moving amoebae; **7** - nucleus; **8** - cyst; **9** - scales in a whole mount preparation; **10 -** base plates of the scales in tangential section; **11 -** top parts of the scales sectioned at various planes; **S** - spines in the cross-section; **12** - nucleus; **13** - dictyosome showing "Golgi attachment" (GA) and a radiating microtubule (MT); **14** - scale in the scale-forming vacuole and mitochondria. Scale bars 10 μm (1-8); 1 μm (9-14).

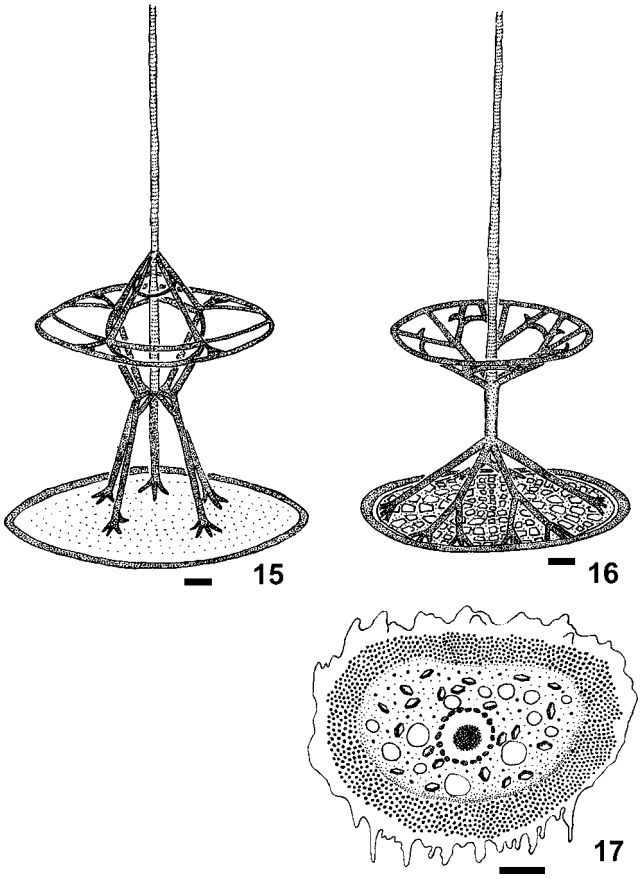

Figs 15-17. 15 - outline of the scale structures of *Cochliopodium spiniferum*; **16** - *Cochliopodium* sp. 3 (after Bark 1973, modified); **17** - locomotive form of *Cochliopodium* sp. 3 (after Bark 1973, modified). Scale bars 0.25 μm (15, 16); 10 μm (17 - estimated from the size of amoebae provided in the description of species).

filaments, originating from the spokes of the funnel (Figs 11, 14). The filaments of the cone were cross-connected between each other at two levels. A vertical spine (Figs 9, 11) projected from the center of the top part of each scale. This spine was slightly tapering and cross-striated with a periodicity of about 0.006 μm. Usually, only a few scales were seen in the sections, which might be caused by the loss of scales in the viscous medium during fixation or embedding steps.

Each nucleus observed in the sections was irregularly rounded, with a central electron dense nucleolus, sometimes with small lacunas (Fig. 12). The Golgi complex was usually located near the nucleus. It consisted of one dictyosome formed by numerous dilated vesicles rather than by a stack of flattened cisternae. An elongated cross-striated MTOC-like structure resembling the "Golgi attachment" (Yamaoka *et al.* 1984) was present near the surface of the dictyosome opposite to the nucleus. Sometimes microtubules were seen radiating from it (Fig. 13). The numerous vesicles of various sizes containing scales at different stages of assembly surrounded the dictyosome (Fig. 14). Mitochondria (Fig. 14) were rounded or ovoid with tubular cristae.

DISCUSSION

Identification

Among the known species of the genus *Cochliopodium*, this amoeba is almost completely identical in LM features to a new but unnamed species "*Cochliopodium* sp. 3" (Fig. 17) comprehensively studied by Bark (1973). The only feature, in which these strains differ, is the ability to encyst, known in the strain described here but never observed in Bark's strain. However, TEM evidence reveals considerable differences in the scale structure. The scales comprising the tectum in Bark's amoebae (Fig. 16) consist of complexly structured base plates, a vertical column made up by the stalks converging towards the top to form a single central core. The simple top part is in the shape of a funnel with the spine in the center. In contrast, in the present strain (Fig. 15) the base plate is amorphous, the stalks never fuse together to form a single central core and the top part of the scale consists of a peripheral funnel, formed by 5 radial spokes, a fine networked disc, a central cone, and a vertical spine. Certain similarities in the structure of the scales, in particular, 5-rayed symmetry and the central spine that is identical in both species, suggests that these species might be closely related, but their distinctness is evident. Another unnamed species with the similar scales was studied by Yamaoka (Yamaoka and Kunihiro 1985, Yamaoka *et al.* 1991). The scales of this species differ from those of my strain in the same way as the scales of Bark's "*Cochliopodium* sp. 3". Besides, their spines appear to be much thicker than those of my strain and carry distinct filamentous material (see Yamaoka *et al.* 1991, Figs 2, 3 at page 12, and Fig. A at page 14). Therefore, the species of Yamaoka is also distinct from my strain, but may be closely related to it due to the similar structure of the scales. Among the named species of *Cochliopodium*, the present strain resembles only *C. bilimbosum* in LM features, but has very different scales. Other species and unnamed strains of *Cochliopodium* studied with EM, namely, *C. minus*,

C. larifeili, *C. gulosum*, *C. barki*, and *Cochliopodium* sp. "NYS strain" (Yamaoka *et al.* 1984; Dyková *et al.* 1998; Kudryavtsev 1999, 2000; Kudryavtsev *et al.* in press) have scales, totally different from the present strain. Other species, for which EM data are not available yet (see Bark 1973 for the list of these species), are different from the present strain in the shape of the locomotive form, the appearance of tectum, and (*C. clarum* Schaeffer, 1926) the structure of the nucleus. Thus, the strain described here is evidently a new species, which I name *Cochliopodium spiniferum* (due to the long spine in the center of a scale).

Taxonomic status of "*Cochliopodium* sp. 3" (Bark 1973)

The strain named "*Cochliopodium* sp. 3" is certainly a new species of *Cochliopodium*. Bark (1973) studied its LM and EM morphology but for unknown reason did not name this strain. It is not possible to do this now, since no type material was deposited. Therefore, the Bark's species requires future re-isolation. *C. spiniferum* is identical to this strain in the LM morphology, but differs in the scale structure - the first such case in *Cochliopodium*. These data rise a question of the possibility to re-isolate "older" species of *Cochliopodium* like those described by West (1901) or Penard (1902) which have never been studied with EM. The modern researcher never knows whether an isolated strain, even identical to a 19th century amoeba in LM data, would differ from it in the structure of scales.

Ultrastructural features

A peculiar electron-dense structure associated with the dictyosome in *Cochliopodium spiniferum* appears to be a MTOC, like in *Cochliopodium barki* (Kudryavtsev *et al.*, 2004). Structurally, this MTOC is not similar to those of other amoeboid protists which are mostly trilaminar, consisting of two electron-dense plates and an electron-transparent layer between them (e. g., Grell and Benwitz 1978, Pussard and Pons 1978, Page 1981, Smirnov 1995-1996, Gothe *et al.* 1999). The apparent presence of a MTOC in *Cochliopodium* makes the set of features of these amoebae extremely unusual, i.e., a generally "gymnamoebian" cell type combined with the tectum and non-typical cytoplasmic MTOC. This complicates the placing of the genus together with the naked lobose amoebae, as suggested by Page (1988) since the presence of a MTOC is rather an exception in the latter group than a rule. Bark's (1973) hypothesis of the relatedness of *Cochliopodium* to chrysophyceans and haptophyceans, based solely on the presence of organic scales on the cell surface, appears to be even weaker supported, since the organic scales are known to date in a wide set of very distant or non-related protistan taxa.

Acknowledgements. Part of this work was made during my stay at the Laboratory of Cell Biology, University of Tübingen, Germany, supported by the DAAD grant 325/lin. I am grateful to Profs. D. Ammermann and C. Bardele for their hospitality and the permission to use microscopes. Support from the Ministry of Education of Russia (grant E02-6.0-78) is acknowledged as well. I also thank one of the reviewers for the correction of English in the manuscript.

REFERENCES

Bark A. W. (1973) A study of the genus *Cochliopodium* Hertwig and Lesser 1874. *Protistologica* **9:** 119-138

Dyková I., Lom J., Macháčková B. (1998) *Cochliopodium minus*, a scale-bearing amoeba isolated from organs of perch *Perca fluviatilis*. *Dis. Aquat. Org.* **34:** 205-210

Gothe G., Böhm K. J., Unger E. (1999) Ultrastructural details of the plasmodial rhizopod *Synamoeba arenaria* Grell. *Acta Protozool.* **38:** 49-59

Grell K., Benwitz G. (1978) Ultrastruktur mariner Amöben IV. *Corallomyxa chattoni*. *Arch. Protistenkd.* **120:** 287-300

Kudryavtsev A. A. (1999) Description of *Cochliopodium larifeili* n. sp., an amoeba with peculiar scale structure, and notes on the diagnosis of the genus *Cochliopodium* (Hertwig and Lesser, 1874) Bark, 1973. *Protistology* **1:** 66-71

Kudryavtsev A. A. (2000) The first isolation of *Cochliopodium gulosum* Schaeffer, 1926 (Lobosea, Himatismenida) since its initial description. II. Electron-microscopical study and redescription. *Protistology* **1:** 110-112

Kudryavtsev A., Brown S., Smirnov A. (2004) *Cochliopodium barki* n. sp. (Rhizopoda, Himatismenida) re-isolated from soil 30 years after its initial description. *Europ. J. Protistol.* (in press)

Page F. C. (1981) A light- and electron-microscopical study of *Protacanthamoeba caledonica* n. sp., type-species of *Protacanthamoeba* n. g. (Amoebida, Acanthamoebidae). *J. Protozool.* **28:** 70-78

Page F. C. (1988) A New Key to Freshwater and Soil Gymnamoebae. Freshwater Biological Association, Ambleside

Penard E. (1902) Faune Rhizopodique du Bassin du Leman. Henry Kündig, Geneva

Pussard M., Pons R. (1978) Étude de la «centrosphère» d'*Acanthamoeba echinulata* Pussard et Pons 1978. *Protistologica* **14:** 247-251

Sadakane K., Murakami R., Yamaoka I. (1996) Cytochemical and ultrastructural studies of the scales of the amoeba *Cochliopodium bilimbosum* (Testacea). *Europ. J. Protistol.* **32:** 311-315

Smirnov A.V. (1995-1996) *Stygamoeba regulata* n. sp. (Rhizopoda) - a marine amoeba with an unusual combination of light-microscopical and ultrastructural features. *Arch. Protistenkd.* **146:** 299-307

West G. S. (1901) On some British freshwater Rhizopods and Heliozoa. *J. Linn. Soc. (Zool.)* **28:** 309-342

Yamaoka I., Kunihiro H. (1985) *Cochliopodium* (Testacea) with new type of scale. *Yamaguchi Seibutsu* **12:** 14-15

Yamaoka I., Kawamura N., Mizuno M., Nagatani Y. (1984) Scale formation in an amoeba, *Cochliopodium* sp. *J. Protozool.* **31:** 267-272

Yamaoka I., Kitanaka K., Murakami R. (1991) *Cochliopodium* (Testacea) in Yamaguchi prefecture. *Yamaguchi Seibutsu* **18:** 10-15

Received on 18th November, 2003; revised version on 19th May, 2004; accepted on 27th May, 2004

Acta Protozool. (2004) 43: 351 - 368

ACTA
PROTOZOOLOGICA

Morphology and Morphogenesis of Two Marine Ciliates, *Pseudokeronopsis pararubra* sp. n. and *Amphisiella annulata* from China and Japan (Protozoa: Ciliophora)

Xiaozhong HU[1,3]*, Alan WARREN[2] and Toshikazu SUZUKI[3]

[1]Laboratory of Protozoology, College of Fisheries, Ocean University of China, Qingdao, P. R. China; [2]Department of Zoology, The Natural History Museum, Cromwell Road, London, UK; [3]Faculty of Fisheries, Nagasaki University, Bunkyo-machi, Nagasaki, Japan

Summary. The morphology and the morphogenesis of two hypotrich ciliates, *Pseudokeronopsis pararubra* sp. n. and *Amphisiella annulata*, collected from the coastal waters off Qingdao (Tsingtao), China and Nagasaki, Japan were studied using live observation and protargol impregnation. Based on current investigations, descriptions of these two species are provided and comparisons with their congeners are given. Diagnosis for *Pseudokeronopsis pararubra* sp. n.: Marine *Pseudokeronopsis*, long elliptical in outline, 180-350×50-90 μm *in vivo* and dark reddish in colour. Ciliature comprising: 64-92 adoral membranelles; bicorona of 15-26 frontal cirri; 1 buccal and 2 frontoterminal cirri; 7-11 transverse cirri; two midventral rows comprising 62-93 cirri and extending to transverse cirri; 48-79 left and 46-80 right marginal cirri; 5-8 dorsal kineties. Numerous (> 100) macronuclear segments. Two types of cortical granules: one orange-red pigment, mainly grouped around cirri and dorsal bristles; the other, colourless and blood-cell-shaped, lying just beneath the former and densely distributed. The morphogenetic process corresponds well with those of its congeners. The most notable point is that the fronto-midventral transverse cirral anlagen never develop in connection with new oral primordium at posterior portion during divisional process in the proter. Supplementary comparison of *Amphisiella annulata* with some marine congeners has been provided in this study. Some morphogenetic and reorganizational stages show that its stomatogenesis seems to be similar to that of its congeners, i.e. the oral primordium originates parakinetally from the amphisiellid median cirral row (ACR) in the opisthe, and the old adoral zone of membranelles seems to be retained completely by the proter. Usually only 6 cirral anlagen (including the anlage for undulating membrane) develop. In the proter, the undulating membranes, the buccal cirrus and cirri left of the ACR provides three streaks, other two anlagen derive from the ACR. In the opisthe, the oral primordium produces the anlage for the undulating membranes and very likely three cirral streaks; the other two anlagen also occur within ACR. The new ACR is formed by alignment of the two rightmost cirral anlagen.

Key words: *Amphisiella*, Hypotrichida, infraciliature, marine ciliates, morphogenesis, *Pseudokeronopsis pararubra* sp. n.

INTRODUCTION

Over the past 10 years, extensive ciliate surveys have been carried out along the coasts of North China, and many new or poorly known forms have been described using modern methods (Song and Wilbert 1997a, b; Song and Hu 1999; Song and Warren 2000; Hu and Song 2000a, b, 2001a, b, c, 2002, 2003; Hu *et al.* 2002; Song *et al.* 2002). Recent work further demonstrates that the biodiversity of marine hypotrichous ciliates is greater than previously supposed (Hu and Suzuki 2004). However, compared with those found in freshwater or terrestrial biotopes, marine forms are still insufficiently studied and many remain unknown regarding their infraciliature and morphogenetic events.

* Present address for correspondence: Xiaozhong Hu, C/o. Dr. Toshikazu Suzuki, Faculty of Fisheries, Nagasaki Univer-sity, Bunkyo-machi, Nagasaki 852-8521, Japan; E-mail: xiaozhonghu@hotmail.com

In this paper we describe one new species and provide additional information on a recently redescribed marine hypotrich, collected from coastal waters in China and Japan.

MATERIALS AND METHODS

Sampling sites. Samples were collected from mariculture water near the coast of Qingdao (Tsingtao, 36°08'N; 120°43'E), China and in Mie Port (32°48'N; 129°46'E), Nagasaki, Japan. Two populations of *Amphisiella annnulata* were isolated from the same locality in January 1996 and November 2000 in Qingdao. *Pseudokeronopsis pararubra* was isolated from both Qingdao and Nagasaki. The Qingdao population of *P. pararubra* was found in the open scallop-culturing water on 20 October, 2000, while the Nagasaki population was collected from the fish-farming water on 17 June, 2003.

General methods. After collection and isolation, specimens were kept in the laboratory, either as pure or raw cultures in Petri dishes, in boiled seawater with squashed rice grains as a substrate for bacterial growth. Cells were observed in life using phase contrast and differential interference microscope. Mixtures of saturated mercury bichloride solution and Bouin's fluid were used to fix samples. Protargol silver impregnation according to Wilbert (1975) was applied to reveal the infraciliature. Measurements were performed at magnifications of 100-1250×. Drawings were carried out with the help of a camera lucida. Terminology and systematic arrangement are according to Borror and Wicklow (1983) and Eigner and Foissner (1994).

RESULTS AND DISCUSSION

Order Hypotrichida Stein, 1859

Family Pseudokeronopsidae Borror *et* Wicklow, 1983

Genus *Pseudokeronopsis* Borror *et* Wicklow, 1983

***Pseudokeronopsis pararubra* sp. n. (Figs 1-3, 6, 7; Tables 1, 2)**

Syn. *Pseudokeronopsis pulchra* Borror *et* Wicklow, 1983 Fig. 20

Diagnosis: Marine *Pseudokeronopsis*, long elliptical in outline, 180-350 × 50-90 μm *in vivo* and dark reddish in colour. Ciliature comprising: 64-92 adoral membranelles; bicorona of 15-26 frontal cirri; 1 buccal and 2 frontoterminal cirri; 7-11 transverse cirri; two midventral rows consisting of 62-93 cirri which extend to transverse cirri; 48-79 left and 46-80 right marginal cirri; 5-8 dorsal kineties. Numerous (>100) macronuclear segments. Two types of cortical granules: one orange-red pigment, mainly grouped around cirri and dorsal bristles; the other, colourless and blood-cell-shaped, lying just beneath the former and densely distributed.

Type location: Marine molluscs culturing waters off the coast of Qingdao (Tsingtao, 36° 08' N; 120° 43' E), China. Salinity 32-37 ‰; water temperature 16-24°C; pH 8.0-8.2.

Type slides: One holotype slide has been deposited in the collections of the Natural History Museum, London, UK, with registration number 2004:6:2:1. One paratype slide of protargol-silver impregnated specimens has been deposited in the Laboratory of Protozoology, Ocean University of China (OUC), P. R. China with registration number: HD-2000102001. The Qingdao population is designated as the type population.

Morphology: The following descriptions are based on observations of two populations, one collected from Qingdao, China, the other from Nagasaki, Japan (Table 1). Body measures 180-350 × 50-90 μm *in vivo*, usually long elliptical in shape when viewed from ventral aspect with anterior end broadly rounded and posterior end narrowed, left margin conspicuously convex and right margin distinctly sigmoidal, widest at middle portion (Figs 1A, 6A); ratio of body length to width about 4-5:1; dorsoventrally flattened about 1: 2 (Fig. 1B). Body dark reddish at low magnification. Adoral zone of membranelles (AZM) about 1/3-1/4 of body length, with distal end bending posteriorly far onto right ventral side (Fig. 1A). Buccal field narrow, with cytostome deeply postioned and pharyngeal fibres conspicuous, *ca* 30-50 μm long in Nagasaki population after impregnation.

Pellicle comparatively thick, but flexible, thus variable in shape (Fig. 1D), with two kinds of cortical granules: one is orange-red pigment, spherical, 1-2 μm in diameter, mainly regularly grouped around ventral cirri and dorsal bristles (Figs 1E,F, 6D-F). These granules are thus distributed in belts or lines along cirral rows and dorsal kineties (Fig. 6B), which renders the whole cell dark reddish in colour. In addition, some were observed randomly positioned. The second type of cortical granules are red blood cell-shaped, about 2-3 μm in diameter, colourless, densely packed and positioned more deeply beneath cell surface than the former type (Figs 1G; 6E, arrows). Usually with several food vacuoles, about 6-12 μm across, and another vacuole (contractile vacuole?) sometimes observed below mid-body in Qingdao population (Fig. 1C, arrow).

Transverse cirri *ca* 15 μm long; other cirri comparatively fine, *ca* 10 μm in length, and motionless for most of the time. Locomotion by slowly crawling on substrate or rotating around main body axis when swimming.

Infraciliature as shown in Figs 1H-K, 6G-K. Adoral zone of membranelles composed of 64-92 membranelles, its distal end extending to right margin of cell and bending posteriad (Fig. 6C, arrows). Paroral membrane short,

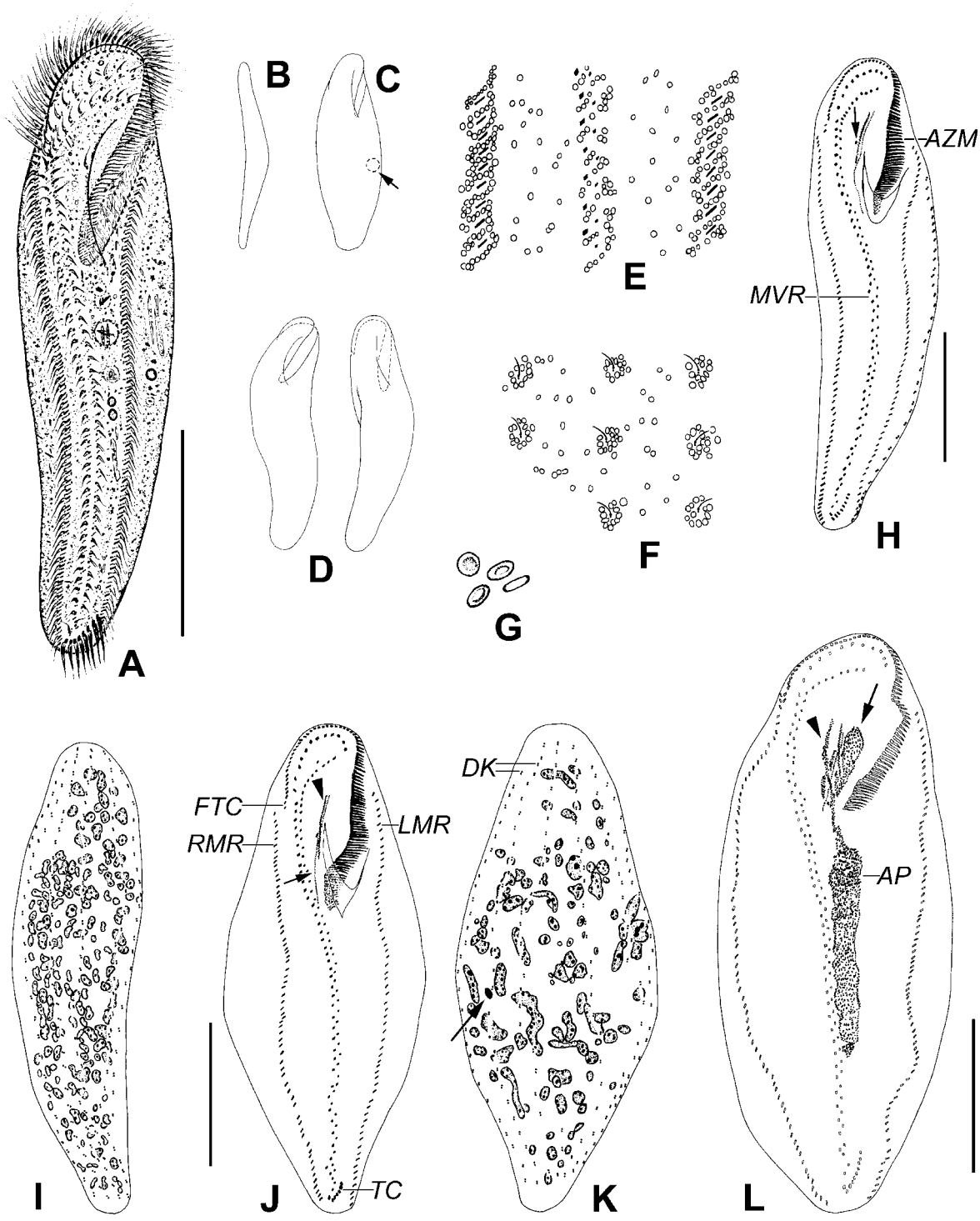

Figs 1A -L. Morphology and morphogenesis of *Pseudokeronopsis pararubra* sp. n. from life **(A-G)** and after protargol impregnation **(H-L)**. **A** - ventral view; **B** - left lateral view; **C** - plumper cell, arrow to show contractile vacuole (?); **D** - different body shapes; **E** - arrangement of pigment granules on ventral side; **F** - arrangement of pigment granules on dorsal side; **G** - red blood cell-shaped cortical granules; **H, I** - ventral and dorsal views of the same individual, showing the infraciliature and nuclear apparatus. Arrow indicates the buccal cirrus; **J, K** - ventral and dorsal views of the same cell, arrow in J to show endoral membrane, arrow in K to indicate micronucleus, arrowhead to mark paroral membrane; **L** - early stage of morphogenesis, arrow to show oral primordium of the proter, arrowhead to indicate the fronto-ventral transverse cirral anlage of the proter. AP - anarchic primordium; AZM - adoral zone of membranelles; DK - dorsal kineties; FTC - frontoterminal cirri; LMR - left marginal cirral row; MVR - midventral rows; RMR - right marginal cirral row; TC - transverse cirri. Scale bars 80 µm.

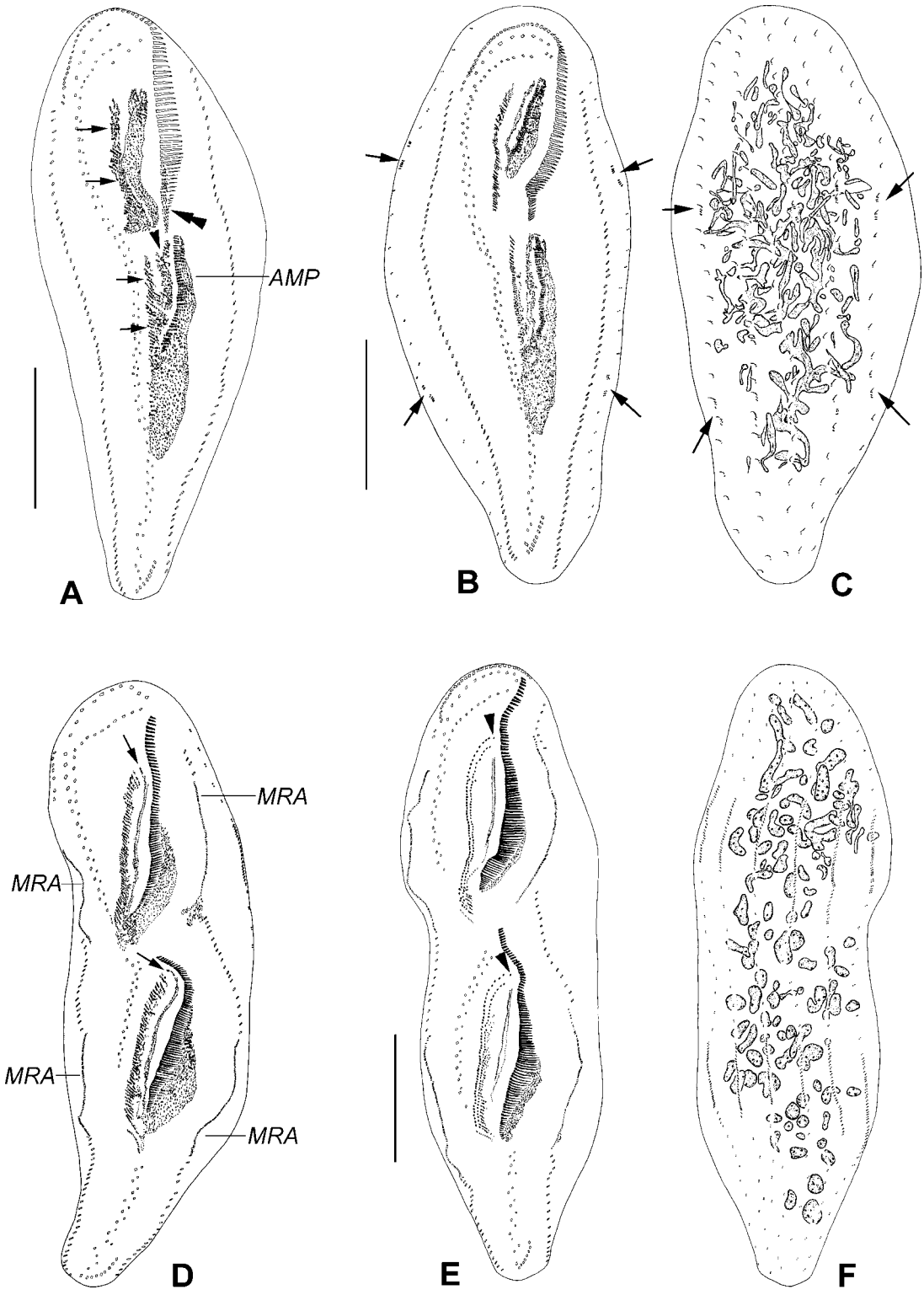

Figs 2A - F. Morphogenesis of *Pseudokeronopsis pararubra* sp. n. after protargol impregnation. **A** - ventral view, arrows to show fronto-ventral transverse cirral anlagen of both the proter and the opisthe, arrowhead to indicate undulating membranes anlagen of the opisthe, double-arrowhead to mark dedifferentiation in the posterior end of the old adoral zone of membranelles; **B, C** - ventral and dorsal views of the same individual, arrows to show dorsal kineties anlagen; **D** - ventral view, arrows to show small anlage separated from the anterior end of the undulating membranes anlagen in both the proter and the opisthe; **E, F** - ventral and dorsal views of the same cell, arrowheads to show frontal cirri derived from anterior end of undulating membranes. AMP - adoral membranelle primordium; MRA - marginal cirral row anlage. Scale bars 80 μm.

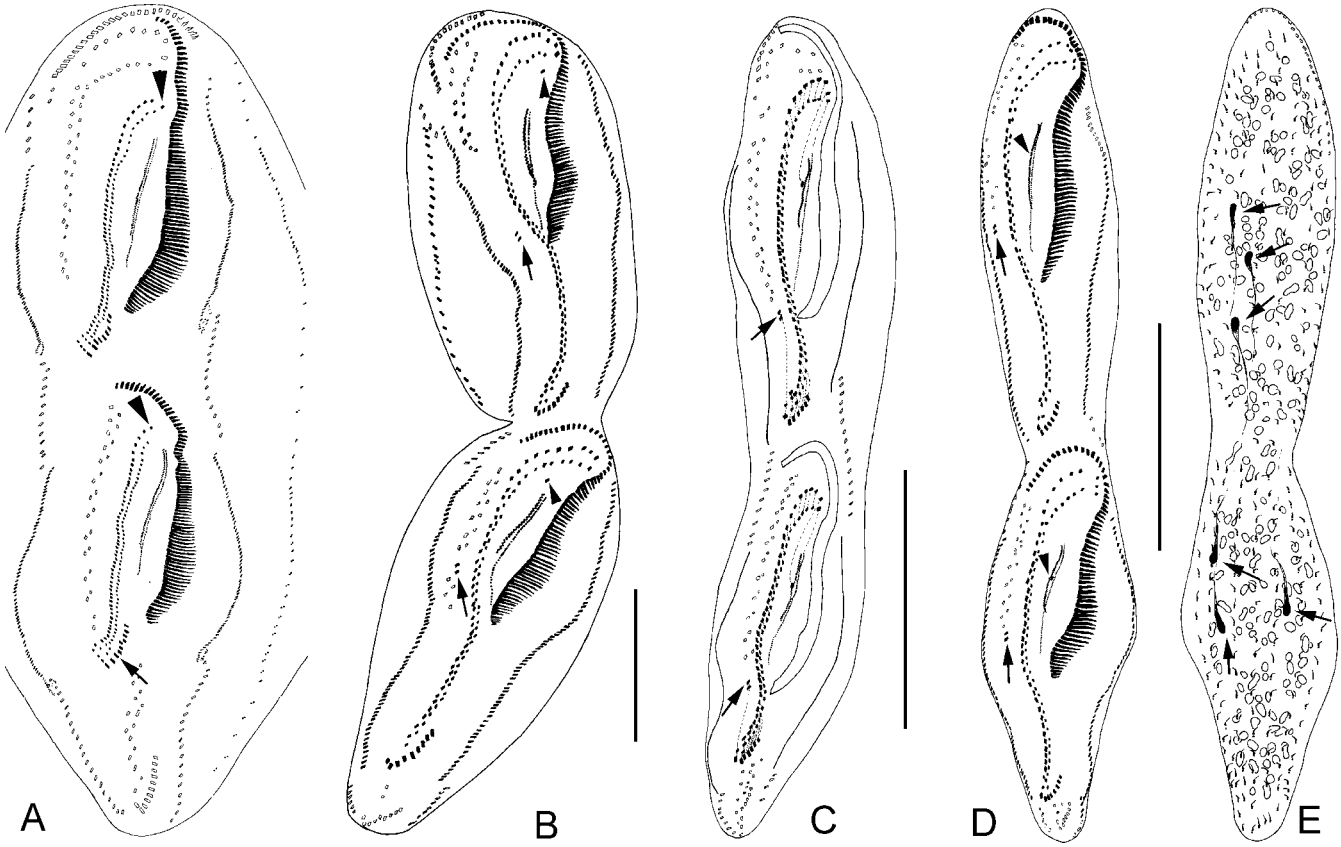

Figs 3A - E. Morphogenesis of *Pseudokeronopsis pararubra* sp. n. after protargol impregnation. **A** - ventral view, arrowheads to show frontal cirri derived from the anterior end of undulating membranes, arrow to mark the third anlage counted from posterior end in the opisthe, which produces four new cirri; **B, C** - ventral views of later dividers, arrows to show frontoterminal cirri moving anteriorly, arrowheads to mark buccal cirri in migration; cirri originating from the same anlage connected by broken lines; **D, E** - infraciliature of ventral and dorsal sides of the same later divider, arrows in D to show frontoterminal cirri moving anteriad, arrowheads to mark buccal cirri, arrows in E to indicate the dividing micronuclei. Scale bars 80 μm.

about half of endoral membrane in length (Figs 1J, 6I). Frontal cirri (FC, Fig. 6I) arranged in two arcs forming a "bicorona", which connect to midventral rows (MVR, Fig. 6J) comsisting of 62-93 cirri and extending posteriad to tranverse cirri (TC, Figs 1J, 6K), so that there is no gap between the posterior end of the midventral rows and the transverse cirri; 7-11 transverse cirri, distributed in J-shape (Figs 1H, J; 6K). Two frontoterminal cirri (FTC, Fig. 1J) between distal end of adoral zone of membranelles and anterior end of right marginal row (Figs 6C, arrowhead; 6H, arrow); single buccal cirrus lies close to paroral membrane (PM), positioned at level of posteior 1/3 (Figs 1H, arrow; 6H, arrowhead). One left and one right marginal cirral row (LMR, RMR) comprising 48-79 and 46-80 cirri, respectively (Figs 1J, 6K). Fibers connected to cirri highly developed (Fig. 6G). 5-8 dorsal kineties (DK) extending almost entire length of cell (Figs 1I, K); dorsal cilia about 5 μm long, easily recognizable *in vivo*.

Macronuclear segments numerous, more than 100 in number, each about 3-6 μm long. Occasionally, micronucleus can be recognized in daughter cells just after division (Fig. 1K, arrow).

Cell division: Since the main morphogenetic events correspond with those of other members in the genus *Pseudokeronopsis*, we here focus primarily on new discoveries for this species.

Stomatogenesis commences with the formation of small groups of basal bodies very close to several left midventral cirri (Fig. 7B, arrows). With the proliferation of basal bodies, these groups join to make a longish field, which is the anarchic primordium of the opisthe (AP, Fig. 1L). During this process, the left midventral cirri remain intact. As the new membranelles of the opisthe organize in a posteriad direction in the adoral membranelles primordia (AMP, Fig. 2A), the undulating membranes anlagen begin to separate to the right of it (Fig. 2A, arrowhead). Meanwhile, several oblique streaks appear

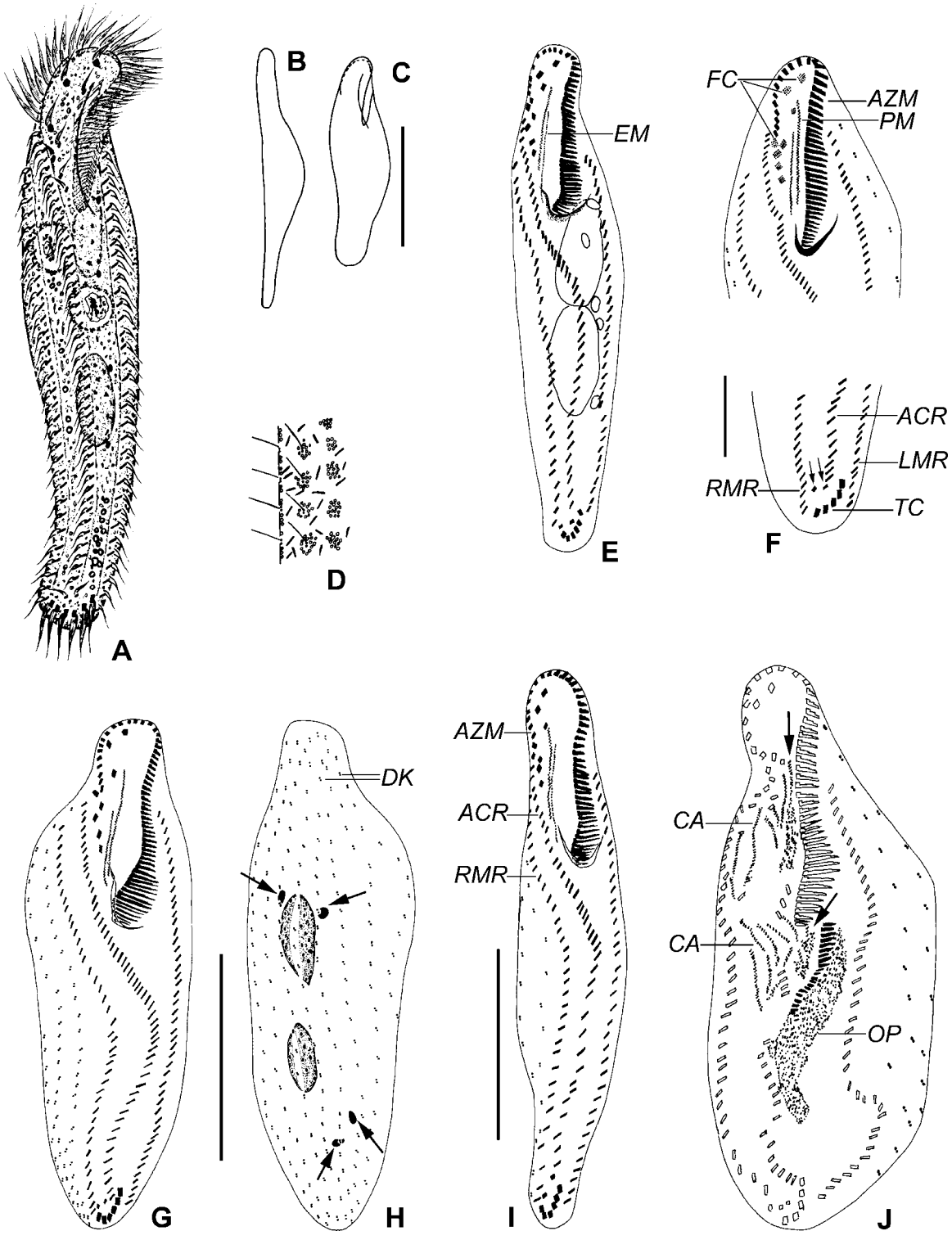

Figs 4A - J. Morphology and infraciliature of two populations of *Amphisiella annulata* from life **(A-D)** and after protargol impregnation **(E-J)**. **A** - ventral view; **B** - left lateral view; **C** - to show body in contracted form; **D** - note dorsal bristles and extrusomes around them, some extrusomes are ejected; **E, I** - infraciliature on ventral side from the population collected in November 2000; **F - H** - from the population collected in January 1996; **F** - infraciliature in anterior and posterior ventral portions, arrows to show pre-transverse cirri; **G, H** - ventral and dorsal views of the same individual, depicting infraciliature, arrows showing micronuclei; **J** - early-middle stage of morphogenesis, arrow to show undulating membranes anlagen. ACR - amphisiellid median cirral row; AZM - adoral zone of membranelles; CA - cirral anlage; DK - dorsal kineties, EM - endoral membrane; FC - frontal cirri; LMR- left marginal cirral row; MRA - marginal cirral row anlage; OP - oral primordium; PM - paroral membrane; RMR - right marginal cirral row; TC - transverse cirri. Scale bars 30 µm (F); 50 µm (I); 60 µm (C); 80 µm (G, H).

Table 1. Morphometric characterization of two populations of *Pseudokeronopsis pararubra* sp. n. All data based on protargol-impregnated specimens from the coastal waters of Nagasaki, Japan (upper line) and Qingdao, China (lower line). CV - coefficient of variation in %, Max - maximum, x - arithmetic mean, Min - minimum, n - number of specimens examined, SD - standard deviation, SE - standard error of the mean. Measurements in µm.

Character	Min	Max	x	SD	SE	CV	n
Body length	174	260	215.6	24.66	4.93	11.4	25
	238	336	288.4	28.68	7.40	9.9	15
Body width	41	66	55.6	7.13	1.43	12.8	25
	78	152	113.6	20.81	5.37	18.3	15
Adoral zone of membranelles, length	70	91	82.6	5.60	1.12	6.8	25
	88	104	95.8	4.68	1.21	4.9	15
Number of adoral membranelles	64	82	71.8	3.86	0.97	5.4	25
	68	92	77.9	6.50	1.74	8.4	14
Number of frontal cirri	15	23	18.4	2.08	0.42	11.3	25
	18	26	21.7	2.73	0.68	12.6	16
Number of midventral cirri	62	91	74.1	7.04	1.44	9.5	24
	65	93	79.0	9.40	2.35	11.9	16
Number of buccal cirri	1	1	1	0	0	0	25
	1	1	1	0	0	0	16
Number of frontoterminal cirri	2	2	2	0	0	0	25
	2	2	2	0	0	0	16
Number of transverse cirri	7	9	7.6	0.65	0.13	8.6	24
	7	11	9.4	1.53	0.29	12.2	16
Number of left marginal cirri	48	68	56.9	5.38	1.10	9.5	24
	57	79	68.5	6.66	1.72	9.7	15
Number of right marginal cirri	46	73	59.5	6.00	1.22	10.1	24
	59	80	69.6	6.66	1.78	9.6	14
Number of dorsal kineties	6	8	6.6	0.65	0.13	9.9	24
	5	7	6.4	0.62	0.15	9.7	16

at the right-anterior position of the anarchic primordium, which forms the fronto-ventral transverse cirral anlagen (Fig. 2A, arrows). At this stage the three parts are connected together at the posterior portion (Figs 2A, B). Later, they separate and further develop into new structures. As the number of adoral membranelles increases in the AMP, a small anlage separates from the anterior end of the undulating membranes anlagen in the opisthe (Fig. 2D, arrow), from which a single frontal cirrus is derived (Figs 2E, 3A, arrowhead). The remaining anlagen split longitudinally to form the paroral and endoral membranes (Figs 2E, 3A-D). During this process, each streak of cirral anlagen divides into 2 segments (cirri) except for the posterior 7-11 streaks, the posterior-most two of which usually generate 4 cirri each (Figs 2E, 3A; 7G, arrow; 7H) but occasionally 5 (Fig. 7G, double-arrowhead), and others form 3 cirri each. Very rarely, the third anlage counted from posterior end generates 4 (Fig. 3A, arrow). Among all these newly formed cirri, the posterior cirrus from the first streak moves to a position beside the paroral membrane and becomes the buccal cirrus (Figs 3B,D, arrowheads); the anterior-most two cirri from the last streak will migrate anteriad to form the frontoterminal cirri (Figs 3B-D, arrow; 7H, arrows); each of the posterior 7-11 streak contributes one transverse cirrus to the daughter cell (Figs 3A-D; 7M, arrows); the remaining new cirri become the frontal and midventral cirri. Marginal cirri and dorsal kineties develop in a usual way, that is, the anlagen appear within old structures and stretch toward both ends to form new ones (Figs 2B-F; 3A-E; 7F,G).

Just as the anarchic primordium in the opisthe appears, a kinetosomal field develops to the right of the buccal cavity and beneath the undulating membranes, which is the oral primordium of the proter (Figs 1L, arrow; 7A, arrow); at the same time the thread-like fronto-ventral transverse cirral anlage is formed independently on the surface between the buccal field and the midventral rows (Fig. 1L, arrowhead). Soon, the cirral anlagen (Figs 2A, arrows; 7K, arrow) and oral primordium (Fig. 7J, arrow) enlarge; meanwhile, the posterior end of the old oral apparatus begins to dedifferentiate (Fig. 2A, double-arrowhead). With the joining of the new basal bodies in the oral primordium, they

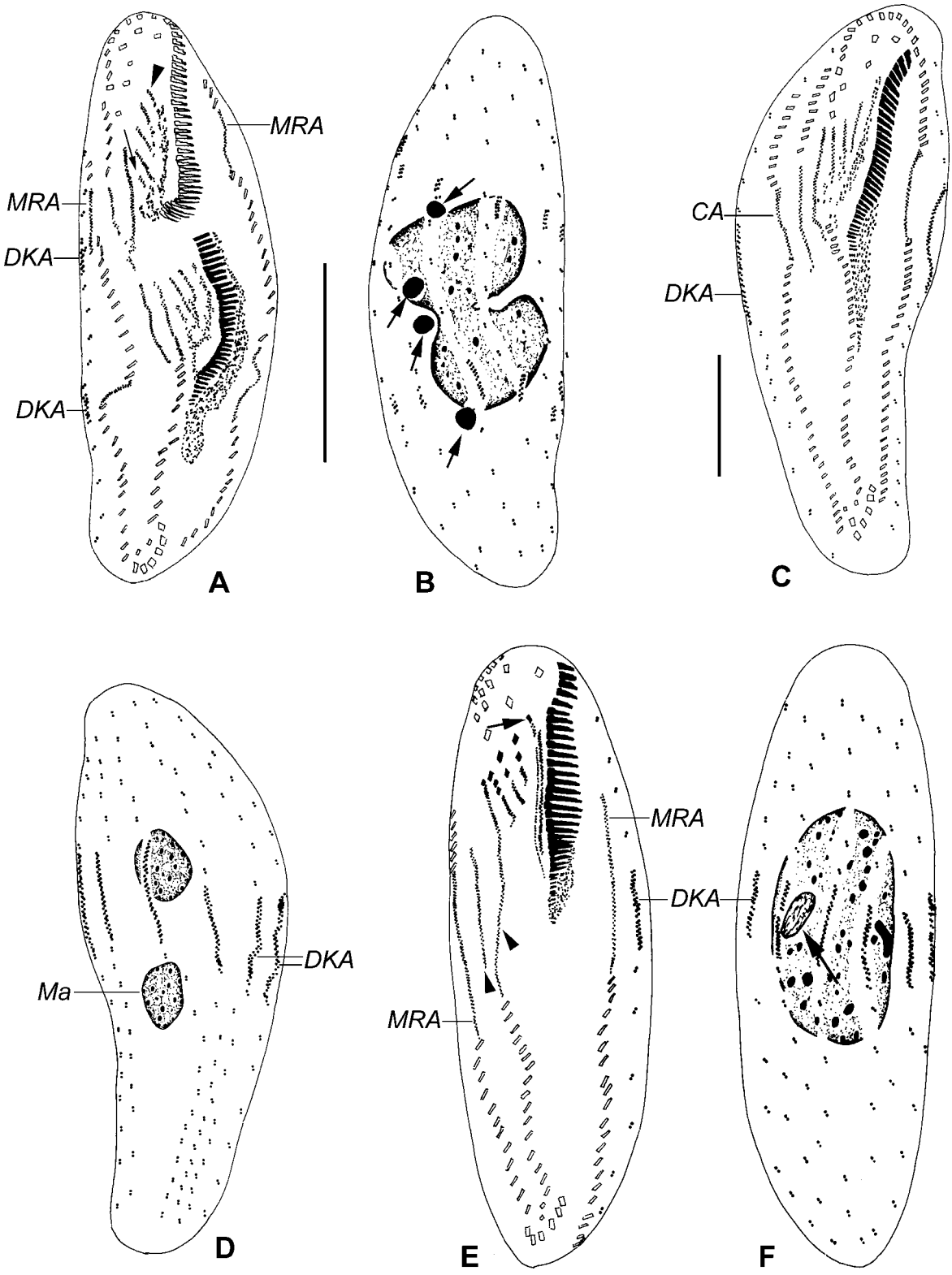

Figs 5A - F. Morphogenesis **(A, B)** and physiological regeneration **(C - F)** of *Amphisiella annulata* after protargol impregnation. **A, C, E** - ventral views of different individuals, arrowhead in A to show a small anlage separated from the anterior end of undulating membranes anlagen, arrow in **A** to mark additional small anlage between cirral anlagen IV and V, arrow in E to indicate frontal cirrus derived from the anterior end of undulating membranes anlagen, arrowheads in E to show the longer cirral anlagen V and VI; **B, D, F** - dorsal views of different cells, arrows to show micronucleus. CA - cirral anlage; DKA - dorsal kinety anlage; Ma - macronuclear nodule; MRA - marginal cirral row anlage. Scale bars 50 µm (A, B); 40 µm (C, D).

gradually organize in a posteriad direction (Figs 2B; 7L, double-arrowhead). Simultaneously the undulating membranes anlage separates and generates the new paroral and endoral membranes as well as the frontal cirrus at their anterior end (Figs 2B, D, E; 3A; 7L, arrow). As in the opisthe, cirral anlagen develop into frontal, buccal, midventral and transverse cirri (Figs 2B, D, E; 3A-D; 7C, arrows; 7L, arrowheads). The replication bands of the macronuclei appear at an early stage of morphogenesis (Fig. 7D, arrowheads). The macronuclear nodules divide without prior fusion (Fig. 7I). Micronuclei divide to be assigned to two daughter cells at late stages (Figs 3E, 7E, arrows).

Comparison with similar species and discussion: As widely noted, species identification in *Pseudokeronopsis*, especially those with pigmented granules, is often difficult because its members possess many overlapping morphological characters (e.g. body size and shape, and the infraciliature), and have very similar morphogenetic patterns (Kahl 1932, Borror and Wicklow 1983, Foissner 1984, Wirnsberger 1987, Wirnsberger *et al.* 1987, Hu and Song 2000b, Song *et al.* 2002). Prior to this investigation, at least five marine species have been described using modern methods, namely: *P. rubra*, *P. flava*, *P. flavicans*, *P. carnea* and *P. qingdaoensis* (Table 2). Of these, *P. qingdaoensis* can be easily separated from *P. pararubra* sp. n. by its body shape (wedge-shaped with posterior end tapered *vs.* long elliptical), higher numbers of transverse (27-45 *vs.* 7-11) and buccal (6-10 *vs.* 1) cirri, and fewer dorsal kineties (3 *vs.* 5-8). In addition these forms differ in the arrangement of their cortical granules (Hu and Song 2000b).

In terms of body size, the arrangement of the granules and the general ciliary pattern, *P. pararubra* sp. n. is very similar to *P. rubra* (Wirnsberger *et al*. 1987, Shi and Xu 2003). However, the former differs from the latter in the following features: body shape *in vivo*, which is often a useful character for species separation (Foissner 1982) (long elliptical *vs.* band-like); the position of buccal cirrus relative to the paroral membrane (i.e. at level of posterior 1/3 *vs.* anterior 1/3); orange-red pigment granules (*vs.* brick-red); the number of frontal cirri (18 and 22 on average, respectively *vs.* 14-16, data from Wirnsberger *et al.*, 1987 and 15 on average in Chinese population) and transverse cirri (7-11, 8 and 9 on average, respectively *vs.* 7 and 6 on average, respectively). Additionally, Wirnsberger *et al.* (1987) gave a revised diagnosis and detailed redescription of *Pseudokeronopsis rubra* and did not mention the red blood cell-shaped cortical granules that are present in *P. pararubra* sp. n. Shi and Xu (2003) redescribed *P. rubra* collected from the South China Sea and also failed to observe these granules suggesting that they are absent in this taxon.

Pseudokeronopsis carnea resembles *P. pararubra* sp. n. in terms of its body size *in vivo*, the colour of the pigmented granules and most biometric characters (Wirnsberger *et al.* 1987). However, the former can be easily separated from the latter by its midventral rows terminating at different levels above the transverse cirri (*vs.* extending all the way to the transverse cirri), a plumper body shape with non-tapering posterior end (*vs.* long elliptical with a conspicuously narrowed caudal region), and having fewer frontal (10-14 *vs.* 15-26) and transverse cirri (6-7 *vs.* 7-11). Considering the strongly shortened midventral rows and orange-red coloured pigment granules present in the Mediterranean population of *Pseudokeronopsis rubra* (Foissner 1984), we agree with Wirnsberger *et al.* (1987) in regarding this as a population of *P. carnea*.

Compared with the new species, *P. flavicans* and *P. flava* are more slender (*vs.* plumper body shape in *P. pararubra* sp. n.), and have a yellow cell colour and yellow-brownish or yellow pigment granules (*vs.* dark red or orange-red), and fewer frontal cirri (*ca* 14 and 9 respectively *vs.* 15-26), transverse cirri (3-6 and 1-3 respectively *vs.* 7-11) and dorsal kineties (4-5 and *ca* 4 respectively *vs*. 5-8). Additionally, these species have a conspicuous gap between the posterior ends of the midventral rows and the transverse cirri (*vs.* no gap in *P. pararubra* sp. n.) (Wirnsberger *et al.* 1987, Song *et al.* 2002).

Hu and Song (2001a) gave a detailed description of a reddish *Pseudokeronopsis* species from Qingdao, China under the name of *P. rubra*. The shortened midventral rows of this population, the conspicuous specialization of cortical granules and the numbers of frontal cirri in the bicorona (11-14) and transverse cirri (2-4) suggest it might be a population of *P. flavicans*. However, some morphological characters are more similar to those of *P. rubra*, i.e. the brick-red pigment granules and the presence of median groove along the midventral rows.

Borror and Wicklow (1983) illustrated *Pseudokeronopsis pulchra in vivo* but did not give any description about its live features or infraciliature. Meanwhile, they just synomized *Holosticha (Keronopsis) pulchra* Kahl, 1932 and *Keronopsis pulchra* in Borror (1972) with their population but supplied no reasons.

However, the original description of this taxon (Kahl 1932, p. 573; Fig. 104_5 on p. 577; obviously incorrectly

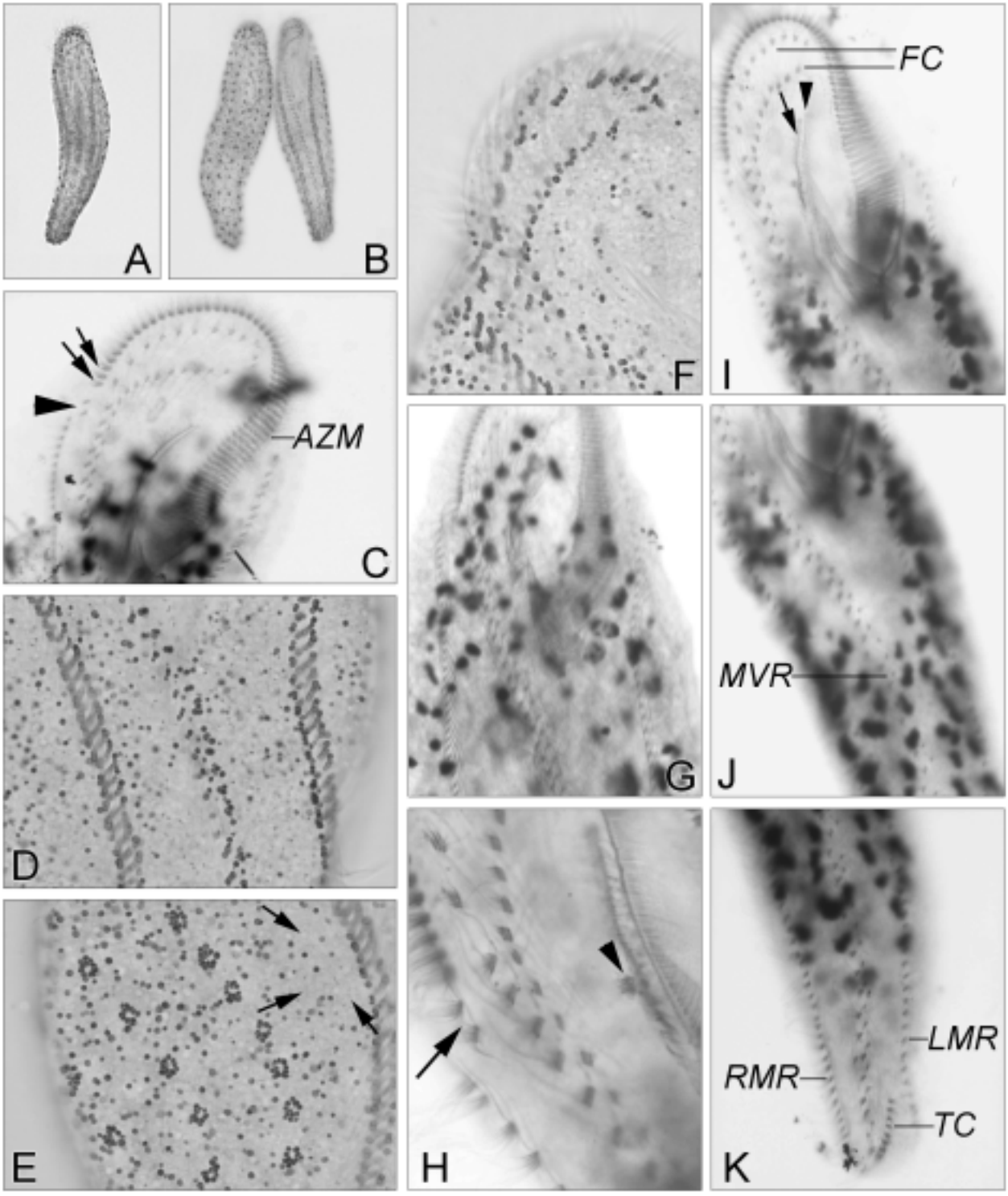

Figs 6A - K. Photomicrographs of *Pseudokeronopsis pararubra* sp. n. from life **(A, B, D-F)** and after protargol impregnation **(C, G-K)**. **A** - ventral view; **B** - two cells, one (left) viewed from dorsal and one (right) from ventral aspect, to denote the arrangement of the pigment granules; **C** - buccal apparatus, arrows to show membranelles at distal end, arrowhead to indicate frontoterminal cirri; **D** - arrangement of pigment granules on ventral side; **E** - arrangement of pigment granules on dorsal side, arrows to show red blood-cell-shaped cortical granules; **F** - arrangement of pigment granules in frontal area; **G** - portion of anterior end of cell, ventral view, to show fibers; **H** - ventral view of part of cell, arrow to show frontoterminal cirri, arrowhead to indicate buccal cirrus; **I - K** - anterior (I), middle (J) and posterior (K) parts of the same cell, ventral view, arrowhead to show paroral membrane, arrow to indicate endoral membrane. AZM - adoral zone of membranelles; FC - frontal cirri; LMR - left marginal cirral row; MVR - midventral rows; RMR - right marginal cirral row; TC, transverse cirri.

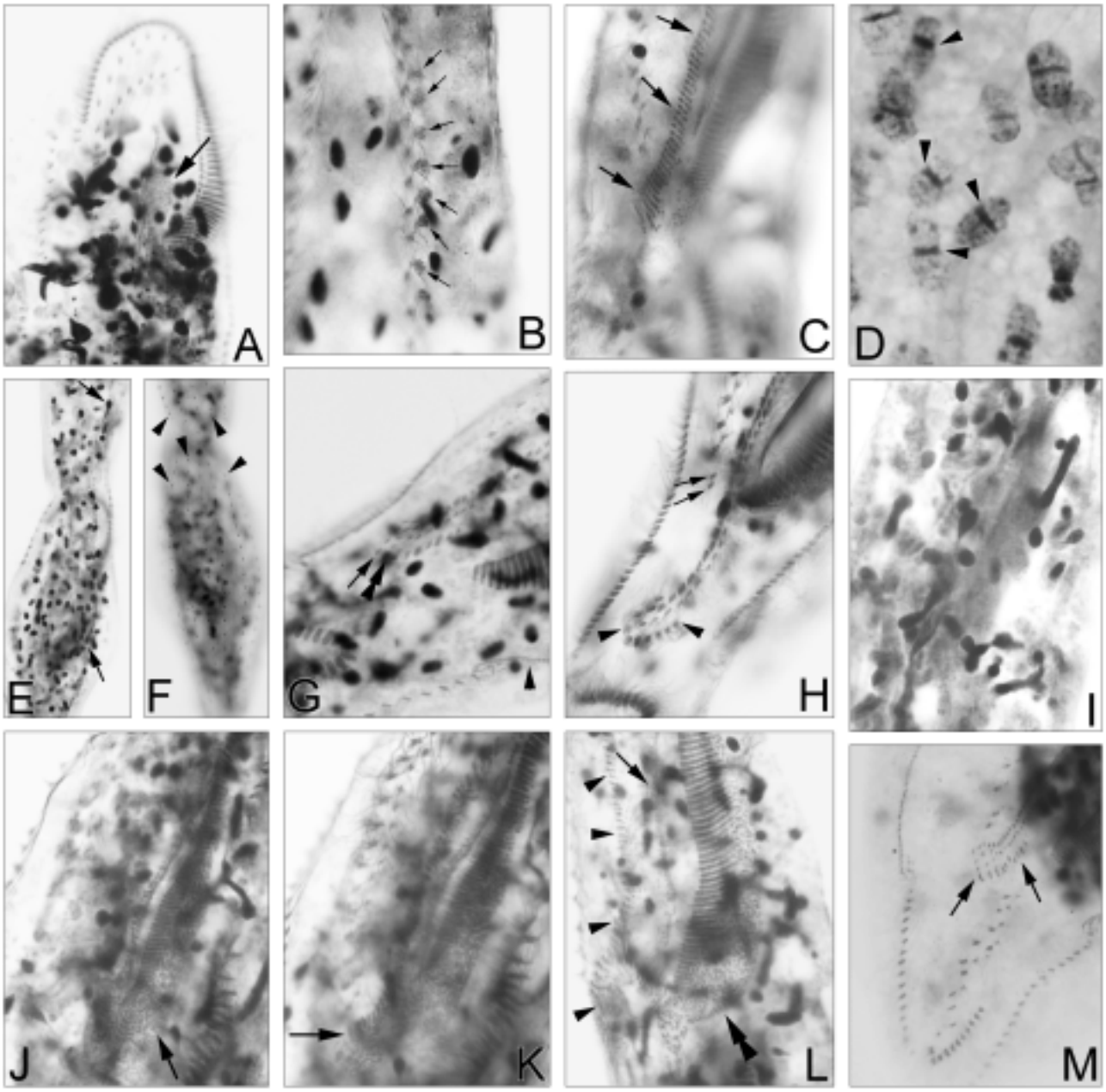

Figs 7A - M. Photomicrographs of *Pseudokeronopsis pararubra* sp. n. after protargol impregnation. **A** - note the oral primordium (arrow) in the proter; **B** - arrows depict small groups of basal bodies very close to left midventral cirri; **C** - depicting fronto-midventral transverse cirral anlagen (arrows) of the proter**; D** - noting the replication bands of macronuclear segments (arrowheads). **E, F** - part of the same later divider, to show dividing micronuclei (arrows) and new dorsal kineties (arrowheads); **G** - ventral view of posterior portion of the proter, arrow to show the last streak producing four cirri, double-arrowhead to mark the next anlage forming five cirri, arrowhead to indicate the anlage for the left marginal cirral row; **H** - ventral view of the posterior part of the proter, arrows to show frontoterminal cirri moving anteriad, arrowheads to mark the new transverse cirri; **I** - noting the division of the macronuclear segments; **J, K** - ventral views of part of the same proter, arrow in **J** to show the oral primordium, arrow in K to mark the fronto-midventral transverse cirral anlagen; **L** - ventral view of part of the proter to show the fronto-midventral transverse cirral anlagen (arrowheads), undulating membranes anlagen (arrow) and oral primordium (double-arrowhead); M - ventral view of the posterior portion of the opisthe, arrows to show the new transverse cirri.

designated as *Keronopsis rubra* f. *heptasticha* in the legend) clearly shows that the anterior-most three cirri of *H. pulchra* are distinctly enlarged. Kahl (1933) provided an additional illustration, which also clearly shows that *H. pulchra* has only 3 frontal cirri. Therefore, the form described by Kahl should not be transferred to the genus *Pseudokeronopsis* since it lacks a distinct bicorona. Borror (1972) illustrated the infraciliature

Table 2. Comparison of the red, orange and other coloured taxa of marine *Pseudokeronopsis* reinvestigated using silver impregnation techniques. Measurement in µm. AM - adoral membranelles, BC - buccal cirrus, DK - dorsal kineties, FC - frontal cirri, MVC - midventral cirri, MVR - midventral rows, PM - paroral membrane, TC - transverse cirri

	P. flava	*P. flavicans*	*P. flavicans*[1]	*P. carnea*	*P. carnea*[2]	*P. rubra*	*P. rubra*	*P. qingdaoensis*	*P. pararubra* sp. n.
Cell size *in vivo*	140-260×40-57	200-300×40-55	160-200×24-40	140-200×28-40	200-320×30-50	170-290×30-70	165-230×54-90	130-240×50-70	180-350×50-90
Body shape	very slender, posteriorly tapered	belt-like, caudally narrowed	slender with posterior end spoon-like	belt-like, caudally slightly or not narrowed	slender with posterior end spoon-like	band-like with posterior end spoon-like	long elliptical with posterior end narrowed	elongated with tapering posterior end	long elliptical with posterior end narrowed
Colour of pigments	yellow brownish	yellow-	brick-red	orange-red	orange-red	brick-red	brick-red	reddish	orange-red
Position of single BC relative to PM	middle part* mid-point	beside	*ca* mid-point*	posterior 1/3*	posterior 1/3*	anterior 1/3	anterior 1/3	**	posterior 1/3
Number of AM	43-59	46-66	46-60	39-80	58-80	50-92	62-88	50-65	64-92
Number of FC	*ca* 9	*ca* 14	11-14	10-14	*ca* 14	14-16	12-18	21-35	15-26
Number of pairs of MVC	28-38	25-40	*ca* 24-38	22-44	*ca* 35	28-47	28-38	*ca* 40	*ca* 30-45
Number of TC	1-3	3-6	2-4	6-7	5-7	*ca* 7	5-8	27-45	7-11
Number of DK	*ca* 4	4-5	4-7	5-6	5	*ca* 6	6-7	3	5-8
Gap between posterior end of MVR and TC	always conspicuous	small and inconspicuous	small to conspicuous	small to conspicuous	conspicuous	absent	absent	absent	absent
References	Wirnsberger *et al.* (1987)	Song *et al.* (2002)	Hu and Song (2001a)	Wirnsberger *et al.* (1987)	Foissner (1984)	Wirnsberger *et al.* (1987)	Shi and Xu (2003)	Hu and Song (2000b)	present study

[1, 2] Both called *Pseudokeronopsis rubra* in these two papers; * based on the protargol illustrations; ** buccal cirri consisting of 6-10 cirri

of *Keronopsis pulchra*. The figure shows that this species has a more or less distinct bicorona suggesting that it should be assigned to the genus *Pseudokeronopsis* (Wirnsberger *et al.* 1987). In addition, the conspicuously shortened midventral rows and the lower numbers of frontal and transverse cirri clearly separate this taxon from *P. pararubra* sp. n. Consequently, the organisms observed by Borror (1972) and by Borror and Wicklow (1983) were very likely misidentified in both cases. Furthermore, the form illustrated by Borror and Wicklow (1983) is very similar to our new species in terms of its body shape, the general ciliary pattern and the number of frontal and transverse cirri. Therefore we consider it very likely a synonym of *P. pararubra* sp. n.

The morphogenesis of *Pseudokeronopsis* spp. has been reported on at least three occasions (Borror 1972, Wirnsberger 1987, Hu and Song 2001a). The new species corresponds well with its congeners in the origin and developmental pattern of the primordia and the anlagen. Only one point needs to be noted here, which is the connection of the oral primordium with the fronto-midventral transverse cirral anlagen in the proter. Based on our observations of this species and of *Pseudokeronopsis flavicans* (Hu and Song 2001a), these two structures appear in different places and never develop a connection at their posterior ends at any stage during the divisional process. However, this is in contrast with that in *P. carnea*, in which these two groups of primordium join posteriorly for a period (Borror 1972, Wirnsberger 1987). According to our studies, however, these two groups of primordia intersect each other at different depths within the cell (i.e. in different optical planes), so the apparently close contact between them, especially when viewed from the ventral side and at lower magnification, is likely an artefact.

Family Amphisiellidae Jankowski, 1979

Genus *Amphisiella* Gourret *et* Roeser, 1888

***Amphisiella annulata* (Kahl, 1928) Borror, 1972 (Figs 4, 5, 8; Tables 3, 4)**

Syn. *Holosticha annulata* Kahl, 1928

Holosticha (*Amphisiella*) *annulata* Kahl, 1928 in Kahl, 1932

Prior to this investigation, this species has not been reported from Yellow Sea, China although it has been noted elsewhere for a few times (Kahl 1932, Borror 1972, Aladro Lubel 1985, Alekperov and Asadullayeva 1999, Berger 2004). The description below is based on observations on the population found in mollusks-culturing waters off the coast of Qingdao, China.

Ecological features: For January 1996 and November 2000 respectively: water temperature about 4°C and 15°C, salinity 29‰ and 33‰, pH 8.0 and 8.3.

Morphology (Figs 4, 8; Table 3): Body measures 100-210 × 24-75 μm *in vivo*, usually elongated elliptical in shape with both ends rounded, left margin conspicuously convex at middle part and right one distinctly sigmoidal (Fig. 4A); ratio of body length to width about 3-5: 1. As in other hypotrichs, body variable in size depending on nutritious state. Dorsoventrally flattened, with ventral side even and dorsal side evidently convex at middle portion (Fig. 4B). Cell flexible and slightly contractile (Fig. 4C). Body colourless to grayish at low magnification. Adoral zone of membranelles about 25% - 33% of body length, with distal end bending posteriorly far onto right ventral side (Figs 4A; 8C, arrows).

Pellicle soft, with colourless extrusomes, less than 0.5 μm in diameter, grouped around dorsal bristles and arranged in lines along dorsal kineties; when ejected, 2-3 μm long (Fig. 4D). Cytoplasm transparent with several refractile granular inclusions, 2-5 μm long. Sometimes 1-2 food vacuoles recognized at mid-body; contractile vacuole not observed, probably absent. Two ellipsoid to long elliptical macronuclear nodules (Ma) positioned posterior to oral field and left of median (Figs 4H, 8B); 2-6 micronuclei (n=21), each about 4 μm long, and about 1-2 located adjacent to one macronuclear nodule (Figs 4A, E, H; 8B, arrows); sometimes micronuclei distantly located far from macronuclear nodules in impregnated cell (Fig. 4H).

Cilia of apical adoral membranelles *ca* 15 μm long. Enlarged frontal cirri about 15 μm in length; transverse cirri *ca* 16-20 μm long; other cirri slightly shorter, 10-12 μm long. Right marginal row located parallel to amphisiellid median cirral row, and cirri in both rows remain motionless for most of the time.

Movement without peculiarities, that is, by crawling on substrate or rotating around long body axis when swimming. Feeds mainly on bacteria.

Infraciliature as shown in Figs 4E-I, 8A-G. Adoral zone of membranelles composed of 33-62 membranelles. Paroral membrane composed of two rows of basal bodies in 'Zig-Zag' form parallel to single-rowed endoral membrane, and anteriorly positioned (Fig. 8G, arrowhead and arrow, respectively). Constantly three slightly enlarged frontal cirri (FC, Figs 4F; 8D, short arrows), one cirrus behind the right frontal cirrus (Fig. 8D, arrowhead), one buccal cirrus and three cirri left of amphisiellied median cirral row (Fig. 8D, long arrow and double-

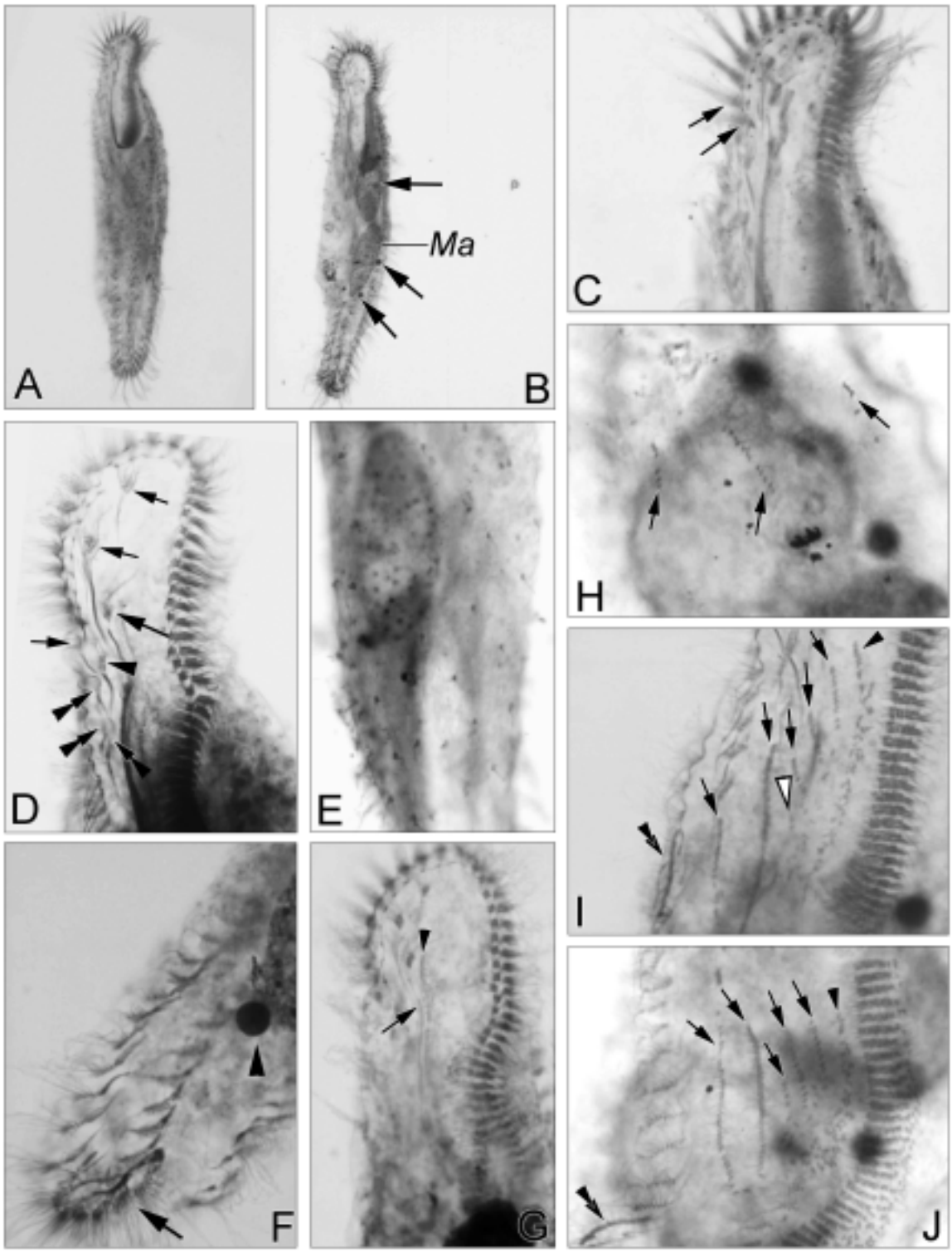

Figs 8A - J. Photomicrographs of *Amphisiella annulata* after protargol impregnation. **A** - infraciliature on ventral side; **B** - macronuclear nodules and micronuclei (arrows); **C, D** - infraciliature in anterior ventral portion, arrows in C to show the membranelles at the distal end, short arrows in D to indicate the frontal cirri, long arrow to show the buccal cirrus, arrowhead to mark the cirrus behind the right frontal cirrus, double-arrowheads to note the cirri left of the amphisiellid median cirral row; **E** - dorsal part of the cell, to note the dorsal kineties; **F** - ventral view of the posterior portion of the cell, arrow to show the transverse cirri, arrowhead to indicate micronucleus; **G** - buccal apparatus, arrowhead to show the paroral membrane, arrow to indicate the endoral membrane; **H** - dorsal view of part of the cell, arrows to show the dorsal kineties anlagen; **I, J** - ventral views of the proter and the opisthe, arrows to show the cirral anlagen, solid arrowheads to indicate the anlagen separated from the anterior end of the undulating membranes anlagen, hollow arrowhead and double-arrowheads to mark additional anlage between cirral anlagen IV and V, and the marginal cirral anlagen, respectively.

Table 3. Morphometric characterizations of two populations of *Amphisiella annulata* (upper line, 1996 population; lower line, 2000 population). Data based on protargol impregnated specimens. Measurements in mm. ACR - amphisiellid median cirral row, CV - coefficient of variation in %, Max - maximum, x - arithmetic mean, Min - minimum, n - number of specimens examined, SD - standard deviation, SE - standard error of the mean. Measurements in µm.

Character	Min	Max	x	SD	SE	CV	n
Body length	120	203	167.3	24.69	6.37	14.8	15
	120	200	152.8	21.88	4.47	14.3	24
Body width	45	80	59.3	10.60	2.74	17.9	15
	28	64	42.1	9.74	2.08	23.1	22
Adoral zone of membranelles, length	48	78	65.7	8.63	2.23	13.1	15
	42	78	55.3	10.04	2.01	18.1	25
Number of adoral membranelles	41	62	52.2	5.70	1.52	10.9	15
	33	57	44.7	6.58	1.34	14.7	24
Number of frontal cirri	3	3	3	0	0	0	15
	3	3	3	0	0	0	25
Number of cirri behind of the right frontal cirrus	1	1	1	0	0	0	15
	1	1	1	0	0	0	25
Number of buccal cirri	1	1	1	0	0	0	15
	1	1	1	0	0	0	25
Number of cirri left of ACR	3	3	3	0	0	0	15
	3	3	3	0	0	0	25
Number of cirri in ACR	45	61	49.9	13.04	5.83	26.2	15
	33	56	42.5	5.98	1.34	14.1	20
Number of pre-transverse cirri	2	2	2	0	0	0	15
	2	2	2	0	0	0	25
Number of transverse cirri	5	7	5.9	0.46	0.12	7.7	15
	6	6	6	0	0	0	20
Number of left marginal cirri	36	46	40.9	3.50	0.93	8.5	15
	25	53	36.5	7.24	1.58	19.8	21
Number of right marginal cirri	36	49	42.4	4.29	1.15	10.1	15
	22	48	34.9	6.69	1.46	19.2	21
Number of dorsal kineties	8	10	8.2	0.53	0.13	6.5	15
	7	8	7.7	0.58	0.13	7.6	19
Number of macronuclear nodules	2	2	2	0	0	0	15
	2	2	2	0	0	0	25
Macronuclei length	16	35	24.3	8.47	2.19	34.8	15
	27	44	34.2	5.15	1.03	15.0	25
Macronuclei width	9	15	12.2	1.57	0.41	12.9	15
	12	28	17.8	4.85	0.97	0.27	25
Number of micronuclei	-	-	-	-	-	-	-
	2	6	3.5	0.98	0.21	28.2	21

- No data available

arrowheads, respectively). Five to seven (usually six) transverse cirri (TC) arranged in J-shape (Figs 4F, G; 8F, arrow). Amphisiellid median cirral row (ACR), of which the cirri are wide (up to 4-5 µm) and narrowly spaced, especially at middle portion (Figs 4E, G), is composed of 33-61 cirri, extending posterior to TC. Additionally 2 pre-transverse cirri located between the posterior end of ACR and TC (Figs 4F, arrows; 4G, I). One left and one right marginal cirral row with their posterior ends not confluent (Figs 4E-G, I), base of each cirrus consisting of two basal body rows. Seven to ten dorsal kineties, of which several rows are shortened at both ends (Figs 4H, 8E); dorsal cilia about 5 µm long, easily recognizable *in vivo*.

Morphogenesis (Figs 4J, 5): A detailed analysis of the morphogenetic process was not carried out because only a few dividers and reorganizers were found, mostly middle to late stages. Nevertheless, these allow us to deduce that stomatogenesis in *A. annulata* is similar to that in its congeners (Wicklow 1982): the oral primordium (OP) originates parakinetally from the ACR (Fig. 4J) in the opisthe, while the old adoral membranelles seems to be retained completely by the proter, and the old undulating membranes must be renewed (Figs 4J,

Table 4. Supplementary comparison of Qingdao populations of *Amphisiella annulata* with a few marine congeners. ACR - amphisiellid median cirral row, AM - adoral membranelles, BL - body length, DK - dorsal kineties, FC - frontal cirri, Ma - macronuclear nodules, TC - transverse cirri. Measurements in µm.

Species name	Body shape	BL	M	FC*	ACR	TC	Ma	DK	Data source
A. ovalis Fernandez-Leborans *et* Novillo, 2001	oval	50-63	16-19	4	18-22	6-7	32-45	4	Fernandez-Leborans and Novillo (1992, 2001)
A. capitata (Perejaslawzewa, 1885)	elongated, slightly cephalized	-	-	11	-	5	2	-	Kahl (1932)
A. oblonga (Schewiakoff, 1893)	elliptical	160	-	4	-	4	2	-	Kahl (1932)
A. thiophaga (Kahl, 1928)	long elliptical	70-100	-	5	-	7	2	-	Kahl (1928, 1932)
A. arenicola Fernandez-Leborans *et* Novillo, 2001	elongated oval	132-162	36-42	7	52-56	5-6	2	5-6	Fernandez-Leborans and Novillo (1992, 2001)
A. annulata (Kahl, 1928)	long elliptical	100-210	33-62	8	33-61	5-7	2	7-10	present study

* including other cirri left of ACR in frontal field

arrow; 5A). Six cirral anlagen (Figs 5A; 8I, J; arrows) eventually develop into the frontal, pre-transverse and transverse cirri and amphisiellid median cirral row plus undulating membranes (usually the anlage generating undulating membranes and one frontal cirrus at its anterior end also called undulating membrane anlage; Figs 5A, arrowhead; 5E, arrow; 8I, J, arrowhead). Rarely there is a small additional anlage between the normal anlagen IV and V (Fig. 5A, arrow). In both dividers, the rightmost two cirral anlagen are formed within the old amphisiellid median cirral row. In the proter, the undulating membranes, the buccal cirrus and some cirri left of the ACR provide three streaks, while in the opisthe, the oral primordium produces the anlage for the undulating membranes and very likely three cirral streaks (Figs 4J; 5A). The marginal row and dorsal kineties evolve as described by Berger (2004), that is, all anlagen occur within the old structures and develop to replace them (Figs 5; 8H-J, arrows and double-arrowhead). The division of the nuclear apparatus does not show a peculiarity. Two marconuclear nodules fuse to a single mass during the middle stages (Figs 5B, F), which subsequently divides twice to be assigned to the daughters.

Comparison: The Qingdao populations of *Amphisiella annulata* correspond well with the redescriptions by Kahl (1932) and Berger (2004) in terms of body shape and size, number of macronuclear nodules as well as ciliary pattern, especially the very narrowly spaced and rather wide cirri of the amphisiellid median cirral row. However, although ring-shaped structures (lithosomes?), the characteristic feature that Kahl (1928) and Berger (2004) described for *Amphisiella annulata*, could not be seen in the cytoplasm of our populations, this is not a proof of misidentification because Kahl (1932) also mentioned that the rings can be absent.

Since Berger (2004) very recently gave a detailed redescription and neotypication of *Amphisiella annulata*, we here provide only supplementary comparisons with some of its congeners (Table 4). Compared with *A. annulata*, *A. ovalis* is much smaller (49.5-63 µm long), has an oval body shape and fewer cirri as well as more macronuclear segments (32-45 *vs.* 2), thus the two can be easily separated (Fernandez-Leborans and Novillo 1992, 2001).

In terms of its body shape, *Amphisiella annulata* also resembles *A. thiophaga*, whose infaciliature is unknown. However, the latter is smaller (70-100 µm)

and has fewer frontal cirri (5 *vs.* 7-9) and sparsely arranged cirri in the amphisiellid median cirral row (Kahl 1932, Borror 1963, Aladro Lubel 1985, Alekperov and Asadullayeva 1999, Berger 2004). Likewise, the infraciliature of *Amphisiella capitata* and *A. oblonga* remain unknown although they differ from *A. annulata* in body shape and in the number of frontal and transverse cirri (Kahl 1932). Fernandez-Leborans and Novillo (1992, 2001) described a new form, *Amphisiella arenicola*, which is similar to *A. annulata* in terms of its body size and the number of adoral membranelles, cirri and macronuclear nodules. However, the former can be separated from the latter by its elongated oval body shape (*vs.* elongated elliptical) and the location of the amphisiellid median cirral row (in middle zone and with a distinct gap between its posterior end and transverse cirri *vs.* posteriorly located and with no gap between its posterior end and the transverse cirri).

As concerns morphogenesis and reorganization, the Qingdao populations lack the additional anlage between the ordinary anlagen IV and V described by Berger (2004) in the Adriatic population of *A. annulata*, so that usually only six ordinary anlagen (I-VI) are formed during division. According to Berger (2004) six transverse cirri in the Adriatic population was formed by the mode that six ordinary cirral anlagen plus an additional anlage contribute one transverse cirrus each at its posterior end except for undulating membrane anlage which does not generate transverse cirrus, 6 cirral anlagen present in Qingdao populations can only produce 5 transverse cirri. However, most cells have six transverse cirri at interphase in our studies. In order to elucidate this difference, we assume that the following possibilities exist: (1) in the instance of only 6 cirral anlagen (most common condition), if each anlage develops one transverse cirrus thus 5 transverse cirri (this number occurs very rarely in our population and the Adriatic population) are eventually formed; if the posterior-most anlage contributes two transverse cirri as demonstrated in *Pseudokeronopsis* spp. by Wirnsberger (1987), so that the filial cell will have 6 transverse cirri (this is very likely the case of Qingdao populations); (2) if an additional anlage occurs (rarely in Qingdao population), then the anlagen probably evolve in the way as shown by Berger (2004) and six transverse cirri are thus formed, one from each anlage.

Acknowledgements. This work was supported by JSPS Postdoctoral Fellowship for Foreign Researcher and Natural Science Foundation of China (project number: 40206021), both awarded to the senior author.

REFERENCES

Aladro Lubel M. A. (1985) Algunos ciliados intersticiales de Isla de Enmedio, Veracruz, México. An. *Inst. Biol. Univ. Méx,. Ser. Zoologia* (1) **55:** 1-59

Alekperov I. K., Asadullayeva E. S. (1999) New, little-known and characteristic ciliate species from the Apsheron coast of the Caspian Sea. *Turkish J. Zool.* **23:** 215-225

Berger H. (2004) *Amphisiella annulata* (Kahl, 1928) Borror, 1972 (Ciliophora: Hypotrichida): morphology, notes on morphogenesis, review of literature, and neotypification. *Acta Protozool.* **43:** 1-14

Borror A. C. (1963) Morphology and ecology of the benthic ciliated protozoa of Alligator Harbor, Florida. *Arch. Protistenkd.* **106:** 465-534

Borror A. C. (1972) Revision of the order Hypotrichida (Ciliophora, Protozoa). *J. Protozool.* **19:** 1-23

Borror A. C., Wicklow B. J. (1983) The suborder Urostylina Jankowski (Ciliophora, Hypotrichida): morphology, systematics and identification of species. *Acta Protozool.* **22:** 97-126

Eigner P., Foissner W. (1994) Divisional morphogenesis in *Amphisiellides illuvialis* n. sp., *Paramphisiella caudata* (Hemberger) and *Hemiamphisiella terricola* Foissner, and redefinition of the Amphisiellidae (Ciliophora, Hypotrichida). *J. Euk. Microbiol.* **41:** 243-261

Fernandez-Leborans G., Novillo A. (1992) Morphology and taxonomy of two new species of marine ciliates (Ciliophora: Spirotriea: Stichtrichida: Amphisiellidae). *Proc. Biol. Soc. Wash.* **105:** 165-179

Fernandez-Leborans G., Novillo A. (2001) A note about two hypotrich ciliate species of the genus *Amphisiella*. *Acta Protozool.* **40:** 225-227

Foissner W. (1982) Ecology and taxonomy of the hypotrichida (Protozoa:Ciliophora) of some austrian soils. *Arch. Protistenkd.* **126:** 19-143

Foissner W. (1984) Infraciliatur, Silberliniensystem und Biometrie einiger neuer und wenig bekannter terrestrischer, limnischer und mariner Ciliaten (Protozoa: Ciliophora) aus den Klassen Kinetofragminophora, Colpodea und Polyhymenophora. *Stapfia* **12:** 1-165

Hu X., Song W. (2000a) Morphology and morphogenesis of a marine ciliate, *Gastrostyla pulchra* (Perejaslawzewa, 1885) Kahl, 1932 (Ciliophora, Hypotrichida). *Europ. J. Protistol.* **36:** 201-210

Hu X., Song W. (2000b) Infraciliature of *Pseudokeronopsis qingdaoensis* nov. spec. from marine biotope (Ciliophora: Hypotrichida). *Acta Zootaxo. Sin.* **25:** 361-364 (in Chinese with English abstract)

Hu X., Song W. (2001a) Morphological redescription and morphogenesis of the marine ciliate, *Pseudokeronopsis rubra* (Ciliophora, Hypotrichida). *Acta Protozool.* **40:** 107-115

Hu X., Song W. (2001b) Morphology and morphogenesis of *Holosticha heterofoissneri* nov. spec. from the Yellow Sea, China (Ciliophora, Hypotrichida). *Hydrobiologia* **448:** 171-179

Hu. X., Song W. (2001c) Redescription of the marine ciliate, *Stichotricha marina* Stein, 1867 (Ciliophora, Hypotrichida) from the mantle cavity of cultured scallop. *Hydrobiologia* **464:** 71-77

Hu X., Song W. (2002) Studies on the ectocommensal ciliate, *Trachelostyla tani* nov. spec. (Protozoa: Ciliophora: Hypotrichida) from the mantle cavity of the scallop *Chalmydis farrei*. *Hydrobiologia* **481:** 173-179

Hu X., Song W. (2003) Morphology, infraciliature and divisional morphogenesis of marine hypotrichs, *Pseudokahliella marina* Foissner *et al.*, 1982 from scallop-culturing water of North China. *J. Nat. Hist.* **37:** 2033-2043

Hu X., Suzuki T. (2004) A new species of *Holosticha* (Ciliophora: Hypotrichida) from the coastal waters of Nagasaki, Japan:

Holosticha nagasakiensis sp. nov. *J. Mar. Biol. Ass. UK* **84:** 9-13

Hu X., Song W., Warren A. (2002) Observations on the morphology and morphogenesis of a new marine urostylid ciliate, *Parabirojimia similis* nov. gen., nov. spec. (Protozoa, Ciliophora, Hypotrichida). *Europ. J. Protistol.* **38:** 351-364

Kahl A. (1928) Die Infusorien (Ciliata) der Oldesloer Salzwasserstellen. *Arch. Hydrobiol.* **19:** 189-246

Kahl A. (1932) Urtiere oder Protozoa I: Wimpertiere oder Ciliata (Infusoria) 3. Spirotricha. *Tierwelt Dtl.* **25:** 399-650

Kahl A. (1933) Ciliata libera et ectocommensalia. *Tierwelt N.- u. Ostsee Lieferung* **23 (Teil II. C_3):** 29-146

Shi X., Xu R. (2003) Morphology and infraciliature of *Pseudokeronopsis rubra* in Jieshi waters of South China Sea. *J. Trop. Oceano.* **22:** 23-29 (in Chinese with English abstract)

Song W., Hu X. (1999) Divisional morphogenesis in the marine ciliates, *Hemigastrostyla enigmatica* (Dragesco & Dragesco-Kernéis, 1986) and redefinition of the geneus *Hemigastrostyla* Song & Wilbert, 1997 (Protozoa, Ciliophora). *Hydrobiologia* **391:** 249-257

Song W., Warren A. (2000) *Pseudoamphisiella alveolata* (Kahl, 1932) nov. comb., a large marine hypotrichous ciliate from China (Protozoa, Ciliophora, Hypotrichida). *Europ. J. Protistol.* **36:** 451-457

Song W., Wilbert N. (1997a) Morphological studies on some free living ciliates (Ciliophora: Heterotrichida, Hypotrichida) from marine biotopes in Qingdao, China with descriptions of three new species: *Holosticha warreni* nov. spec., *Tachysoma ovata* nov. spec. and *T. dragescoi* nov. spec. *Europ. J. Protistol.* **33:** 48-62

Song W., Wilbert N. (1997b) Morphological investigations on some free living ciliates (Protozoa, Ciliophora) from China Sea with description of a new hypotrichous genus, *Hemigastrostyla* nov. gen. *Arch. Protistenkd.* **148:** 413-444

Song W., Wilbert N., Warren A. (2002) New contribution to the morphology and taxonomy of four marine hypotrichous ciliates from Qingdao, China (Protozoa: Ciliophora). *Acta Protozool.* **41:** 145-162

Wicklow B. J. (1982) The Discocephalina (n. subord.): ultrastructure, morphogenesis and evolutionary implications of a group of endemic marine interstitial hypotrichs (Ciliophora, Protozoa). *Protistologica* **18:** 299-330

Wilbert N. (1975) Eine verbesserte Technik der Protargolimprägnation für Ciliaten. *Mikrokosmos* **64:** 171-179

Wirnsberger E. (1987) Division and reorganization in the genus *Pseudokeronopsis* and relationships between urostylids and oxytrichida (Ciliophora, Hypotrichida). *Arch Protistenkd.* **134:** 149-160

Wirnsberger E., Larsen H. F., Uhlig G. (1987) Rediagnoses of closely related pigmented marine species of the genus *Pseudokeronopsis* (Ciliophora, Hypotrichida). *Europ. J. Protistol*. **23:** 76-88

Received on 6th February, 2004; revised version on 5th July, 2004; accepted on 30th July, 2004

Acta Protozool. (2004) 43: 369 - 371

ACTA
PROTOZOOLOGICA

A New Coccidian Parasite, *Isospora andesensis*, from the Common Bush Tanager (*Chlorospingus ophthalmicus)* of South America

Alisha C. TEMPLAR[1], Thomas E. McQUISTION[1] and Angelo P. CAPPARELLA[2]

[1]Department of Biology, Millikin University, Decatur, Illinois; [2]Department of Biological Sciences, Illinois State University, Normal, Illinois, USA

Summary. A new species of *Isospora* is described from the fecal contents of the common bush-tanager, *Chlorospingus ophthalmicus hiaticolus*, an avian host from Peru. Sporulated oocysts are subspherical to ovoid, 22.6 × 18.7 (20-24 × 17-20) µm, with a smooth, colorless, bilayered wall, the inner wall is slightly thinner and darker than the outer wall. The average shape index is 1.2. No micropyle or oocyst residuum are present, but the oocyst contains one polar granule. Sporocysts are ovoid, 14.1 × 8.5 (13-15 × 8-9) µm, average shape index of 1.7 with a smooth, single layered wall and composed of a triangular-shaped Stieda body but no substieda body. The tip of the Stieda body is dark gray to black. The subspherical sporocyst residuum is composed of fine, uniform granules. Sporozoites are vermiform with an ovoid, posterior refractile body and an ovoid centrally located nucleus and randomly arranged in the sporocyst.

Key words: Coccidia, *Isospora andesensis* sp. n.

INTRODUCTION

The common bush-tanager (*Chlorospingus ophthalmicus hiaticolus*) forages primarily in groups of 10 to 20 birds, usually with mixed flocks of other tanagers (Ridgley and Tudor 1989). Common bush-tanagers are primarily found in the coastal mountains of the Andes, and their diet consists of fruit and insects (Valburg 1992). This paper describes the only isosporan parasite that has been reported in the genus *Chlorospingus*.

MATERIALS AND METHODS

Fecal samples were obtained from the common bush tanager during a bird collecting expedition in Peru during July 2002. Upon collection, the fecal samples were placed in 2.5% (w/v) $K_2Cr_2O_7$ solution and maintained at cool temperatures in the field before being

Address for correspondence: Thomas E. McQuistion, Department of Biology, Millikin University, Decatur, Illinois 62522 USA; Fax: (217) 362-6408; E-mail: tmcquistion@mail.millikin.edu

sent to the third author's laboratory for examination. Procedures for processing, examining, and measuring oocysts are described by McQuistion and Wilson (1989) using an Olympus BX-51 microscope with phase-contrast and differential interference contrast microscopy. All measurements are given in micrometers with the size ranges in parenthesis following the means. Oocysts were five months old when examined, measured, and photographed.

RESULTS

Isospora andesensis sp. n.

Description of oocysts: Oocysts subspherical to ovoid, 22.6 × 18.7 (20-24, SD = 1.18 × 17-20, SD = 0.96) (N = 30) with a smooth, bilayered wall; the inner wall is thinner and darker than the outer wall. The shape index (length/width) is 1.2 (1.1-1.3, SD = 0.07). Micropyle and oocyst residuum absent but one ovoid polar granule is present. Sporocysts are ovoid, 14.1 × 8.5 (13-15, SD = 0.57 × 8-9, SD = 0.53) (N = 27); shape index is 1.7 (1.6-1.8, SD = 0.09). The Stieda body is triangular shaped with the tip or apex dark gray to black with no apparent substieda body suggesting a membrane enclosing the sporozoites and sporocyst residuum. The sporozoites are vermiform with an ovoid, posterior refractile body and a centrally located nucleus. The 4 sporozoites are randomly arranged in the sporocyst with a subspherical residuum composed of fine, uniform granules.

Type-host: *Chlorospingus ophthalmicus hiaticolus* (Passeriformes: Thraupidae), sample taken July 17, 2002.

Type-specimens: A phototype series and formalin preserved sporulated oocysts are deposited in the Harold W. Manter Laboratory of Parasitology, University of Nebraska State Museum, Lincoln, Nebraska 68588, accession no. HWML 45412 (for formalin specimens) and HWML 45413 (for phototypes).

Type-location: Peru, San Martin Departamento; *ca* 24 km ENE of Florida (village) 5° 43'23"S, 77° 45'01"W, *ca* 2500 m elevation.

Prevalence: 3/7 (43%) was infected within the same locality, but at varied elevations.

Site of infection: Unknown; oocysts found in feces.

Etymology: The specific epithet, *ensis*, is the Latin word meaning from, and is in reference to the location of the avian host, the Andes Mountains.

Remarks: The oocysts are easily broken and collapse after one hour in sugar solution. There were hundreds of oocysts present in the samples taken from the three infected birds.

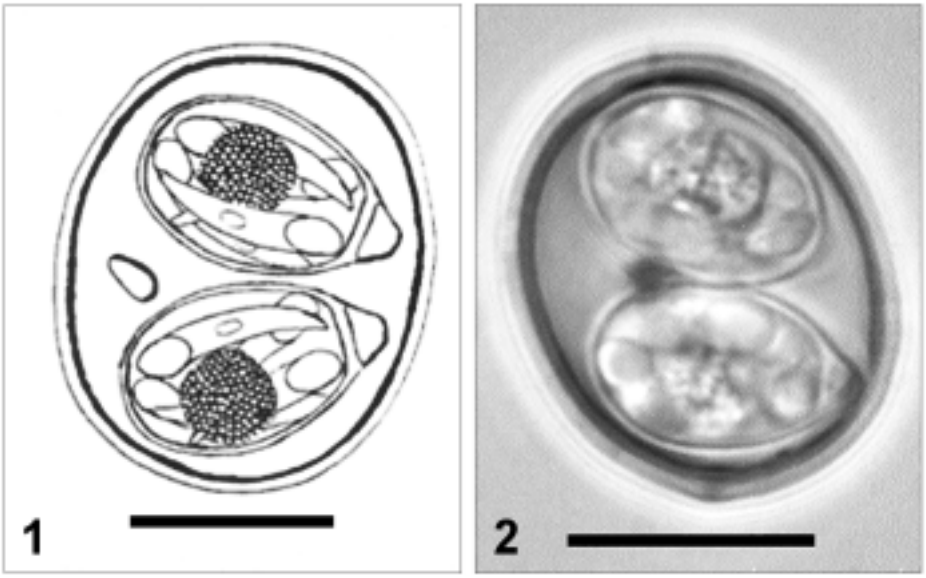

Fig. 1. Composite line drawing of sporulated oocyst of *Isospora andesensis* sp. n. from *Chlorospingus ophthalmicus*. Scale bar 10 µm.
Fig. 2. A differential interference contrast photomicrograph of sporulated oocyst of *Isospora andesensis* sp. n. Scale bar 10 µm.

DISCUSSION

Tanagers (Order Passeriformes, Family: Thraupidae) are not definable as a monophyletic group (Isler and Isler 1987, Ridgely and Tudor 1989). No taxonomic character exists that specifically defines the tanagers (Ridgley and Tudor 1989). They are mainly tropical in distribution, and reach maximum diversity in the Andes, where mixed flocks may have up to a dozen or more tanager species in them (Ridgley and Tudor 1989).

Boughton *et al*. (1938) reported coccidia in three genera of Andean tanagers, the southern palm tanager, *Thraupis palmarum palmarum*, the Brazilian silver-beaked tanager, *Rhamphocelus brasilius*, the magpie tanager, *Cissopis leveriana*, and southern silver-beaked tanager, *Rhamphocelus carbo carbo*. However, all were reported from captured birds in zoos and none of the coccidia were described or named. Lainson (1994) described *Isospora thraupis* from the palm tanager, *Thraupis palmarum melanoptera*, a possible sympatric species with *Chlorospingus ophthalmicus.* Although the average oocysts of *Isospora thraupis* are similar in size (19.9 × 19 µm) and shape index (1.0) to *Isospora andesensis* sp. n. (22.6 × 18.7 µm and 1.2), the sporocysts and sporozoites are quite different between the two species. *I. thraupis* has an inconspicuous Stieda body and a very small, but distinct substieda body. *I. andesensis* sp. n. has a prominent, triangular-shaped Stieda body and no substieda body. Sporozoites of *I. thraupis* have two refractiles bodies while *I. andesensis* sp. n. sporozoites have only one refractile body. Additionally, no polar granule is reported in *I. thraupis* oocysts while *I. andesensis* sp. n. has one polar granule.

Acknowledgements. The authors thank the Academy of Natural Sciences of Philadelphia for funding the bird collecting expedition, Mr. Zachary A. Cheviron for host identification and capture location data, Amanda Hill for the composite drawing and Ms. Mary Ellen Martin for assistance in naming the parasite. Microscopy equipment was funded by National Science Foundation grant number DBI 0116693.

REFERENCES

Boughton D. C., Boughton R. B., Volk J. (1938) Avian hosts of the genus *Isospora* (Coccidiidae). *Ohio J. Sci*. **38:** 149-163

Isler M. L., Isler P. R. (1987) The Tanagers: Natural History, Distribution, and Identification. Smithsonian Institution Press, Washington, D.C.

Lainson R. (1994) Observations on some avian coccidia (Apicomplexa: Eimeriidae) in Amazonian Brazil. *Mem. Inst. Oswaldo Cruz Rio de J*. **89:** 303-311

McQuistion T. E., Wilson M. (1989) *Isospora geospizae*, a new coccidian parasite (Apicomplexa: Eimeriidae) from the small ground finch (*Geopspiza fuliginosa*) and the medium ground finch (*Geospiza fortis*) from the Galapagos Islands. *Syst. Parasitol.* **14:** 141-144

Ridgley R. S., Tudor G. (1989) The Birds of South America. University of Texas Press, Austin, Texas

Valburg L.K. (1992) Flocking and frugivory: the effect of socialgroupings on resource use in the common bush-tanager. *Condor* **94:** 358-363

Received on 1st June, 2004; revised version on 2nd August, 2004; accepted on 3rd August, 2004

Acta Protozool. (2004) 43: 373 - 377

ACTA
PROTOZOOLOGICA

Short Communication

Prolonged Activation of Transcription Regulating Factors in *Trypanosoma brucei brucei* Nuclear Proteins by Interferon-γ Stimulation

Ahmed SHARAFELDIN[1], Thomas BITTORF[2], Robert A. HARRIS[4], Eilhard MIX[3] and Moiz BAKHIET[1]

[1]Center for Infectious Medicine, Karolinska Institute, Huddinge University Hospital, Stockholm, Sweden; [2]Department of Medical Biochemistry and [3]Department of Neurology, University of Rostock, Germany; [4]Center for Molecular Medicine, Karolinska Hospital, Stockholm, Sweden

Summary. In African trypanosomiasis the host-derived cytokine interferon-γ (IFN-γ) has been identified as a potent growth promoter of the causative agent *Trypanosoma brucei brucei (T.b.b.)*. The mechanism of growth promotion involves activation of tyrosine protein kinases (TPKs). In the present study, it is shown that in contrast to the situation in multicellular eukaryotic organisms, IFN-γ-stimulated TPKs in *T.b.b.* do not activate transcription factors (TFs) of the signal transducers and activators of transcription (STAT) family, but they activate the TF AP-1, and transcription regulating factors, which bind to E74 (ETS-like proteins) and to hSIE (STAT-like proteins), respectively. Prolonged activation of the transcription regulating factors was determined by electrophoretic mobility shift assay (EMSA) of IFN-γ stimulated *T.b.b*. In addition, c-fos, a component of the transcription factor AP-1, was detected immunocytochemically and by SDS-PAGE with subsequent Western blotting after IFN-γ stimulation of the trypanosomes. The findings support the reported growth enhancing properties of IFN-γ on trypanosomes and for the first time identify transcription regulating factors, which may be selectively involved in IFN-γ- dependent responses of protozoa.

Key words: IFN-γ, transcription factor, *Trypanosoma brucei.*

Abbreviations: AP-1 - activated protein-1, EMSA - electrophoretic mobility shift assay, ETS - external transcribed spacer, hSIE - high-affinity serum-inducible element, IFN-γ - interferon gamma, NF-κB - nuclear factor protein-κB, NO - nitric oxide, PARP - procyclic acidic repetitive protein, PBS - phosphate buffered saline, STAT - signal transducers and activators of transcription, *T.b.b.* - *Trypanosoma brucei brucei*, TFs - transcription factors, TLTF - T lymphocyte triggering factor, TPKs - tyrosine protein kinases, VSG - variant surface glycoprotein.

INTRODUCTION

Trypanosoma brucei is an extracellular hemoflagellate protozoan parasite creating major health problems in sub-Saharan Africa. It is the causative agent of human African trypanosomiasis or sleeping sickness, and 'nagana' disease in animals. The parasites multiply freely in the blood of their infected hosts and are capable of evading the host immune system by switching their outer body surface protein (Turner and Barry 1989). *Trypanosoma brucei* infection induces a massive polyclonal activation of B-lymphocytes, generalized immunosuppression with multiple changes in the cells of the lym-

Address for correspondence: Ahmed Sharafeldin, Karolinska Institute, Cardiovascular Research Unit, Cellular and Molecular Immunology Unit, Center for Molecular Medicine (CMM), L8:03, Karolinska Hospital, 171 76 Stockholm, Sweden; Fax: + 46 8 313147; E-mail: Ahmed.Sharafeldin@cmm.ki.se

phoid tissues, and induction of suppressive T-cells and macrophages (Askonas *et al.* 1979). In addition, early induction of various other immune mediators such as nitric oxide (NO) (Sternberg and McGuigan 1992) and IFN-γ (Olsson *et al*. 1991) are also associated with the infection.

IFN-γ is an important cytokine for the host response against different infections, especially viral infections. However, recent studies demonstrated that in *Trypanosoma brucei* infection this cytokine plays an important role for the benefit of the trypanosomes. It was shown that IFN-γ could stimulate the growth and proliferation of *Trypanosoma brucei brucei* (*T.b.b.*) *in vitro* and *in vivo* (Bakhiet *et al*. 1996). A parasite-released protein called T lymphocyte triggering factor (TLTF) induces $CD8^+$ T lymphocytes to produce IFN-γ (Olsson *et al*. 1991, 1993; Bakhiet *et al*. 1996). The gene for this protein was cloned and the recombinant version was shown to induce IFN-γ secretion by $CD8^+$ but not $CD4^+$ T lymphocytes (Vaidya *et al*. 1997). The mechanism of IFN-γ activation of *T.b.b* was studied step-wise. A direct effect of IFN-γ on *T.b.b.* was the rapid and strong tyrosine phosphorylation detected in *T.b.b.* lysates by Western blotting after five minutes of stimulation (Mustafa *et al*. 1997). Downstream components of the signal pathway, especially transcription factors (TFs), transcription regulating factors responsible for *T.b.b.* growth promotion and TLTF expression, have not been identified to date.

Gene transcription in *T.b.b.* has been studied extensively in order to understand the molecular events leading to the expression of different variant surface glycoprotein (VSG) genes. These studies involved gene expression for VSG and procyclic acidic repetitive protein (PARP). In contrast to most eukaryotic cells, transcription in trypanosomes appears to encompass more than one gene in a polycistronic way of gene transcription that generates many pre-mRNAs carrying the information for more than one protein (Johnson *et al*. 1987). Three trypanosomal RNA polymerases analogous to eukaryotic RNA polymerases direct gene transcription in these primitive eukaryotes (Marchetti *et al*. 1998), and the gene expression of VSG and PARP are directed by RNA polymerase I (Clayton *et al*. 1990, Zomerdijk *et al*. 1991, Rudenko *et al*. 1992). It was also demonstrated that two reactions are required for processing the pre-mRNA in the trypanosomes, *trans*-splicing to add the cap at the 5' end, and completing the 3' end by polyadenylation (Murphy *et al*. 1986).

Transcription in eukaryotes involves the assembly of DNA binding proteins called TFs and other transcription regulating factors. TFs are proteins that bind to *cis*-acting elements of DNA and guide the binding of RNA polymerase II to start the transcription of specific mRNA (Szabo *et al*. 2000).

MATERIALS AND METHODS

Animals, infection and preparation and cultivation of *T.b.b*

Five DA rats were injected intraperitoneally (i.p.) with 10^5 of *T.b.b.* variable antigen type An Tat 1/1, derived from monomorphic stabilizer EATRO 1125 (WHO central serum bank for sleeping sickness, Antwerp, Belgium). Six days later, blood was collected from the rats by heart puncture in heparin-containing glass tubes. Blood was diluted 3:1 in phosphate buffered saline (PBS) supplemented with 1% glucose, pH 8.0 (PBSG). The suspension was centrifuged at 1,400 rpm for 10 min at 4°C. Trypanosomes were collected from the interface layer. PBSG- equilibrated DEAE columns (Pharmacia, Uppsala, Sweden) were used to separate *T.b.b.* from the remaining red blood cells.

Trypanosomes were collected on ice and their final concentration was adjusted to $5x10^8$/ml. Subsequently, they were incubated in RPMI (GIBCO BRL, Paisley, UK) supplemented with 10% foetal bovine serum (FBS) (GIBCO) for 6 h at 37°C in order to inhibit the *in vivo* activation of the IFN-γ-induced signal pathways.

Trypanosoma brucei brucei were then washed and their concentration was adjusted to $8x10^6$ per ml. They were stimulated with 400U/ml recombinant rat IFN-γ for 15, 60 or 240 min, respectively. A control group remained unstimulated. The stimulation was terminated and *T.b.b.* were recovered by centrifugation at 14,000 rpm. The supernatant was discarded and the pellet was snap-frozen in liquid nitrogen and stored at -85°C.

Infections of the rats are conducted in accordance with accepted ethical practice approved by the ethical committee at Karolinska Institute.

Preparation of nuclear extracts and electrophoretic mobility shift assay (EMSA)

Nuclear extracts were prepared essentially as described (Andrews and Faller 1991). For EMSA analysis nuclear proteins corresponding to 1×10^6 trypanosomes were incubated with 16 fMol double stranded oligonucleotides containing consensus binding sites for the transcription factors NF-κB (5'-AGT TGA GGG GAC TTT CCC AGG C-3') and AP1 (5'-CGC TTG ATG ACT CAG CCG ATC-3') as well as hSIE for STAT-like factors (5'- GTC GAC ATT TCC CGT AAA TCG TCG A) and E74 for ETS-like factors (5'-GAA TAA CCG GAA GTA AC-3'). The oligonucleotides were end-labeled with [γ-^{32}P]-ATP (Amersham Pharmacia Biotech, Freiburg, Germany) by polynucleotide kinase. The shift assays were performed in a total volume of 20 µl of the following buffer: 10 mM Tris-HCl, pH 7.5; 50 mM KCl, 0.1 mM EDTA, 1 mM dithiothreitol, 1 mg/ml bovine

serum albumin (BSA), 5% glycerol, 0.1% NP40, 1 µM Pefabloc (Roche Molecular Biochemicals, Mannheim, Germany). The reactions, also containing poly(dI-dC) (1 mg/ml; Roche), were performed at room temperature for 30 min and initiated by the addition of nuclear extract. Complexes were analyzed by electrophoretic separation on a 6% polyacrylamide gel in 0.25 × TBE buffer. Dried gels were exposed to X-ray film for autoradiographic analysis.

Immunocytochemical staining of IFN-γ stimulated *T.b.b.*

Trypanosoma brucei brucei were purified from rat blood as described above and cultured at 37°C for 6 h. They were then stimulated with 400 U/ml recombinant rat IFN-γ, for 15, 60 or 240 and 480 min, respectively, or were un-stimulated (control group). They were mounted on gelatine-coated slides and air-dried. *T.b.b.* were fixed with 6% paraformaldehyde in PBS for 30 min, and after 4 washes in 0.1% PBS/saponin endogenous peroxidase was blocked using an avidin-biotin blocking kit (Vector Laboratories Inc. Burlingame, CA). Slides were then blocked in 10% normal goat serum (1h at room temperature) before challenge with 2.5 µg/ml of anti-c-fos polyclonal antibody (Santa Cruz Biotechnology Inc., CA, USA). After 4 washes in PBS, biotinylated anti-rabbit antibody (Jackson ImmunoResearch Laboratories, PA, USA) at a dilution of 1:300 was applied. The slides were incubated with avidin-biotin-peroxidase complex (Vector). Staining was performed using a DAB-staining kit (Vector). As control, primary antibodies were omitted or irrelevant primary antibody was used.

SDS-PAGE and Western blotting of IFN-γ stimulated *T.b.b.* lysates

Using the same conditions of stimulation as described above, *T.b.b.* lysates were prepared from the pellet by adding lysis buffer containing 20 mM TRIS-HCl (pH 7.5), 137 mM NaCl, 0.1% SDS, 0.5% sodium deoxycholate, 1% Triton X-100, 10% glycerol, 2 mM EDTA, 1 mM phenylmethylsulphonylfloride (PMSF), 0.15 U/ml aprotinin, and 1 mM sodium orthovanadate. After 3-4 min on ice supernatants were removed and kept at -80°C. The protein content in the cytoplasmic extracts was determined using the protein assay of BioRad Hercules, CA). The samples from the cytoplasmic extracts were fractionated by SDS-PAGE. The separated proteins were transferred electrophoretically to a nitrocellulose membrane (BioRad). Membranes were blocked in 5% dry milk in TBST - to prevent non specific binding - in a shaker for 1 h. The primary antibody polyclonal anti-c-fos (diluted 1:1000) was added for 1h. After washing, the membranes were incubated for 1h with the secondary antibody (horseradish peroxidase-conjugated anti-rabbit immunoglobulins (DAKO A/S, Glostrup, Denmark, diluted 1:2000). The protein was detected using enhanced chemiluminescence system (Amersham Pharmacia Biotech) on an autoradiographic film.

RESULTS

EMSA investigation shows that the TFs AP-1 and NF-κB, an ETS-like factor binding to E74 and a STAT-like factor binding to hSIE are all constitutively expressed in the nuclei of the bloodstream form of *T.b.b.* at low levels, as depicted in Fig. 1. The expression of AP-1, E74 and hSIE was up-regulated after 15 min (for AP-1 and E74) to 60 min (for hSIE) of IFN-γ stimulation, whereas NF-κB expression remained at the same level. Maximum expression of AP-1as observed in the long and short exposure, E74 and hSIE was detected after 240 min of IFN-γ stimulation. STAT expression was not detectable by the applied method (data not shown). The expression of the classical immediate early gene c-fos, a component of the AP-1 family, was further investigated by immunocytochemistry and Western blot. Immunocytochemical staining demonstrated the translocation of c-fos to trypanosome nuclei (Fig. 2). In the unstimulated trypanosomes c-fos staining was only observed in the cytoplasm (Fig. 2B), while upon IFN-γ stimulation this factor started to be recruited to the nucleus (Figs 2C, D). The expression pattern of c-fos in Western blot of *T.b.b.* lysates shown in Fig. 3 confirms the suggested activating properties of IFN-γ for this factor.

DISCUSSION

In the present study we investigated the changes caused by IFN-γ stimulation of *T.b.b.* with regard to the expression of the TFs: AP-1 and NF-κB as well of the DNA binding-sites E74 for a ETS-like factor and hSIE for a STAT-like factor.

In eukaryotes, the assemblies of TFs bound to DNA direct RNA polymerase binding to initiate mRNA synthesis. RNA polymerases alone cannot bind efficiently to DNA. TF activities are regulated through different mechanisms such as phosphorylation (de Groot *et al*. 1993). In addition, transcription activity is influenced by several other DNA-binding proteins like those binding to E74 and hSIE sites. An important physiological function of these factors is the control of cell proliferation, achieved through their ability to regulate the expression and function of cell cycle regulators (Shaulian and Karin 2001).

Transcription in *T.b.b.* differs in some aspects from those in multicellular eukaryotes (Marchetti *et al*. 1998). Three types of RNA polymerases direct transcription in the parasite, but details of this process are still unclear. In the present study we demonstrate DNA binding activities of three transcription regulating factors among the nuclear proteins of IFN-γ-stimulated trypanosomes, which are not primarily involved in IFN-γ dependent signalling in multicellular eukaryotes, whereas the con-

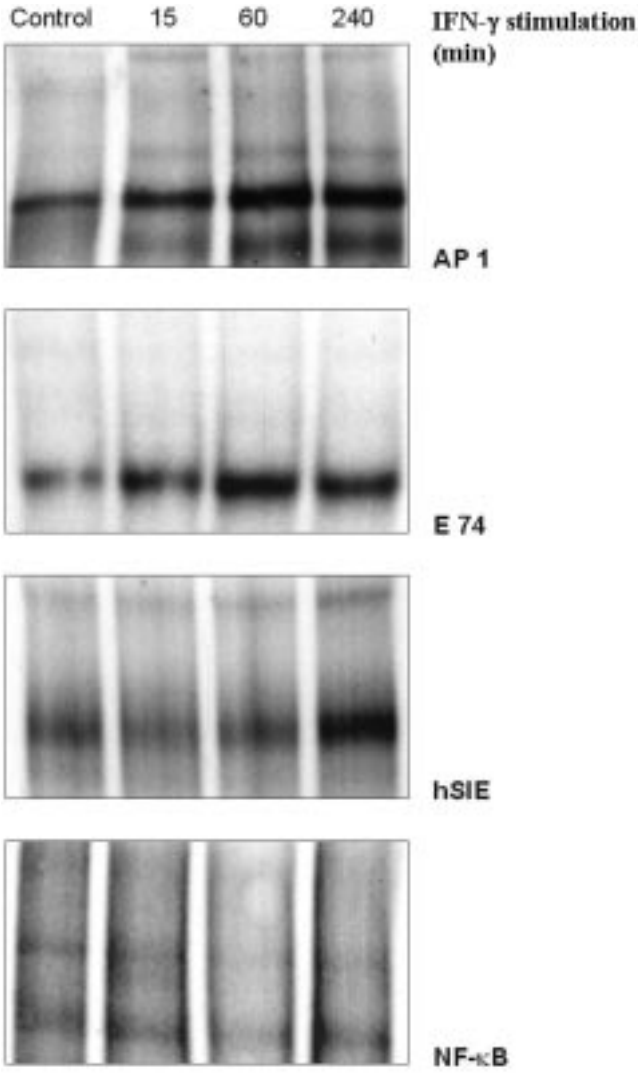

Fig. 1. DNA binding activities of AP-1, E 74, hSIE, and NF-κB are detected by EMSA using nuclear proteins of IFN-γ stimulated *Trypanosoma brucei brucei* Time points indicate time (min) of exposure of *T.b.b.* to IFN-γ after the parasites were adapted to the culture medium for 6h in order to inhibit *in vivo* activation of signal pathways.

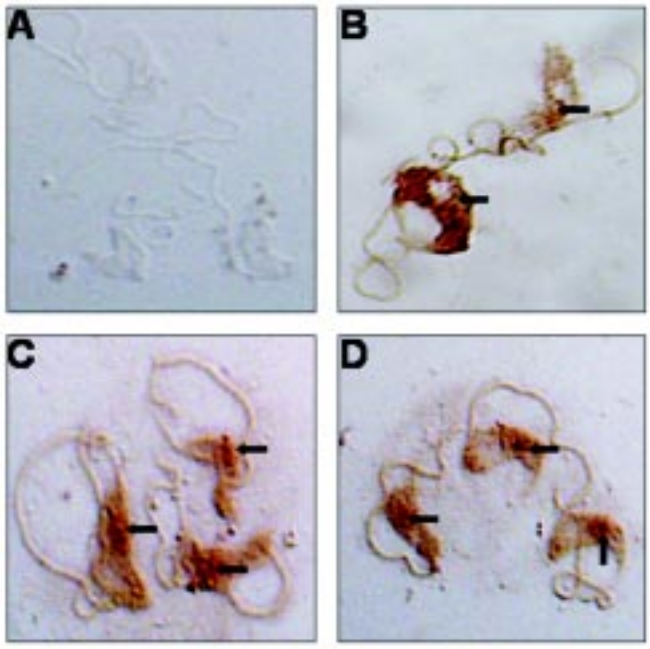

Fig. 2. Detection of c-fos by immunocytochemical staining of IFN-γ stimulated *Trypanosoma brucei brucei* **A:** depicts the negative control omitting the primary antibody. **B:** depicts the expression of c-fos under normal growth condition of the unstimulated trypanosomes. **C:** demonstrates the recruitment of c-fos to the nuclear area. **D:** shows the translocation of c-fos to *T.b.b.* nuclei, which are indicated by arrows.

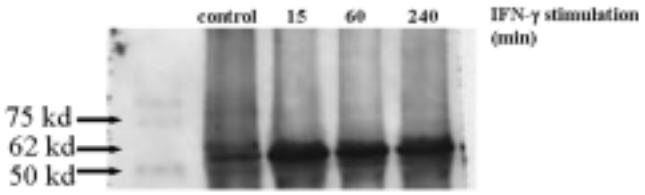

Fig. 3. Western blot detection of c-fos in *Trypanosoma brucei brucei.* The 62kD band represents c-fos protein expression after the indicated time (min) of exposure of the parasites to IFN-γ. The parasites were previously adapted to the culture medium for 6 h in order to inhibit *in vivo* activation of signal pathways.

ventional TFs of the IFN-γ induced signal pathway STAT 1 and 2 were not detected (data not shown). Out of the detected transcription regulating factors AP-1 comprises a family of TFs consisting of homodimers and heterodimers of Jun and Fos, and has been shown to control rapid responses of mammalian cells to stimuli that induce proliferation, differentiation, and transformation (Sharma and Richards 2000). E74 is the DNA binding site of a member of the external transcribed spacer ETS family. The physiological functions of this family were first characterized during *Drosophila* development. DNA binding activity to E74 is induced by the hormone 20-hydroxyecdysone (ecdysone). This activity enhances changes in gene transcription, cell physiology, and tissue organization (Hsu and Schulz 2000). The high-affinity serum-inducible element hSIE and the TF nuclear factor protein-κB NF-κB are involved in different cellular processes such as cell growth, development and apoptosis. NF-κB is induced to control a variety of physiological aspects of immune and inflammatory responses. This protein is regulated by the interaction between Rel and IκB.

The prolonged up-regulation of AP-1 suggests that it might play a role in trypanosome developmental pro-

cesses, since it was reported to control proliferation and differentiation (Sharma and Richards 2000). As it was shown by EMSA the factor was activated to bind to trypanosomes DNA in IFN-γ stimulated parasites, while this activation was not observed in unstimulated parasites, suggesting a role for the cytokine IFN-γ in enhancing the gene transcription process in the trypanosomes.

IFN-γ is a potent activator of the STAT signalling pathway in multicellular eukaryotic cells (Alsayed *et al*. 2000), and it induces a rapid and strong tyrosine phosphorylation in *T.b.b.* (Mustafa *et al*. 1997). Our findings suggest that subsequent to tyrosine phosphorylation the transcription regulating factors AP-1, ETS-like factor (binding to E74), and STAT-like factor (binding to hSIE), but not NF-κB are induced in *T.b.b.* In multicellular eukaryotic cells the binding of IFN-γ to its stimulated response element ISREs induces the expression of different factors, which initiate gene transcription for this cytokine or other proteins (Imam *et al*. 1990). The main signal pathway induced by IFN-γ in multicellular eukaryotes is the Janus kinase (JAK)-STAT pathway, for which no evidence has been found in IFN-γ stimulated *T.b.b.* to date. The induction of the transcription regulating factors AP-1, ETS-like factor (binding to E74) and STAT-like factor (binding to hSIE) in *T.b.b.* was weaker, but prolonged as compared to the common TF induction in multicellular eukaryotes. Their prolonged up-regulation may compensate for the lower level of factor expression in order to achieve efficient mRNA production of IFN-γ-induced target genes.

Acknowledgment. This investigation received financial support from the Swedish foundation for Strategic Research, and from the Swedish Medical Research Council. The WHO Central Serum Bank for Sleeping Sickness delivered trypanosome materials.

REFERENCES

Alsayed Y., Uddin S., Majchrzak B., Druker B. J., Fish E. N. Platanias L. C. (2000) IFN-gamma activates the C3G/Rap1 signaling pathway. *J. Immunol*. **164:** 1800-1806

Andrews N. C., Faller D. V. (1991) A rapid micropreparation technique for extraction of DNA-binding proteins from limiting numbers of mammalian cells. *Nucleic Acids Res*. **19:** 2499

Askonas B. A., Corsini A. C., Clayton C. E., Ogilvie B. M. (1979) Functional depletion of T- and B-memory cells and other lymphoid cell subpopulations-during trypanosomiasis. *Immunology* **36:** 313-321

Bakhiet M., Olsson T., Mhlanga J., Buscher P., Lycke N., van der Meide P. H., Kristensson K. (1996) Human and rodent interferon-gamma as a growth factor for *Trypanosoma brucei*. *Eur. J. Immunol*. **26:** 1359-1364

Clayton C. E., Fueri J. P., Itzhaki J. E., Bellofatto V., Sherman D. R., Wisdom G. S., Vijayasarathy S., Mowatt M. R. (1990) Transcription of the procyclic acidic repetitive protein genes of *Trypanosoma brucei*. *Mol. Cell Biol*. **10:** 3036-3047

de Groot R. P., den Hertog J., Vandenheede J. R., Goris J., Sassone-Corsi P. (1993) Multiple and cooperative phosphorylation events regulate the CREM activator function. *EMBO J*. **12:** 3903-3911

Hsu T., Schulz R. A. (2000) Sequence and functional properties of Ets genes in the model organism *Drosophila*. *Oncogene* **19:** 6409-6416

Imam A. M., Ackrill A. M., Dale T. C., Kerr I. M., Stark G. R. (1990) Transcription factors induced by interferons alpha and gamma. *Nucleic Acids Res*. **18:** 6573-6580

Johnson P. J., Kooter J. M., Borst P. (1987) Inactivation of transcription by UV irradiation of *T. brucei* provides evidence for a multicistronic transcription unit including a VSG gene. *Cell* **51:** 273-281

Marchetti M. A., Tschudi C., Silva E., Ullu E. (1998) Physical and transcriptional analysis of the *Trypanosoma brucei* genome reveals a typical eukaryotic arrangement with close interspersion of RNA polymerase II- and III-transcribed genes. *Nucleic Acids Res*. **26:** 3591-3598

Murphy W. J., Watkins K. P., Agabian N. (1986) Identification of a novel Y branch structure as an intermediate in trypanosome mRNA processing: evidence for trans splicing. *Cell* **47:** 517-525

Mustafa E., Bakhiet M., Jaster R., Bittorf T., Mix E., Olsson T. (1997) Tyrosine kinases are required for interferon-gamma-stimulated proliferation of *Trypanosoma brucei brucei*. *J. Infect. Dis*. **175:** 669-673

Olsson T., Bakhiet, M. Edlund C., Hojeberg B., Van der Meide P. H., Kristensson K. (1991) Bidirectional activating signals between *Trypanosoma brucei* and CD8+ T cells: a trypanosome-released factor triggers interferon-gamma production that stimulates parasite growth. *Eur. J Immunol*. **21:** 2447-2454

Olsson T., Bakhiet M., Hojeberg B., Ljungdahl A., Edlund C., Andersson G., Ekre H. P., Fung-Leung W. P., Mak T., Wigzell H. (1993) CD8 is critically involved in lymphocyte activation by a *T. brucei brucei*-released molecule. *Cell* **72:** 715-727

Rudenko G., Lee M. G., Van der Ploeg L. H. (1992) The PARP and VSG genes of *Trypanosoma brucei* do not resemble RNA polymerase II transcription units in sensitivity to Sarkosyl in nuclear run-on assays. *Nucleic Acids Res*. **20:** 303-306

Sharma S. C., Richards J. S. (2000) Regulation of AP1 (Jun/Fos) factor expression and activation in ovarian granulosa cells. Relation of JunD and Fra2 to terminal differentiation. *J. Biol. Chem*. **275:** 33718-33728

Shaulian E., Karin M. (2001) "AP-1 in cell proliferation and survival." *Oncogene* **20:** 2390-2400

Sternberg J., McGuigan F. (1992) Nitric oxide mediates suppression of T cell responses in murine *Trypanosoma brucei* infection. *Eur. J. Immunol*. **22:** 2741-2744

Szabo S., Khomenko T., Gombos Z., Deng X. M., Jadus M. R., Yoshida M. (2000) Review article: transcription factors and growth factors in ulcer healing. *Aliment Pharmacol. Ther*. **14 (Suppl 1):** 33-43

Turner C. M., Barry J. D. (1989) High frequency of antigenic variation in *Trypanosoma brucei rhodesiense* infections. *Parasitology* **99:** 67-75

Vaidya T., Bakhiet, Hill K. L., Olsson T., Kristensson K., Donelson J. E. (1997) The gene for a T lymphocyte triggering factor from African trypanosomes. *J. Exp. Med*. **186:** 433-438

Zomerdijk J. C., Kieft R., Shiels P. G., Borst P. (1991) Alpha-amanitin-resistant transcription units in trypanosomes: a comparison of promoter sequences for a VSG gene expression site and for the ribosomal RNA genes. *Nucleic Acids Res*. **19:** 5153-5158

Received on 12th June, 2004; revised version on 2nd August, 2004; accepted on 3rd August, 2004

INSTRUCTIONS FOR AUTHORS

Acta Protozoologica is a quarterly journal that publishes current and comprehensive, experimental, and theoretical contributions across the breadth of protistology, and cell biology of lower Eukaryote including: behaviour, biochemistry and molecular biology, development, ecology, genetics, parasitology, physiology, photobiology, systematics and phylogeny, and ultrastructure. It publishes original research reports, critical reviews of current research written by invited experts in the field, short communications, book reviews, and letters to the Editor. Faunistic notices of local character, minor descriptions, or descriptions of taxa not based on new, (original) data, and purely clinical reports, fall outside the remit of *Acta Protozoologica*.

Contributions should be written in grammatically correct English. Either British or American spelling is permitted, but one must be used consistently within a manuscript. Authors are advised to follow styles outlined in The CBE Manual for Authors, Editors, and Publishers (6th Ed., Cambridge University Press). Poorly written manuscripts will be returned to authors without further consideration.

Research, performed by "authors whose papers have been accepted to be published in *Acta Protozoologica* using mammals, shall have been conducted in accordance with accepted ethical practice, and shall have been approved by the pertinent institutional and/or governmental oversight group(s)"; this is Journal policy, authors must certify in writing that their research conforms to this policy.

Nomenclature of genera and species names must agree with the International Code of Zoological Nomenclature (ICZN), International Trust for Zoological Nomenclature, London, 1999; or the International Code of Botanical Nomenclature, adopted by XIV International Botanical Congress, Berlin, 1987. Biochemical nomenclature should agree with "Biochemical Nomenclature and Related Documents" (A Compendium, 2nd edition, 1992), International Union of Biochemistry and Molecular Biology, published by Portland Press, London and Chapel Hill, UK.

Except for cases where tradition dictates, SI units are to be used. New nucleic acid or amino acid sequences will be published only if they are also deposited with an appropriate data bank (e.g. EMBL, GeneBank, DDBJ).

All manuscripts that conform to the Instructions for Authors will be fully peer-reviewed by members of Editorial Board and expert reviewers. The Author will be requested to return a revised version of the reviewed manuscript within four (4) months of receiving the reviews. If a revised manuscript is received later, it will be considered to be a new submission. There are no page charges, but Authors must cover the reproduction cost of colour illustrations.

The Author(s) of a manuscript, accepted for publication, must transfer copyrights to the publisher. Copyrights include mechanical, electronic, and visual reproduction and distribution. Use of previously published figures, tables, or brief quotations requires the appropriate copyright holder's permission, at the time of manuscript submission; acknowledgement of the contribution must also be included in the manuscript. Submission of a manuscript to *Acta Protozoologica* implies that the contents are original, have not been published previously, and are not under consideration or accepted for publication elsewhere.

SUBMISSION

Authors should submit manuscript to: Dr Jerzy Sikora, Nencki Institute of Experimental Biology, ul. Pasteura 3, 02-093 Warszawa, Poland, Fax: (4822) 8225342; E-mail: jurek@nencki.gov.pl or j.sikora@nencki.gov.pl.

At the time of submission, authors are encouraged to provide names, E-mails, and postal addresses of four persons who might act as reviewers. Extensive information on *Acta Protozoologica* is available at the website: **http://www.nencki.gov.pl/ap.htm**; however, please do not hesitate to contact the Editor.

Hard copy submission: Please submit three (3) high quality sets of text and illustrations (figures, line drawing, and photograph). When photographs are submitted, arranged these in the form of plate. A copy of the text on a disk or CD should also be enclosed, in PC formats, preferably Word for Windows version 6.0 or higher (IBM, IBM compatible, or MacIntosh). If they do not adhere to the standards of the journal the manuscript will be returned to the corresponding author without further consideration.

E-mail submission: Electronic submission of manuscripts by e-mail is acceptable in PDF format only. Illustrations must be prepared according to journal requirement and saved in PDF format. The accepted manuscript should be submitted as a hard copy with illustrations (two copies, one with lettering + one copy without lettering) in accordance with the standards of the journal.

ORGANIZATION OF MANUSCRIPTS

Text: Manuscripts must be typewritten, double-spaced, with numbered pages (12 pt, Times Roman). The manuscript should be organized into the following sections: Title, Summary, Key words, Abbreviations, Introduction, Materials and Methods, Results, Discussion, Acknowledgements, References, Tables, and Figure legends. Figure legends must contain explanations of all symbols and abbreviations used. The Title Page should include the title of the manuscript, first name(s) in full and surname(s) of author(s), the institutional address(es) where the work was carried out, and page heading of up to 40 characters (including spaces). The postal address for correspondence, Fax and E-mail should also be given. Footnotes should be avoided.

Citations in the text should be ordered by name and date but not by number, e.g. (Foissner and Korganova 2000). In the case of more than two authors, the name of the first author and *et al.* should be used, e.g. (Botes *et al.* 2001). Different articles by the same author(s) published in the same year must be marked by the letters a, b, c, etc. (Kpatcha *et al.* 1996a, b). Multiple citations presented in the text must be arranged by date, e.g. (Small 1967, Didier and Detcheva 1974, Jones 1974). If one author is cited more than once, semicolons should separate the other citations, e.g. (Lousier and Parkinson 1984; Foissner 1987, 1991, 1994; Darbyshire *et al.* 1989).

Please observe the following instructions when preparing the electronic copy: (1) label the disk with your name; (2) ensure that the written text is identical to the electronic copy; (3) arrange the text as a single file; do not split it into smaller files; (4) arrange illustrations as separate files; do not use Word files; *.TIF, *.PSD, or *.CDR graphic formats are accepted; (5) when necessary, use only italic, bold, subscript, and superscript formats; do not use other electronic formatting facilities such as multiple font styles, ruler changes, or graphics inserted into the text; (6) do not right-justify the text or use of the hyphen function at the end of lines; (7) avoid the use of footnotes; (8) distinguish the numbers 0 and 1 from the letters O and l; (9) avoid repetition of illustrations and data in the text and tables.

References: References must be listed alphabetically. Examples for bibliographic arrangement:

Journals: Flint J. A., Dobson P. J., Robinson B. S. (2003) Genetic analysis of forty isolates of *Acanthamoeba* group III by multilocus isoenzyme electrophoresis. *Acta Protozool.* **42:** 317-324

Books: Swofford D. L. (1998) PAUP* Phylogenetic Analysis Using Parsimony (*and Other Methods). Ver. 4.0b3. Sinauer Associates, Sunderland, MA

Articles from books: Neto E. D., Steindel M., Passos L. K. F. (1993) The use of RAPD's for the study of the genetic diversity of *Schistosoma mansoni* and *Trypanosoma cruzi*. In: DNA Fingerprinting: State of Science, (Eds. S. D. J. Pena, R. Chakraborty, J. T. Epplen, A. J. Jeffreys). Birkhäuser-Verlag, Basel, 339-345

Illustrations and tables: After acceptance of the paper, drawings and photographs (two copies one with lettering + one copy without) must be submitted. Each table and figure must be on a separate page. Figure legends must be placed, in order, at the end of the manuscript, before the figures. Figure legends must contain explanations of all symbols and abbreviations used. All line drawings and photographs must be labelled, with the first Author's name written on the back. The figures should be numbered in the text using Arabic numerals (e.g. Fig. 1).

Illustrations must fit within either a single column width (86 mm) or the full-page width (177 mm); the maximum length of figures is 231 mm, including the legend. Figures grouped as plates must be mounted on a firm board, trimmed at right angles, accurately mounted, and have edges touching. The engraver will then cut a fine line of separation between figures.

Line drawings should be suitable for reproduction, with well-defined lines and a white background. Avoid fine stippling or shading. Prints are accepted only in *.TIF, *.PSD, and *.CDR graphic formats (Grayscale and Colour - 600 dpi, Art line - 1200 dpi) on CD. Do not use Microsoft Word for figure formatting.

Photographs should be sharp, glossy finish, bromide prints. Magnification should be indicated by a scale bar where appropriate. Pictures of gels should have a lane width of no more than 5 mm, and should preferably fit into a single column.

PROOF SHEETS AND OFFPRINTS

After a manuscript has been accepted, Authors will receive proofs for correction and will be asked to return these to the Editor within 48-hours. Authors will be expected to check the proofs and are fully responsible for any undetected errors. Only spelling errors and small mistakes will be corrected. Twenty-five reprints (25) will be furnished free of charge. Additional reprints can be requested when returning the proofs, but there will be a charge for these; orders after this point will not be accepted.

Indexed in: Current Contents, Biosis, Elsevier Biobase, Chemical Abstracts Service, Protozoological Abstracts, Science Citation Index, Librex-Agen, Polish Scientific Journals Contents - Agric. & Biol. Sci. Data Base at: **http://psjc.icm.edu.pl**, Microbes.info "Spotlight" at **http://www.microbes.info**, and electronic version at Nencki Institute of Experimental Biology website in *.PDF format at http://www.nencki.gov.pl/ap.htm now free of charge.

ACTA PROTOZOOLOGICA

ORIGINAL ARTICLES

SHORT COMMUNICATION

2004 NOVEMBER

VOLUME 43 NUMBER 4